Fall 12-2021

Subtalar Joint Definition in Biomechanical Models

Julia Noginova
Old Dominion University, jnogi001@odu.edu

SUBTALAR JOINT DEFINITION IN BIOMECHANICAL MODELS

by

Julia Noginova
B.S. May 2014, George Mason University

A Dissertation Submitted to the Faculty
of Old Dominion University in Partial Fulfillment of the
Requirements for the Degree of

DOCTOR OF PHILOSOPHY

BIOMEDICAL ENGINEERING

OLD DOMINION UNIVERSITY

December 2021

Approved by:

Stacie I. Ringleb (Director)

Hunter J. Bennett (Member)

Sebastian Y. Bawab (Member)

Krishna N. Kaipa (Member)

ABSTRACT

SUBTALAR JOINT AXIS DEFINITION IN BIOMECHANICAL MODELS

Julia Noginova
Old Dominion University, 2021
Director: Dr. Stacie I. Ringleb

The effect of including a subtalar joint in a dynamic musculoskeletal model has not been fully explored or validated. The subtalar joint is often modeled as a one DOF hinge with the tri-planar axis defined as a combination of inclination and deviation angles measured from the ground and midline of the foot, respectively. The overall purposes of this dissertation were to explore how the inclusion of the subtalar joint and the definition of origin location and axis orientation affect the kinematics, joint kinetics, and muscle activations of the knee, ankle, and subtalar joint during dynamic tasks of walking and running through sensitivity analyses and validation using OpenSim (SimTK, Stanford, CA).

The findings of this dissertation conclude that if the subtalar joint is to be included in a model, the location of the axis origin needs to be considered and accurately defined, especially if the inclination/deviation angles of the rotational axis will be modified to represent a more subject-specific definition. The models in this study were validated for walking using available *in vivo* joint contact data from the Grand Knee Challenge. Further inferences were made on the validity of the models for running based on similarities seen in the EMG and muscle activation patterns. The conclusions from this work are drawn from analysis of walking and running, which are primarily sagittal plane motions. Future studies analyzing more complex motion such as cutting or walking on uneven terrain, where there is more transverse and coronal plane motion,

may further highlight the importance of the subtalar joint in musculoskeletal modeling as it plays a more active role during foot adaption.

This dissertation is dedicated to my very patient and very loving family who have never stopped believing in me.

A special dedication to my mother, who knew even before I did, that I would apply and work towards my doctorate degree.

ACKNOWLEDGMENTS

I would like to extend my acknowledgement to Dr. Stacie Ringleb for the guidance and knowledge that I have received in my time as her student. She really defined what it meant to be a mentor, both in research and inspiring me to break through any barriers that may come my way. I hope to become as impressive and impactful as I move forward.

Next, I would like to acknowledge my committee members, Dr. Bennett, Dr. Bawab, and Dr. Kaipa for all their support, without which I would not have been able to complete this work.

I would also like to thank Dr. Handley for being like a second mom to me, at school and outside, for the past 15 years.

And lastly, I would like to thank Tom for providing me with the push that I needed to quit dragging my feet and finish my dissertation. He helped me realize that I don’t need to wait until graduating to begin the life that I want.

TABLE OF CONTENTS

Page

LIST OF TABLES

Table Page

LIST OF FIGURES

Figure Page

Figure Page

CHAPTER 1: INTRODUCTION

1.1 ANATOMY

The ankle-joint complex, comprised of the talocrural and subtalar joints (STJ), is the connection formed between the lower leg proximally, and the rigid foot distally (Brockett and Chapman, 2016). The segments of the hindfoot can be broken down into the shank (tibia & fibula), the heel bone (calcaneus), and the ankle bone (talus) (Figure 1-1) (Chan and Rudins, 1994; Nichols et al., 2016).

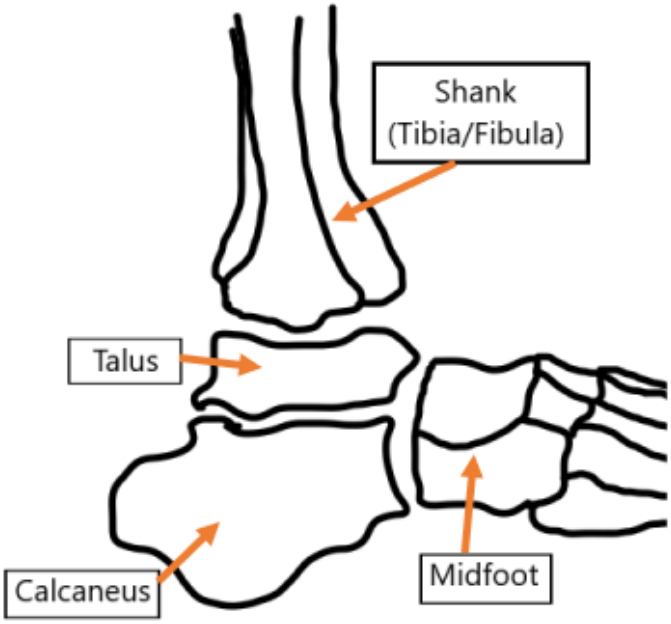

Figure 1-1: Anatomy of the bones of the lower limb and foot that make-up the hindfoot, talocrural and subtalar joints.

The talocrural, is a synovial joint that is formed between the tibia superiorly and the talus inferiorly (Stagni et al., 2003). Found adjacently, the concave facet on the inferior aspect of the talus articulates with the convex posterior facet of the calcaneus, making up the subtalar joint

which has the largest surface area of all the joints (Budny, 2004; Chan and Rudins, 1994; Fernandez et al., 2020). The talus is 60% covered by articular cartilage but lacks any muscle insertion (Maceira and Monteagudo, 2015; Rockar, 1995). Therefore, these two joints must rely on the stability of the hindfoot to keep the congruence and normal motion of the talus. Motion and stability of the ankle complex depends on the specific bone geometry and contours of the many articulating surfaces, the musculotendon forces acting on the joint, as well as the strength and integrity of the surrounding collateral ligaments (McCullough et al., 2011). While no muscles attach to the talus, there are many that cross the ankle-joint complex that work to stabilize the foot and assist in controlling the foot during dynamic activity (Chan and Rudins, 1994; Jastifer and Gustafson, 2014). The major muscles that contribute to foot-shank motion are the: Extensor Hallucis Longus (EHL), Extensor Digitorum Longus (EDL), Tibialis Anterior (TA), Tibialis Posterior (TB), Flexor Digitorum Longus (FDL), Flexor Hallucis Longus (FHL), Peroneus Longus (PL), Peroneus Brevis (PB), and the Achilles Tendon (aka Triceps Surae) which can be broken down into, Gastrocnemius and Soleus (Delp et al., 1990). These muscles can be grouped by function as either ankle plantarflexers, dorsiflexors, everters, or inverters. The ankle everters/inverters are also regularly classified as subtalar supinators/pronators (Rockar, 1995). The action of any muscle is dependent on the position and location of insertion relative to the talocrural or subtalar joint axis (Close et al., 1967; Maceira and Monteagudo, 2015; Rockar, 1995).

1.2 KINEMATICS

During gait, the role of the hindfoot is to offer both support and propulsion to the rest of the leg (Stagni et al., 2003). The talocrural joint functions to distribute the vertical stresses of

gravity, also known as ground reaction force, that are applied throughout the entire foot during weightbearing (Bonnel et al., 2010). While the subtalar joint works with the talocrural to create the functional unit of the ankle, it also plays a crucial role in the mobility of the foot (Keefe and Haddad, 2002). The subtalar joint allows for the absorption of rotations of the leg during stance phase as well as readily accommodates foot position for uneven terrain surfaces (Lundberg and Svensson, 1993; Taylor et al., 2001). This adaptation of the joint to uneven ground comes about from the subtalar joint's natural tri-planar motion (Keefe and Haddad, 2002).

The anterior, middle, and posterior facets, (Figure 1-2) created by the articulation of the talus and calcaneus, allow the subtalar joint to freely move and glide in all three planes of motion (Keefe and Haddad, 2002).

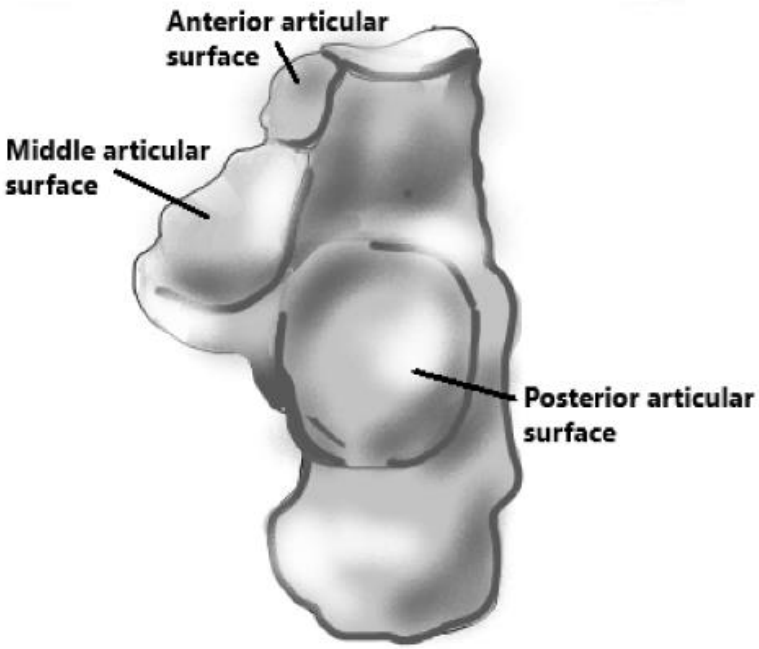

Figure 1-2: Posterior, medial, and anterior facets on the calcaneus that articulate with the talus to allow tri-planar motion.

This tri-planar axis is often cited as running through the center of the talar head and was shown to run postero-lateral-inferior to antero-medial-superior (Fernandez et al., 2020; Jastifer and Gustafson, 2014; Wright et al., 1964). The complex articulation allows the subtalar joint to act as a flexible structure to accommodate for uneven ground while also becoming a rigid lever to distribute propulsive forces across the foot during gait (Aynardi et al., 2015; Budny, 2004). However, due to the irregular geometry of the bones, the plane of motion for this joint does not correspond to any one cardinal body plane (i.e. sagittal, frontal, transverse) but rather is a resultant of all three planes of motion together (Chan and Rudins, 1994; Rockar, 1995). Motion along this oblique axis is referred to as supination/pronation. While the naming convention of these motions differ, it is generally accepted that supination is composed of inversion in the frontal plane, adduction in the transverse plane, and plantarflexion in the sagittal plane while pronation is defined as the combination of eversion, abduction, and dorsiflexion (Budny, 2004; Kjaersgaard-Andersen et al., 1987; Piazza, 2005).

The anatomical position and orientation of a joint axis affect the magnitude of rotation of the joint as well as determine the joint moments created by the interplay of the muscles, ligaments, and ground reaction force (Engsberg, 1987). For this reason, investigators have used *in vitro* models to manipulate and isolate the talocrural and subtalar joints in an attempt to locate and orient the average axis of rotation for each joint (Isman and Inman, 1969; Leardini et al., 2001; Manter, 1941; Root et al., 1966). Since the surrounding muscles and ligaments provide stabilizing forces to the joints as well, *in vivo* evaluation of joint axes and motion during load bearing has also been evaluated with the aid of intercortical bone pins (Arndt et al., 2004) and modern imaging techniques (Beimers et al., 2008; Fernandez et al., 2020; Sheehan et al., 2007).

1.2.a. AXIS OF ROTATION

According to Inman, an average axis of rotation that revolves in all three planes of motion can be simplified and expressed by two angles (Isman and Inman, 1969). In the talocrural joint, the inclination angle is defined between the long axis of the tibia and the joint axis in the frontal plane. Whereas the deviation angle is between the midline of the foot and the projection of the talocrural joint on the horizontal plane (Isman and Inman, 1969). Behavior of joints are often related as simple machines for ease of modeling biomechanical properties (Dettwyler et al., 2004; Jastifer and Gustafson, 2014). For example, it has been determined that the talocrural joint acts as a fixed axis that follows naturally along a body plane (Lewis et al., 2006). In other words, based off of previous *in vitro* work, the axis of rotation for the talocrural joint is found to be horizontal, or 90°, from the frontal plane (Dettwyler et al., 2004). Isman and Inman (1969), in a study comparing rotation axes in 46 cadavers, observed a slight variation with the talocrural joint axis deviated 82.7° ± 3.7° from the frontal plane and 84° ± 7° from the transverse plane. Bogert et al (1994) used an optimization approach to determine talocrural and subtalar joint axes *in vivo* and found similar inclination, 85.4° ± 7.4°, and deviation, 89° ± 15.1°, angles. Since the talocrural joint's average axis of rotation follows so closely to a cardinal body plane, it makes sense that it is the main contributor to plantarflexion/dorsiflexion along the sagittal plane.

The subtalar joint axis also runs through the talus pointing towards the back of the heel. Thus many models simplify the axis and treat both as simple revolute joints (Budny, 2004; Delp et al., 1990; Leitch et al., 2010; Lewis et al., 2006). However, with more recent investigation, there has been much debate if the subtalar joint behaves as a fixed axis (Isman and Inman, 1969; Manter, 1941) or if the angulation of the subtalar joint is joined with sliding of the talus, creating a screw-

like motion along the axis of the subtalar joint (Langelaan, 1983; Leardini et al., 2001; Lundberg and Svensson, 1993). And with the debate of the behavior of the subtalar joint axis comes considerable variation in the concluded orientation for the subtalar joint axis (Table 1-1). There is high variability, not just in the anatomical values of mean inclination/deviation angles, but in the inter-subject variability as well (Arndt et al., 2004; Bogert et al., 1994; Lundberg and Svensson, 1993). This variability accounts for the large ranges of subtalar joint orientation values; for example, Isman and Inman (1969) reported the subtalar joint inclination and deviation angles to range between 20-68° and 4-47°, respectively (Figure 1-3) (Isman and Inman, 1969).

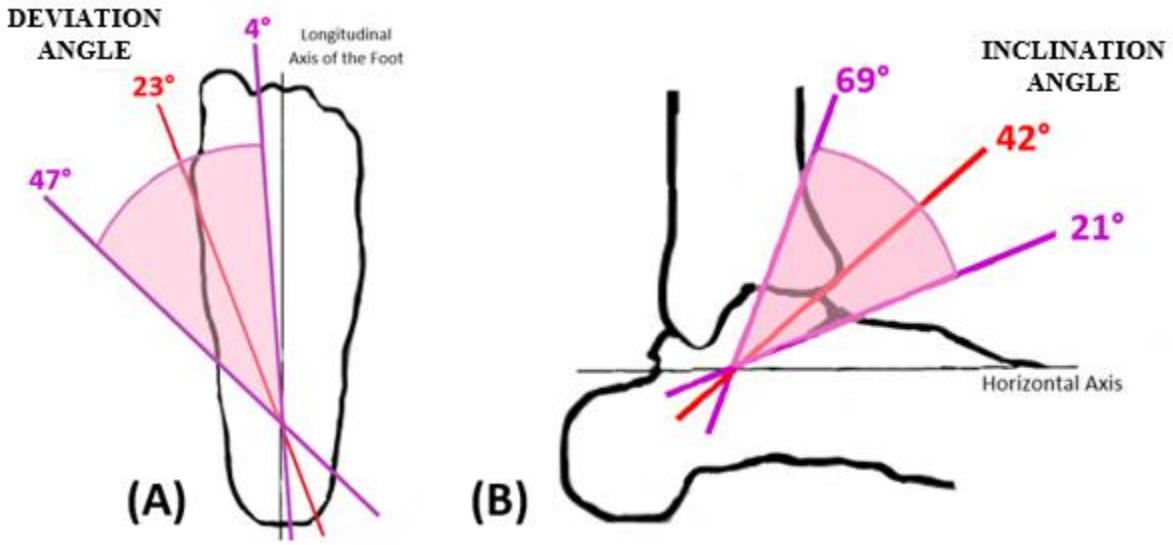

Figure 1-3: Subtalar joint axis orientation defined as components of (A) deviation angle from midline of the foot and (B) inclination angle from the horizontal plane. The purple shading represents the range of values established by Inman, with the line indicating mean values for both.

When comparing between the two angle components, the deviation angle measures have been reported with larger standard deviation estimates (Table 1-1) from the concluded mean.

Author	Sagittal Plane/ Inclination	Transverse Plane/ Deviation	Method
Manter (Manter, 1941)	42° (29°-47°)	16° (8°-24°)	In vitro, anatomical
Root (Root et al., 1966)	41° ± 8° (22°-55°)	17° ± 2° (8°-29°)	In vitro, anatomical
Inman (Isman and Inman, 1969)	41° ± 9° (20°-68°)	23 ± 11° (4°-47°)	In vitro, anatomical
Leardini (Leardini et al., 2001)	53° ± 6° (44°-61°)	38° ± 5° (33°-47°)	In vitro, anatomical
Lewis (Lewis et al., 2006)	30.6° ± 6.4 ° (23°-41°)	23.2° ± 10.4 ° (10°-40°)	In vitro, anatomical
Lundberg (Lundberg and Svensson, 1993)	33° ± 16° (29°-38°)	32° ± 16° (23°-37°)	In vivo, X-ray
Arndt (Arndt et al., 2004)	31.4° – 36.45°	15.7°-23.5°	In vivo, anatomical
Van de Bogert (Bogert et al., 1994)	35.3° ± 4.8°	18.0° ± 16.2°	In vivo, anatomical
Beimers (Beimers et al., 2008)	51.4° ± 4.3° (45.2°-59.1°)	5.4° ± 7.8° (-9.4°-22.7°)	In vivo, CT (simulated load)
Sheehan (Sheehan et al., 2007)	Variable depending on angle	Variable depending on angle	In vivo, MRI (simulated load)
Fernandez (Fernandez et al., 2020)	43° ± 5.7° (45.2°-59.1°)	6 ± 8.6° (45.2°-59.1°)	In vivo, CT (full weightbearing)

Table 1-1: Brief list of past investigators reported subtalar joint axis inclination and deviation angles and the method in which the angles were determined. Mean value with standard deviation as well as (range) when given.

Van de Bogert reported that across 14 subjects, the subtalar joint deviation angle was almost 3 times larger compared to standard deviations of the inclination angles (15° compared to 5°, respectively) (Bogert et al., 1994; Engsberg, 1987; Leitch et al., 2010). The considerable variation seen, both inter-patient and between studies, shows that it is important to assess subject-specific kinematics and axis definition instead of using a generic characterization to describe joint function (Birch and Deschamps, 2014).

The inclination and deviation angles of the subtalar joint axis are important as the average axis of rotation affects both the kinematics and kinetics of the joint during active dynamic motion. It has been determined that a higher subtalar joint inclination angle allows more tibial rotation in the transverse plane, which in turn, leads to an increase in adduction/adduction range of motion (Budny, 2004; Kirby, 1987). Conversely, the lower the pitch of the inclination angle, the more rotation is seen in the calcaneus in the frontal plane. This increase in frontal plane motion results in an increase in inversion/eversion ranges of motion (Budny, 2004; Chan and Rudins, 1994; Kirby, 1987). The deviation angle of the rotational axis, measured from the sagittal plane, affects the amount of dorsiflexion-plantarflexion that the joint rotates, with the contribution being minimized as the axis moves closer to the sagittal plane (Budny, 2004; Chan and Rudins, 1994).

In many of the determinations of talocrural and subtalar joint axes orientation, a single value has been used to define the axis for the full ranges of motion. However, there have been observed changes of both position and orientations of the joint axes during motion leading many to suggest that one single fixed axis of rotation may not be enough to fully describe all motions seen at the joints (Engsberg, 1987; Leardini et al., 2001). Lundberg performed experiments in which the motions of talocrural dorsiflexion/plantarflexion and supination/pronation were broken

up into several static, 10 degrees of motion increments (Lundberg et al., 1989). It was concluded that the talocrural joint axis differed between increments and changed continuously throughout the ranges of motion (Lundberg et al., 1989). Similarly, in a series of roentgen experiments performed by Langelaan (1983) to determine subtalar joint axis of rotation, it was found that for each intermediate position, a unique subtalar joint location and orientation was measured (Langelaan, 1983). Using intracortical pins, similar patterns were seen *in vivo* in the talocrural and subtalar joint axes during stance phase of walking. Whereas previous studies had collected kinematics at 10° increments, investigators analyzed finite and instantaneous helical axes of the subtalar joint by separating the whole joint motion into two half arcs (Arndt et al., 2004). The results showed that the finite helical axis (FHA) were variable during the arcs of motion. This supports the finding by Langelaan (1983) and Engsberg (1987) that joint axes are not constant throughout the arcs of motion (Arndt et al., 2004; Dettwyler et al., 2004; Engsberg, 1987; Langelaan, 1983; Lundberg et al., 1989).

Another source of the large discrepancies in ranges of subtalar joint axis orientation comes from differences and error in the varying methodologies of subtalar joint axis calculation. Tracking the isolated subtalar joint motion alone is difficult due to surrounding skin artifact, lack of external talar landmarks, relative size of the talus and nearby bodies, complex geometry of the joint, coupled motion with the talocrural joint, etc. (Arndt et al., 2004; Beimers et al., 2008; Fernandez et al., 2020). Several methods have been used to try to determine the axis and isolated motion of the subtalar joint. Cadaveric simulations offer a controlled evaluation of subtalar joint kinematics by being able to “lock” the talocrural joint in place. However, many were evaluated using anatomical landmarks or were evaluated in the unloaded condition. This in turn, disregards the contribution of the ligaments, tendons, and surrounding structures to stability and

joint rotation (Reule et al., 2011). Both *in vitro* and *in vivo* studies have started to use imaging techniques, such as roentgen stereophotogrammetry (x-ray), CT, and MRI in both loaded and unloaded conditions. As Table 1-1 shows, the deviation angles of the subtalar joint axis have been determined to be smaller in these studies. It was determined that subtalar joint range of motion is often estimated to be 3x smaller when using CT imaging technique as compared to external subtalar joint motion estimates (goniometer) (Pearce and Buckley, 1999). The imaging techniques allow for estimation of joint angle vectors in a 3D space instead of just components of an inclination and deviation angle (Fernandez et al., 2020; Nichols et al., 2017; Parr et al., 2012).

Generally speaking, the means of measuring and describing segment anatomical axes has varied between authors, both on methodology of data collection (i.e. *in vivo* vs *in vitro*, static vs dynamic, anatomical landmark vs imaging, weight-bearing vs non-loaded, etc.) (Carson et al., 2001; Michelson et al., 2004) as well as the coordinate system used to describe bone motion (i.e. Euler, Joint Coordinate System, Helical) (Baeyens et al., 2005; Ball and Greiner, 2008; Berme et al., 1990; Choisne et al., 2012; Grood and Suntay, 1983; Spoor and Veldpaus, 1980; Woltring et al., 1985; Ying et al., 2004). These differences in anatomical coordinate system definition between studies limit the comparability of results from one study to the next (Carson et al., 2001). In an aim to resolve these differences and allow for straight-forward comparisons, the International Society of Biomechanics (ISB) has created standards for researchers to follow when reporting kinematic data of major segments of the human body (Brown et al., 2009; Wu and Cavanagh, 1995). These define the recommended location and direction of the segment joint coordinate system. For example, the ISB has defined the talocrural coordinate system as having an origin located on the talus at the inter-malleolar point, found midway between the medial and lateral malleoli (Wu et al., 2002). The reference frame is defined with the X-axis following the

long axis of the foot pointing towards the toes, the Y-axis as the longitudinal axis that is perpendicular to the foot and points towards the tibia, and the Z-axis being the cross product of the two, pointing laterally (Wu et al., 2002). Currently there are no specific standards for the rest of the foot, though many cite the ISB ankle standards when giving a reference frame to the subtalar joint.

1.2.b RANGE OF MOTION

The great variability in joint axis orientation, either due to inter-subject variability or how the axes are reported, also affects reported ranges of motion. This makes it difficult for investigators and clinicians to make the distinction between normal and abnormal motion (Choisne et al., 2013). There are widely conflicting reports of what the range of motion of the healthy talocrural and subtalar joint are and what "normal" motion should look like. For example, during clinical examinations, it has been reported that average range of motion for the subtalar joint is about 25° to 30° of inversion and 5° to 10° of eversion (Budny, 2004). However, according to Wright et al. (1964), in an analysis of the stance phase of walking, the average rotation observed at the subtalar joint is only about 6° of motion. These differences in values may be attributed to how each study is conducted. Previously reported studies vary in how the foot is loaded (talus vs calcaneus), how much loading is being applied, the method of measuring joint angle, and how the final results are reported (Fujii et al., 2010). Some studies report one maximum value that represents the total range that the joint motion spans. This value can vary anywhere between 6° to 45° of total subtalar joint range of motion (Brantigan et al., 1977; Hicks et al., 2015; Wright et al., 1964). Other studies have determined total ranges of motion by dividing the full range into the two motion arcs and comparing that motion to neutral

position. McMaster described the subtalar joint as having 30° of total motion along its multi-planar axis, with 25° of those being in inversion and 5° in eversion (McMaster, 1976). Others investigators have reported anywhere from 50-60° of total subtalar joint range of motion with an even split between inversion/supination and eversion/pronation (Jastifer and Gustafson, 2014). Allinger and Engsberg(1993) evaluated the range of motion of the subtalar joint in each of the three planes separately and found that the greatest motion was in dorsiflexion/plantarflexion (20°-35°), eversion/inversion (10°-20°), and then abduction/adduction (10°-10°). Similarly, Maceira and Monteagudo (2015) found that 2/3 of subtalar motion comes from supination and the rest from pronation. While subtalar joint passive motion can reach 30°, only 10° of supination and 5° of pronation is necessary for normal gait. This supports Wright et al.'s (1964) low estimation of subtalar joint motion as well as Ardnt et al.'s (2004) that found that maximum rotations of the subtalar joint during stance were 8.3° eversion/inversion, 3.7° dorsiflexion/plantarflexion, and 6.1° abduction/adduction.

While the range of motion may be small (especially when weightbearing), together with the talocrural joint, the range of motion of the full ankle-complex is larger than reported ranges of either alone (Siegler et al., 1988). This is due to the highly coupled kinematics of the talocrural and subtalar joints that move simultaneously (Siegler et al., 1988). This often makes it difficult to isolate and measure the axis of the individual joints as well as their separate contribution towards the total hind-foot motion (Lewis et al., 2006). It has been reported that during dorsiflexion/plantarflexion, the talocrural is the primary contributor to calcaneal motion relative to the tibia with little, if any, occurring at the subtalar joint (Wong et al., 2005). However, the subtalar joint contributes more to inversion-eversion with a reported 2:1 ratio of subtalar to talocrural joint motion (Taylor et al., 2001; Wong et al., 2005). This ratio increases to

3:1 for supination motion and up to 4:1 reported for internal-external rotation (Bahr et al., 1998; Taylor et al., 2001). In one cadaver study, the percentage of subtalar joint contribution was a bit less in all measured motion with a contribution of 31-34% during calcaneal internal rotation, 30-35% external rotation, 37-42% of inversion and 43-51% of eversion (Pellegrini et al., 2016).

This shows that while the talocrural and subtalar joint have primary functions of foot dorsiflexion/plantarflexion and inversion/eversion, the contribution of each joint to overall foot motion cannot be simplified to just one degree of freedom flexion-extension motion (Arndt et al., 2004; Bonnel et al., 2010; Nichols et al., 2016; Taylor et al., 2001).

1.3 MUSCLE MOMENT ARMS

The range of motion of the subtalar joint relies on the action of the muscles that work to maintain balance of the foot (Close et al., 1967; Jastifer and Gustafson, 2014). It has been concluded that this muscle function is dependent on the tendon location in relation to the joint axis, the distance from the axis, relative strength, and weight-bearing conditions (Close et al., 1967; Lewis et al., 2006; Maceira and Monteagudo, 2015; Reule et al., 2011; Rockar, 1995; Wade et al., 2019). For most joints, there are muscle function pairs that work antagonistically to move the segments. The extrinsic muscles that insert posterior to the talocrural axis are considered plantarflexors, while vice versa, those with insertion points located anterior to the ankle axis work as dorsiflexors (Chan and Rudins, 1994). The main ankle dorsiflexors are the Extensor Hallucis Longus, Extensor Digitorum Longus, and the Tibialis Anterior since they are found above the talocrural joint axis (Figure 1-4). Conversely, the Tibialis Posterior, Flexor Digitorum Longus, Flexor Hallucis Longus, Achilles Tendon, Peroneus Brevis and Peroneus Longus are below the axis thus making them plantarflexors.

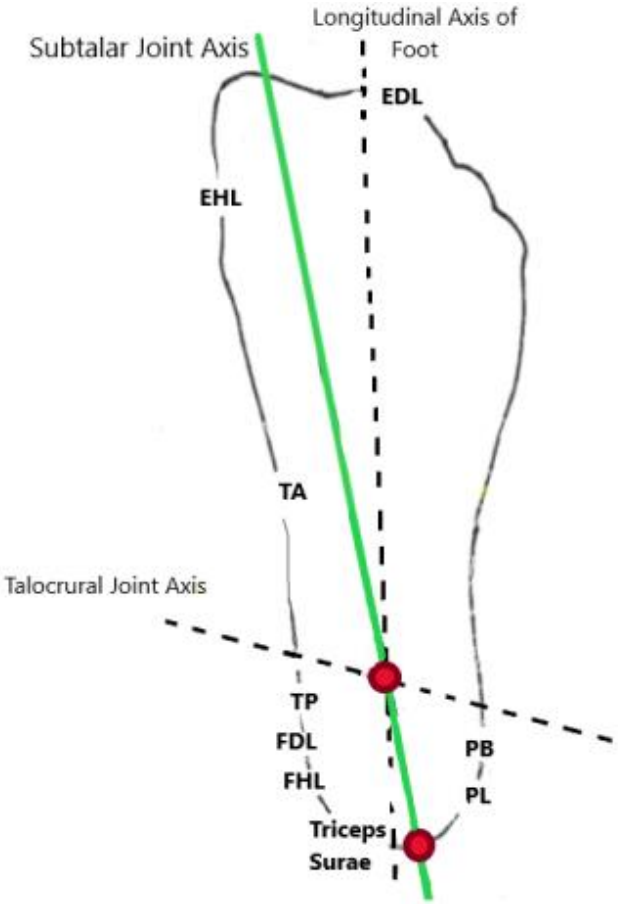

Figure 1-4: The talocrural and subtalar joint axes and relationship to insertions of muscles of the ankle and subtalar joint.

Many of these muscles have a dual function depending on where the tendon crosses the subtalar joint axis. The subtalar joint inverters/supinators are EHL, TA, TB, FDL, FHL, Triceps Surae as they are found on the medial side of the subtalar axis (Figure 1-4) (Chan and Rudins, 1994; Maceira and Monteagudo, 2015; Rockar, 1995). The evertor/pronators of the foot have insertions located on the lateral side of this axis and are the EDL, PL, PB (Close et al., 1967; Rockar, 1995).

Almost as important as the line of action of a muscle to the understanding of muscle capability is the relative distance the tendon is from the axis (Lewis et al., 2006; Rockar, 1995). This distance is known as the muscle moment arm. Muscle tendons that pass closer to the joint

axis are considered “ambiguous” due to their proximity (Lewis et al., 2006). The shorter the relative distance from muscle insertion to axis, the smaller the lever arm the muscle has in order to exert force upon the joint (Rockar, 1995). Generally, muscles with larger muscle moment arm have a greater torque, or effectiveness in muscle action to act on the joint (Reule et al., 2011). Changes in joint axis position or orientation, either due to injury or altered foot anatomy, could significantly alter function of the muscles of the lower extremity (Close et al., 1967). Reule et al. found that there were significant differences in subtalar joint axis orientation, specifically the deviation angle, between normal healthy feet and those with Achilles tendon pathologies (Reule et al., 2011). This medial shift in subtalar axis meant that for some subjects the subtalar joint axis actually ran through the Achilles tendon instead of running outside of the tendon, thus changing the function of the muscle as well as its effectiveness to exert any muscle action on the joint.

1.4 CLOSED KINETIC CHAIN

Many of the findings on the orientation of the joint axes and role of the ligaments in stability of the ankle have been determined based off of kinematic analysis from passive motions (Nichols et al., 2017). However, as seen in Table 1-1 of the subtalar joint axis orientation, the measured inclination/deviation angles have been shown to differ between static *in vitro* measurements and *in vivo* weight-bearing conditions. These differences are especially profound when looking at the deviation angles, which in CT weight-bearing conditions has been approximated to be ~6° of deviation from the midline of the foot while *in vitro* studies based off anatomical landmarks have reported deviation angles up to 38° (Beimers et al., 2008; Fernandez et al., 2020; Isman and Inman, 1969; Leardini et al., 2001; Manter, 1941). It has been shown that the forces applied during the weight-bearing state change the relative motion of both the talus

and calcaneus, affecting the mechanism of pronation/supination of the hindfoot (Rockar, 1995; Taylor et al., 2001). When the foot isn't loaded, like during the swing phase of gait, it is defined as being in the open-kinetic chain. In this state, supination is defined as calcaneal inversion in the frontal plane, adduction in the transverse, and plantarflexion in the sagittal (Taylor et al., 2001). There is little to no relative motion of the talus and tibia during. However, in the closed-kinetic chain, the now weight-bearing foot has load being applied to the calcaneus through ground reaction and intra-articular forces (Taylor et al., 2001). Together, these prevent the calcaneus from adducting and plantarflexing like it normally would during open-kinetic chain supination. In order to still complete the normal supination motion, the talus takes over in the transverse and sagittal plane components (Taylor et al., 2001). However, because the talus is incredibly hard to track clinically, it may not be a reliable method to measure of the motions of the subtalar joint when loaded by just using anatomical landmarks alone. Furthermore, the subtalar joint is not the only joint that the is affected by changes to weight bearing state. During the gait cycle, the tibia rotates, anywhere from 10-25° degrees internally during the load acceptance phase and externally rotates back to neutral for the rest of the cycle (Rockar, 1995). Since the tibiotalar joint only accounts for 11° of these rotations, the subtalar joint accommodates for the rest (Rockar, 1995). As the talus translates medio-inferiorly and rotates internally, the calcaneus on the posterior end everts but also the adjacent calcaneocuboid and talonavicular joints located anteriorly rotate until they form a rigid lever (Ito et al., 2017). This free rotation of the subtalar joint allows the foot to be flexible during load-acceptance to accommodate for uneven ground while also becoming rigid enough during toe-off to propel the body forward (Jastifer and Gustafson, 2014).

1.5 MUSCULOSKELETAL MODELS

In order to analyze the relative joint motion, many investigators rely on biomechanical or musculoskeletal models for accurate assessment of normal human movement, with and without injury (Lewis et al., 2006; Lewis et al., 2007; Nichols et al., 2017). These computational models utilize the concepts of multibody dynamics and sets of mathematical equations to describe relative motion of the body segments and forces, both internally and externally, that are applied to the physical system (Hicks et al., 2015). Body segments are often overly simplified and treated as rigid vectors while joints are modeled after mechanical simple machines (ball and socket, hinge, etc.) (Dettwyler et al., 2004; Jastifer and Gustafson, 2014). For ease of modeling and calculation, the simplified musculoskeletal geometry follows a generic description except for special focus on the muscle and joints being specifically evaluated (Hicks et al., 2015). For example, when evaluating hip or knee rotations and reaction forces, the rest of the body including the torso and lower foot are defined as simply as possible. By reducing the body and relationship between the joints too much, the role and complex function of the segment as well as their contribution to the rest of the kinetic chain may be lost. In modeling the foot, the 26 separate bones are commonly treated as five or fewer segments, with most musculoskeletal models treating the lower leg segment as just the shank, the talus, and the foot (Brown et al., 2009; Carson et al., 2001; Dettwyler et al., 2004; Jenkyn and Nicol, 2007; Malaquias et al., 2017). With the foot represented as just a rigid segment, the complex motion is reduced to only foot progression angle and net plantarflexion/dorsiflexion (Carson et al., 2001). This is especially true when the joints of the hindfoot are simplified as well.

Quantitative assessments such as joint angles, joint moments, and muscle forces are all dependent on definition of joint origin location, axis orientation, and the degrees of freedom at

the joint (Lewis et al., 2009; Lewis et al., 2006). For this reason, musculoskeletal models need to be as realistic as possible for accurate estimations. However, the joint axes positions and orientations within the ankle complex have such high variability between subjects. This considerable variation may reduce the ability of generic models to accurately predict joint angles and moments (Lewis et al., 2006). Therefore, the utilization of subject-specific models that accurately represent the degrees of freedom and axes of rotation may be necessary in assessment of complex joints and complex, dynamic motions (Nichols et al., 2017).

Models that treat the foot as a rigid vector also simplify the rotations of the foot such that the talocrural and subtalar joints are often represented as 1 degree of freedom (DOF) hinge joints (Almonroeder et al., 2013; Delp et al., 1990; Nichols et al., 2016). Furthermore, in dynamic analysis the subtalar joint is often held "locked" in a neutral position, thus treating the two separate joints of the ankle as one (Almonroeder et al., 2013; Delp et al., 1990). One reasoning for this is that because certain motions, like cycling, walking, and running, are mostly completed in the sagittal plane, simplified two-dimensional models are deemed sufficient enough to be used to study joint coordination and energetics (Hicks et al., 2015). However, since normal subtalar joint motion is in three planes of motion, "locking" it from moving or limiting its degrees of freedom may add a real limitation in accurately modelling dynamic motion. Nichols et al. (2016) found that when comparing calculated joint angles of a model using 1 DOF at both the talocrural and subtalar joints vs 3 DOF each, the 1 DOF model did a better job at predicting talocrural joint angles for most rotations analyzed. Similar results were concluded in a study that found that an 8-DOF foot model resulted in more accurate kinematics when compared to a model with 15-DOF (Malaquias et al., 2017). It was found in both these studies that increasing the DOF within the model decreased the accuracy to predict motion. The added DOF may have increased the

complexity of the inverse kinematics problem and thus allowing for more errors in calculating a solution (Malaquias et al., 2017). While the higher DOF model decreased predictive accuracy in the talocrural joint calculations, neither the 1 DOF nor 3 DOF models were able to adequately predict subtalar joint motion during gait (Nichols et al., 2016). This inability to accurately predict joint motion may also come from uncertainty that comes from using skin-marker data to try to measure joint articulation in a laboratory setting (Andersen, 2018). Since the talus moves so freely during dynamic motion, it is almost impossible to accurately track without invasive bone pins (Arndt et al., 2004; Rockar, 1995). Instead, investigators use skin markers to define motion of the calcaneus relative to the tibia. However as mentioned, measuring the motion of the hindfoot makes it difficult to determine how much contribution of the total motion is from the talocrural and how much from the subtalar joint.

Recently there has been a shift from generic musculoskeletal models based off cadaveric studies and kinematic data collected from passive motion towards subject-specific models that yield higher anatomical accuracy and representation of joint axes of rotation (Andersen, 2018; Correa et al., 2011; Nichols et al., 2017). This is crucial as the high variability reported in subtalar joint axis location and inclination/deviation angles may result in substantial errors that reduce the ability of generic model to accurately predict joint motions and muscle moment arms (Lewis et al., 2009; Lewis et al., 2006). Nichols et al. (2017) compared calculated tibiotalar and subtalar joint kinematics when using subject-specific subtalar joint axes vs a generic model. It was concluded that the angle comparisons between generic and subject-specific models were significantly different for both joints, 12.9° ± 4.3° for the tibiotalar and 24.4° ± 5.9° subtalar axis. Though the differences were significant, incorporating the subject-specific axes into the biomechanical models did not considerably affect prediction of talocrural or subtalar joint

kinematics (Nichols et al., 2017). A limitation of this study is that the subject-specific axes orientations were calculated using talar morphology from *in vivo* CT scans while the generic axis used as a reference for comparison is based off passive joint motions collected *in vitro*. Since subtalar joint axis orientation varies greatly depending on foot position and loading conditions, comparison between methodologies may not be a fair representation. The findings of this study match previous validation studies conducted for the knee that show that patient specific geometry did not improve knee contact force predictions (Andersen, 2018; Correa et al., 2011). Together these show that, while more anatomically correct, the bone geometry in a model may not be as big of a component to joint calculations as the axis of rotation or surrounding tendons.

Musculoskeletal simulations allow for analysis of muscle and contact forces that cannot be easily obtained non-invasively, however in order for the models to be accepted on a wider scale they need to be appropriately validated (Andersen, 2018; Correa et al., 2011; Hicks et al., 2015). Direct validation comes from comparing the outputs to readily available *in vivo* measurement to prevent inaccurate calculations and conclusions to be drawn from biomechanical models (Ding et al., 2016). Validation becomes even more important when the generic model is altered to account for subject-specific consideration or when analyzing dynamic movements of non-healthy individuals (Correa et al., 2011). Examples of readily available measurements that can be used to validate models are joint range of motion (ROM) measures obtained from a goniometer and EMG signals to measure muscle activations. In recent years with the development of instrumented implants, models can now explicitly validate joint contact force while also indirectly validating the contributing muscle force that produced the articulating contact force (Andersen, 2018; Ding et al., 2016).

Through the direct comparisons using instrumented knee implants and skin-EMG, the accuracy of numerous models' estimation of contact force has been validated, many of which were accounting for subject-specificity or during various dynamic motions such as walking, bouncy gait, smooth gait, etc. (Andersen, 2018; Ding et al., 2016; Fregly et al., 2012; Hast and Piazza, 2013; Jung et al., 2016). However, there are currently no studies in which individuals with instrumented knee implants were asked to engage in more dynamic motion beyond gait and squatting (i.e. running). While there are no measures of the knee contact force during running, there are readily available EMG datasets that can be used to validate a model's muscle activity at various running speeds (Hamner and Delp, 2013). There has yet to be any comparisons between models validated for walking by using EMG and instrumented implant versus models using just EMG signals, like those used during running analysis. Similarly, to the author's knowledge, no studies have made any conclusions on the ankle and subtalar joint contact forces during dynamic motion as there are no instrumented implants for these joints. Since the lower kinetic chain is comprised of the knee, ankle, and foot, it is likely that if a model is sufficient enough to accurately evaluate knee contact forces then it is appropriate for ankle and subtalar joint contact force predictions (Chan and Rudins, 1994).

1.6 SPECIFIC AIMS

Overall: Determine a set of standards or suggested guidelines on how the subtalar joint should be defined in dynamic musculoskeletal models

Specific Aim 1: Determine how the subtalar joint axis origin location affects the ankle muscle functions and the effect this has on computed joint angles and moments.

Hypothesis 1: Moving the subtalar joint origin from the distal heel to an origin location closer to the talocrural joint will improve subtalar joint muscle moment arms and joint measures of kinematics, moments, and reaction force.

Specific Aim 2: Determine how the axis orientation of the subtalar joint affects the lower kinetic chain (i.e. subtalar, ankle, and knee) and if these changes are dependent on the complexity of motion (walking, running at 2 different speeds)

Hypothesis 2a: The model will be sensitive to changes of the subtalar joint orientation, no matter the origin location. The deviation angle will have a stronger effect compared to inclination angle on the joint measures for the knee, ankle, and subtalar joint.

Hypothesis 2b: The more complex the motion, the larger the significance of manipulating the subtalar joint orientation. Running at 5 m/s will result in larger peak values for all joints and measures than running at 2 m/s, followed by normal gait.

Specific Aim 3: Validate how well musculoskeletal models can predict muscle activation and joint contact force of various dynamic tasks (walking, running at 2 speeds) using EMG and instrumented knee to compare locked and unlocked subtalar joint conditions.

Hypothesis 3a: The musculoskeletal models used in this study will be validated for analysis of walking based on comparison to instrumented implant and EMG data. The EMG-to-activation of walking will be compared to matching EMG-to-activation patterns collected during running. If these produce similarly close results, the model will likely produce similarly accurate knee contact force estimates.

Hypothesis 3b: Locking the subtalar joint during dynamic analysis will significantly affect the muscle activation of the major ankle muscles as there is no motion that contributes to inversion/eversion.

CHAPTER 2: METHODS

2.1 EXPERIMENTAL DATA ACQUISITION

2.1.a. GRAND KNEE CHALLENGE

Introduced as a journal-based challenge in the American Society of Mechanical Engineers' *Journal of Biomechanical Engineering*, the 'Grand Challenge Competition to Predict in Vivo Knee Loads' (referred to as the Grand Knee Challenge (GKC) for the rest of the document) aims at advancing musculoskeletal modeling of the knee (Chen et al., 2016; Fregly et al., 2012). The goal of the competition is for researchers to use the openly available data to critically evaluate their model's ability to compute knee muscle and contact forces during dynamic motion and validate their results using data collected from patient with force-measuring knee implant (Fregly et al., 2012). The first challenge, released in 2010, provided 'competitors' with in vivo tibial contact force through the instrumented knee implant (eTibia), skin marker trajectory and ground reaction force from motion capture, EMG, muscle strength, as well as pre- and post-operative CT data (Fregly et al., 2012). The initial GKC included motion trials of normal gait and medial-lateral sway using a modified Cleveland Clinic marker set consisting of 43 dynamic markers and 12 static markers. In following iterations of the challenge, with a total of 6 taking place between 2010-2016, the available data for investigators to modify their models has increased to include: instrumented knee contact torque, X-ray data MR data , as well as implant-bone geometry of femur, patella, tibia/fibula, talus, calcaneus, midfoot, metatarsals, and phalanges (Kinney et al., 2013). Motivated by determining accuracy of realistic day-to-day motion, the variety of dynamic motions measured has also opened up to include: walking pole, medial thrust, bouncy, smooth, crouch, forefoot-strike, long walking pole , treadmill gait, slow and turning gait (Fregly et al., 2012; Kinney et al., 2013).

2.1.b. RUNNING DATASET

Openly available data encourages collaborative effort and advancement in musculoskeletal modeling. There has been a rising trend in the biomechanical and musculoskeletal modeling community towards open- or shared access to information; not just in sharing the results but in the data, models, scripts, analysis being completed by researchers in the community (SimTK). Through project-hosting platforms such as SimTK, there is a growing repository of datasets including: walking, running, instrumented prostheses, upper limb, energetics, etc. (SimTK). One such dataset made available comes from a study on muscle contribution to the body at various speeds of running (Hamner and Delp, 2013). Unlike the GKC that specifically provided data for others to run the analysis and validation, Hamner and Delp (2013) collected and analyzed their data as a part of their own study and chose to make the datasets available to the public. The repository contains experimental data (marker position, ground reaction force, muscle EMG) for 10 subjects running at multiple speeds ranging from 2-5 m/s. Provided along with the collected experimental data are subject-specific models that were created and scaled based on a custom 54 retroreflective marker-set. The dataset also has computed results from their analysis of joint angles, joint moments, as well as other muscle-driven simulations across the different speeds of running (Hamner and Delp, 2013).

2.2 MODELING

2.2.a. MODEL DEFINITION

OpenSim (SimTK, Stanford, CA) is an open-source computational musculoskeletal modeling software, first developed by Delp et al (1990), that provides the framework for

dynamic musculoskeletal computation and simulation based on multi-body dynamics and resolving of mathematical equations (Almonroeder et al., 2013; Delp et al., 1990). Researchers use the models created in OpenSim to then study the effects of musculoskeletal geometries, joint motion, and muscle-tendon properties on the calculated muscle and joint forces and moments in dynamic conditions (Maheshwari, 2014). One such model that is most commonly referenced and utilized for computation in OpenSim is the default Gait2392 lower-extremity model.

Bones: In the software, OpenSim, bones are represented as rigid segments fitted with polygons to define the bony surface (Delp et al., 1990; Irmischer, 2017). Each segment contains mass properties that can then be scaled according to a subject's height/weight, otherwise known as their anthropometric data. The Gait2392 model is made up of rigid segments defining the pelvis, as well as bi-lateral definitions of the femur, patella, tibia, talus, calcaneus, and toes. as stated before, polygon mesh is used to define the bony surface of the pelvis and femur segments (Delp et al., 1990). Shank and the distal foot segments structures are adopted using computer fitting technique as established by Stredney et al.(1985).

Muscles: One of the elements of the body geometry that can be affected in scaling is the insertion or attachment of any muscle-tendon units that are defined to that body (Irmischer, 2017). Muscles span across bodies to generate forces that, in turn, result in joint motion (Maheshwari, 2014). In OpenSim, muscles are listed as specialized force element whose function and muscle path can generally be defined as a straight-line from origin to insertion (Delp et al., 1990; Irmischer, 2017). There are some specific instances, like when muscles wrap over bones, in which case the "wrapping points" are represented by way of intermediate via points (Delp et al., 1990). In the default Gait2392 model, this is best scene for the quadricep tendons, where additional insertion points are added for knee-flexion angles that exceed 80°. For the muscles of

the ankle and subtalar joint, they are all represented as simple line segments with function based on relation of anatomical landmarks found on bone surfaces to joint axes.

Joints: Lastly, the joint definition in OpenSim specifies the relation of movement between two bony rigid body segments. This joint motion is represented a function of 6 possible DOF of transformation, 3 for rotation and 3 for translation, and this defines the 'child' segment motion with respect to the 'parent' segment (Irmischer, 2017). The Gait2392 lower extremity model has 23 total DOF spread across the pelvis, as well as right and left: hip, knee, patellofemoral, ankle, subtalar, and metatarsophalangeal joints. The hip joints are represented by 3-DOF ball-and-socket joints while the knee joint follows definition by Yamaguchi and Zajac (1989) which simplifies the interaction of femur, patella, and tibia as just 1 DOF. And finally, the ankle, subtalar, and mtp are all modeled as frictionless revolute joints (in other words, 1 DOF each) with location and orientation matching descriptions provided by Isman and Inman (1969) (Delp et al., 1990; Isman and Inman, 1969).

2.2.b. SCALING

It is the responsibility of researchers to understand the how the elements of a models are defined as well the underlying equations and processes of analysis that are necessary to provide realistic human motion estimates (Hicks et al., 2015; Irmischer, 2017). Scaling is important, even when using a generic model, as it better accounts for the anthropometric differences that exist person to person (Hicks et al., 2015). During scaling, the subject-specific weight of each person is used to adjust the mass properties of the model. In this study, this was especially important as the models used were simplified to the pelvis and lower extremities; therefore, the models were scaled to the relative mass and inertial properties of the included body segments. Additionally, the dimensions of the bodily segments were scaled based on the distance between

marker locations obtained during static trial. With the body segment properties changing based on anthropometric height and weight, so do the properties of the elements that attach to these segments, specifically the force generating properties and muscle-tendon attachments (Correa et al., 2011; Hast and Piazza, 2013).

2.2.c. INVERSE KINEMATICS

The next step in modelling the effect of subtalar joint orientation during normal gait and running is to determine the joint angles of the knee, ankle, and subtalar joint throughout stance for each condition. This is done by using OpenSim's toolbox to compute the inverse kinematics (IK) of these joints (Hast and Piazza, 2013). For each time frame, the scaled model uses experimentally collected marker trajectory data to come up with a "best fit" coordinate or pose. The aim is to minimize the residuals, or the sum of weighted squared errors, between the experimental markers and best-fit coordinate. The best-fit pose at the end gives experimental coordinate values, or angles, for all joints being evaluated in the model.

2.2.d. INVERSE DYNAMICS

The motion of each joint comes from the interaction of the muscles, ligaments, as well any internal and external forces. To estimate the net loads (forces and torques) that are being applied to the system that cause the specific motion, inverse dynamics (ID) analysis is used (Hicks et al., 2015; Walter et al., 2015). OpenSim's inverse dynamics tool takes the scaled model, motion from the generalized coordinates, as well as external load (like ground reaction force) into consideration to calculate the net forces and torques (i.e. moment) at each joint using the classical mechanical concept of Newton's 2nd Law: F=ma. The net joint torques, especially for the subtalar joint, are especially sensitive to change in this study as they are dependent on both axis location and orientation for their calculations (Lewis et al., 2006).

2.2.e. STATIC OPTIMIZATION

When analyzing human motion, optimization (static or dynamic) is often used to simulate the recruitment of muscles to estimate individual muscle forces (Irmischer, 2017). Static optimization (SO) uses the inverse-dynamics based simulations of net joint moments to resolve the muscle redundancy problem (Andersen, 2018). In other words, since there are multiple muscle excitation patterns that can be used to solve for the input kinematics, an optimization criteria is established to minimize the weighted sum of squared muscle activations (Almonroeder et al., 2013). The products of static optimization include muscle activations, forces, and controls. Since muscle forces are one of the largest factors in joint contact force estimation, it is important for these individual muscle predictions to be as accurate as possible (Andersen, 2018).

2.2.f. JOINT REACTION ANALYSIS

Similar to inverse dynamics, joint reaction (JR) analysis computes the resultant forces and moments at a joint. However, this analysis goes beyond the output of inverse dynamics as it takes into consideration forces and moments transferred between consecutive bodies (i.e. other joints) as well as the forces acting upon the joint due to muscle activations that were computed through static optimization.

2.3 DATA PROCESSING

The objective of this dissertation was to evaluate how changes to subtalar joint axis characterization affects musculoskeletal model's ability to produce joint measures for the whole lower kinetic chain (knee, ankle, subtalar joint) and to determine a guideline of how the subtalar joint should be defined during dynamic simulations. This was done by (1) determining how the STJ origin location affects muscle function of the muscles surrounding the ankle joint complex,

(2) evaluating how STJ inclination/deviation angles affect kinematics, kinetics, and joint contact forces for the lower limb during dynamic movement, and (3) validating how well musculoskeletal models can account for differences in subtalar joint orientations.

Experimental data for this study was obtained from two open-source datasets made available to researchers. To evaluate how changes to subtalar joint axis definition affects musculoskeletal model in normal gait tasks, overground walking data was obtained from the 3rd, 4th, and 6th competition of the GKC (Fregly et al., 2012). Subjects in this study were fitted with an instrumented implant that either comprised of four uniaxial force transducers with knee force resulting in the sum of 4 sensors or a 6-axis load cell that outputs knee force as coordinates (Fx, Fy, Fz) (Fregly et al., 2012; Knarr and Higginson, 2015). Along with the in vivo knee loads acquired from the instrumented implant (eTibia), marker trajectory, ground reaction force (GRFs), and surface EMG data were obtained from the GKC dataset for three trials of normal gait for each subject.

OpenSim (SimTK, Stanford, CA, v3.3) was used to analyze the effect of subtalar joint definition on musculoskeletal simulation. For normal gait, the Lai full-body model was adjusted to reflect the pelvis and instrumented lower limb (left limb for 3rd, and right for 4th and 6th competition) (Lai et al., 2017). This results in a 13 DOF model with 40 Hill-type contractile elements. For all simulations, the metatarsophalangeal (mtp) joint is kept locked while the subtalar joint is kept unlocked unless specifically noted otherwise; all other joints are unlocked during analysis. Using anthropometric data including height, weight, and relative distances between skin markers & anatomical landmarks in static trials, the adjusted-Lai model is scaled in OpenSim to create subject-specific models.

The default ankle and subtalar joint axis definition in the Lai model matches that as first established by Delp et al (1990) (Delp et al., 1990; Lai et al., 2017). This coordinate system axis has its origin location found at the most disto-lateral aspect of the calcaneus with orientation of the axis pointing up and inward through the talus with inclination and deviation angles of 37.2° and 8.7°, respectively. This represents the default subtalar joint axis model, 'Delp-Heel'. To evaluate how changes to subtalar joint axis origin location affect the models, the location of the joint in OpenSim is adjusted such that the origin is [0, 0, 0] in the parent-body, which is the talus. This results in the new origin location being incident with the ankle joint axis, or in between the malleoli of the ankle. When referring to models with this new origin location, they will be denoted by '-Ankle' suffix.

In the Lai model, the orientation of the joints is in reference to the child body reference frame and is expressed in Euler XYZ body-fixed rotation angles (Lai et al., 2017). To evaluate how much the inclination and deviation angles separately affect joint measures, the STJ orientations are modified to reflect the inclination or deviation angles when taken to their maximum/minimum values as defined by Isman and Inman (1969) while keeping the other at the default found in Lai et al (2017). Table 2-1 below shows the subtalar joint orientations and their respective inclination/deviation angles manipulated to their respective max/min as well as Isman and Inman's (1969) mean values compared to the Delp orientation. In total there are 12 models: 2 axes origin locations x 6 subtalar joint axis orientations.

	Delp	IncMin	IncMax	DevMin	DevMax	Inman
Inclination	37.2°	21°	69°	37.2°	37.2°	42°
Deviation	8.7°	8.7°	8.7°	4°	47°	23°

Table 2-1: Subtalar joint orientation models used during analysis of walking and their respective inclination and deviation angles

Similar to normal walking data, a dataset of running at various speeds was obtained through open-access resources (Hamner and Delp, 2013; SimTK). Of the 10 male subjects provided in the data, 3 were chosen for analysis and comparison. The data included skin marker trajectory, ground reaction force, and EMG signals of running at speeds of 2 m/s, 3 m/s, 4 m/s, and 5 m/s (Hamner and Delp, 2013). To determine the effect of subtalar joint axis definition in relation to speed, the slowest (2 m/s) and fastest (5 m/s) speeds were chosen for evaluation. Also included in the dataset were pre-established subject-specific models for each participant. The models created by Hamner and Delp (2013) also include just the pelvis and one lower limb and closely follow the body and joint definitions as described by Delp et al (1990). The major differences between the Hamner and Lai models include: a lack of patellofemoral joint in the Hamner model, the amount of muscle-tendon units included (43 vs 40, respectively), as well as passive muscle properties introduced in the Lai model (Hamner and Delp, 2013; Lai et al., 2017).

With the already created subject-specific models for the three subjects, the same process of manipulating the subtalar joint axis definition was followed. The only difference is that instead of comparing maximum and minimum inclination/deviation angles, the Delp and Inman orientations were compared to helical axis estimates gathered from in vivo weight-bearing CT (Fernandez et al., 2020). The table (Table 2-2) below shows the subtalar joint orientations

analyzed for running tasks as well as the conditions of the study in which they were determined. In total there are 6 models created to analyze running: 2 origin locations X 3 axis orientations.

	Delp	Inman	CT
	mathematical	*In vitro*, non-weightbearing	*In vivo*, weightbearing
Inclination	37.2°	42°	43°
Deviation	8.7°	23°	6°

Table 2-2: Subtalar joint orientation models used during analysis of running at 2 m/s and 5 m/s with their respective inclination/deviation angles as well as technique of how the orientations were estimated.

2.4 DATA ANALYSIS

Using a custom-MATLAB code (MathWorks, Natick, MA, USA, R2019b) and OpenSim analysis toolbox, the scaled and adjusted models for each subject (from both the GKC and Running datasets) and the marker trajectory data are used as input to solve the inverse kinematics problem. This computes the generalized model joint coordinates for each time frame of the entire trial. Following IK, inverse dynamics is performed using the measured GRF and calculated joint angles as input. From this analysis, the net joint torques are determined. The next step is to compute muscle activation and force histories through the process of static optimization. For this analysis, the optimization criteria are such that the weighted sum of squared muscle activations was minimized. Knee, ankle, and subtalar joint forces are then calculated through joint reaction analysis. These represent the sum of internal and external loads applied to the body, which include loads from other joints as well as estimated muscle forces that were produced during static optimization analysis. Since all of these measures are computed for each time frame over

the entire trial, the MATLAB code uses the measured GRF to determine the timing of stance phase for the lower limb. From there, the stance phase is normalized to 100 points to be able to easily compare between trials and subjects as a percent of stance phase.

For normal gait using data from the GKC, the analysis is completed for each of the three walking trials. These are then averaged together after normalized to 100 points to produce one curve for the joint angles, moments, muscle activations, and contact forces. Only one trial was analyzed per running speed in the running data to analyze joint measures, however the average of three cycles was taken to account for any variability between stance cycles.

2.5 VALIDATION/STATISTICS

Evaluating the validity of musculoskeletal models, especially after adjusting for subject-specific considerations, is an important part of answering research or clinical questions and prevents the chances of erroneous conclusions (Hicks et al., 2015). When possible, it is best to validate results based on direct comparison with simultaneously collected experimental data. Thanks to the inclusion of measured instrumented knee loads (GKC) and EMG data (GKC and Running datasets), the results of knee joint contact force and muscle forces can be compared.

The instrumented knee implant (eTibia) loads measured during normal walking are compared to computed knee joint contact forces for each Lai subtalar joint axis model that was created. Validation and statistical significance is determined by calculating Root Mean Square Error (RMSE) and correlation between the *in vivo* load and computed values. RMSE is calculated by taking the square root of the squared sum of differences between estimated and predicted values. The closer the value is to 0, the smaller the error between observed and estimated. Another measure to determine validity is Pearson's correlation coefficient. This gives

a value falling between –1 to +1 where the closer to 1 the correlation factor is, the stronger a positive relationship between measured and calculated values. While the RMSE gives an indication of how close the values are, the correlation represents the similarity in shape or pattern of the curves, not necessarily the values themselves.

To compare muscle action during dynamic task, of both walking and running (2 m/s and 5 m/s), the modeled muscle activation can be indirectly compared to EMG signals. EMG's allow for noninvasive measurement of muscle force during a dynamic motion, but are often unreliable or cannot fully measure muscle activations, especially for deeper or covered muscles (Anderson and Pandy, 2001; Meyer et al., 2013). Since they are difficult to normalize, there is no direct way of comparing to computed muscle activations but they still give a good agreement when analyzing onset/offset and pattern of excitation (Hicks et al., 2015). There have been suggested guidelines for how to classify correlation values. Walter gave determinations based on score with: poor (0.0-0.5), moderate (0.5-0.7), good (0.7-0.9), or strong (0.9-1.0) (Andersen, 2018; Walter et al., 2015).

Where *in vivo* measures are not available (joint rotations, moments, etc.), the effect of changing the subtalar joint origin location and axis orientation is analyzed by using the default Delp axis definition used in both Lai and Hamner models as the 'standard'. Using statistical software, SPSS (IBM Corp, Armonk, NY, V27), Student's two-tailed paired t-tests are performed for each STJ axis and orientation model against the 'standard' with significance set at $p < 0.05$. Paired t-tests are used to compare peak discrete variables from each of the analyses during stance phase,

CHAPTER 3: THE EFFECT OF SUBTALAR JOINT AXIS LOCATION ON MUSCLE MOMENT ARMS

3.1 INTRODUCTION

Musculoskeletal models are used to analyze dynamic motion and are built by simplifying the definitions of bones, muscles, and joints into a generic kinematic model (Nichols et al., 2017). While generic models make computing inverse and forward dynamics easy, more subject-specific consideration may be necessary in modeling complex joint motion. The talocrural and subtalar joint (STJ) provide primary dorsiflexion/plantarflexion and inversion/eversion during gait, respectively, with the subtalar joint being the biggest contributor to load acceptance leading to stance phase (Lundberg and Svensson, 1993). However, frequently the subtalar joint is overlooked in biomechanical models by "locking" the joint during analysis therefore treating the two separate joints as one joint complex that rotates about the intermalleolar axis.

Even when left "unlocked", the subtalar joint's tri-planar rotation is simplified to a 1-DOF rotation about a generic axis. However, when comparing numerous *in vitro, in vivo*, weightbearing, and non-weightbearing studies there is still much disagreement concerning how the subtalar joint axis should be defined (Arndt et al., 2004; Fernandez et al., 2020; Lundberg and Svensson, 1993; Manter, 1941; Sheehan et al., 2007). The most common STJ coordinate system (orientation and location) referenced in literature is that by Isman and Inman (1969). According to Isman and Inman (1969), the subtalar joint orientation can be defined by an oblique axis of rotation with an inclination angle, measured from the horizontal plane, ranging from 68.5-20.5˚ (mean 42˚) and a deviation angle, measured from the midline of the foot, that ranges 4-47° (mean 23°). When defining this joint in musculoskeletal models, like in the commonly used OpenSim Gait2392 model (Delp et al., 1990), the subtalar joint is treated as a 1 DOF joint

with the oblique axes' inclination and deviation angles set at 37.2° and 8.7°, respectively (Delp et al., 1990). While the default subtalar joint axis values used in the Gait2392 model lie within Isman and Inman's (1969) range as stated by Delp et al. (1990), these values are much lower than the averages reported by Isman and Inman (1969).

Furthermore, the Delp model has the location of the subtalar joint axis origin based at the most distal part of the calcaneus. This is based off studies that have found the subtalar joint axis to run from the talus down, back, and outward through the lateral aspect of the heel (Fernandez et al., 2020; Wright et al., 1964). While to the author's knowledge there have been no subtalar joint specific standards, the ISB standards for ankle joint recommend that the calcaneus coordinate system origin should be coincident with that of the ankle, i.e. midway between the two malleoli of the talus, and not the heel of the foot (Wu et al., 2002). With the large spread of subtalar joint orientations, the origin location could affect how and where the axis crosses through the talus.

The choice in coordinate system location (i.e., origin location) and orientation can affect joint analyses such as inverse kinematics, inverse dynamics, joint loads, and muscle moment arm calculations (Nichols et al., 2017). A muscle's moment arm defines its action as well as can be used to determine the muscle's effectiveness at exerting force on a particular joint (McCullough et al., 2011; Sherman et al., 2013). The location of a muscle's insertion relative to the joint axis determines the muscle function (plantarflexor, dorsiflexor, everter, inverter) while the distance away from the axis affects the amount of force that the muscle can producing an action (Lewis et al., 2006; Rockar, 1995). The main ankle muscles that contribute to balance and control of the foot are : Extensor Hallucis Longus (EHL), Extensor Digitorum Longus (EDL), Tibialis Anterior (TA), Tibialis Posterior (TB), Flexor Digitorum Longus (FDL), Flexor Hallucis Longus (FHL),

Peroneus Longus (PL), Peroneus Brevis (PB), and the Achilles Tendon (aka Triceps Surae) which can be broken down into, Gastrocnemius and Soleus (Delp et al., 1990). The action of each muscle can be determined anatomically by tendon insertion (Figure 3-1). Muscles that insert posterior to the talocrural joint are plantarflexors, while dorsiflexors are anterior to the axis. Similarly, muscles that insert medially on the foot are considered invertors while those found lateral to the subtalar joint are evertors (Table 3-1).

It is unknown how changes to the subtalar joint's coordinate system will affect the moment arms and thus function of the muscles. The purpose of this study was to determine how the subtalar joint origin location and axis orientation definitions affect the muscle moment arms of the ankle/subtalar joint throughout subtalar joint range of motion.

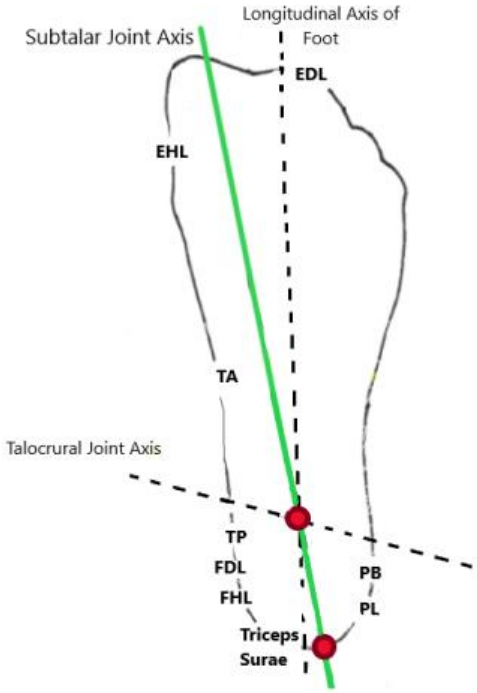

Figure 3-1: Muscle tendon insertions relative to talocrural and subtalar joint axes

Function on the Ankle	Muscles that contribute to the action
Plantarflexor	FDL, FHL, AT, PB, PL, TB
Dorsiflexor	EDL, EHL, TA
Invertor	EHL, FDL, FHL, TA, TB
Evertor	EDL, PB, PL

Table 3-1: Ankle function groups and the muscles that provide action for that motion

3.2 METHODS

Subject marker position and anthropometric data were obtained from three separate competitions (3rd, 4th, and 6th) of the open-source GKC (Fregly et al., 2012). The GKC used a modified Cleveland Clinic marker set to define body segments lengths and track motions during self-selected speeds of walking. These were imported into OpenSim (v3.3) to scale and adjust a full-body musculoskeletal model (Lai et al., 2017) to just include the pelvis and lower instrumented limb (right limb for 4^{th} and 6^{th}, left limb for 3^{rd}). To evaluate the effect of subtalar joint orientation and origin location on subtalar joint muscle moment arms - two models each, one per location, were created using the scaled Lai model with the default Delp STJ orientation and the Inman STJ orientation. The modelled combinations are as follows: 1) Delp STJ axis orientation at talocrural joint (Delp-Ankle), 2) Delp STJ axis orientation at distal calcaneus (Delp-Heel), 3) Inman STJ axis orientation at talocrural joint (Inman-Ankle), and 4) Inman STJ axis orientation at distal calcaneus (Inman-Heel), respectively. Using OpenSim's

GUI toolbox for analysis, the muscle moment arms vs subtalar joint angle were plotted for each of the four model variations (Delp - Heel, Delp - Ankle, Inman - Heel, and Inman - Ankle) for 8 muscles that act on the subtalar joint [EDL, EHL, FDL, FHL, PerBrev, PerLong, TibAnt, TibPost]. The muscle moment arms were analyzed from -20 to +20 degrees of subtalar joint angle as this represents the average subtalar joint range of motion and matches previous muscle moment arm studies (Klein et al., 1996; McCullough et al., 2011; Spoor et al., 1990). Muscle moment arm values were compared to measurements completed *in vitro* (Klein et al., 1996) of five key muscles: the FHL, TibAnt, TibPost, PerBrev, PerLong. Mean moment arm values were determined to be significantly different if they fall outside 2 standard deviations of the *in vitro* measured mean as this would fall outside range of replicable human values (Hicks et al., 2015).

Marker trajectory and ground reaction force obtained from the GKC datasets of normal gait were used to analyze how the changes due to STJ axis orientation and axis location affect the joint angles and moments of the lower kinetic chain (subtalar, ankle, and knee joints). Statistical significance was determined using two-tailed paired t-tests with the default Delp-Heel model used as the ‘standard’ by which to compare against.
Significance set at $p<0.05$.

3.3 RESULTS

3.3a INFLUENCE OF JOINT ORIENTATION

When comparing the muscle moment arms after modifying the subtalar joint axis orientation alone (Delp - Heel vs Inman - Heel), the Inman orientation produces larger muscle moment arm values (Table 3-2) for all muscles that were analyzed. The largest difference in

mean moment arm values is for the Tibialis Anterior which has an average moment arm of -9.49 mm in the Delp - Heel model while Inman - Heel gives an average moment arm of 13.05 mm (note: negative values indicate inversion moment, positive indicates eversion). Now considering the relation between orientations with the adjusted origin location, both Delp axis orientation models (Delp - Heel, Delp - Ankle) report muscle moment arms that fall within 2 standard deviations of the *in vitro* mean moment arms for all five of the muscles (FHL, TibAnt, TibPost, PerBrev, and PerLong) as reported by Klein et al (Klein et al., 1996). The Inman - Heel STJ axis model also has the FHL and PerLong moment arms calculated to fall within 2 std deviation, however, with the Ankle origin location, the Inman orientation model has the PerBrev, TibPost, and TibAnt all producing muscle moment arm values that are outside of the 2 std deviation range (Figure 3-2).

Table 3-2: Average muscle moment arm values with standard deviation for each muscle for the axis orientation (Delp/Inman) and origin location (Heel/Ankle) combinations. Averages from Klein et al. compared for muscles with available values.

		PerLong		PerBrev		TibAnt		TibPost		FHL		EDL		EHL		FDL	
		avg	std	avg	std	avg	std	avg	std	avg	std	avg	std	avg	std	avg	std
Klein et al		21.8	4.3	20.5	3.9	-3.8	4.4	-19.2	3.6	-7.8	3	---	---	---	---	---	---
Delp	Ankle	25.03	1.22	26.56	0.96	-8.8	0.29	-17.6	1.16	-14.59	0.79	15.82	0.5	0.6	0.02	-17.02	1.02
	Heel	26.05	0.93	27.61	1.18	-9.49	0.26	-18.17	1.42	-15.55	1	15.46	0.49	-0.54	0.12	-17.92	1.28
Inman	Ankle	21.72	1.03	24.46	0.89	1	0.03	-16.68	1.1	-15.49	0.84	21.54	0.69	9.26	0.29	-16.19	0.97
	Heel	31.24	1.72	33.95	1.36	13.05	1.32	-7.33	0.24	-5.21	0.17	33.07	1.42	21.49	1.52	-5.99	0.2

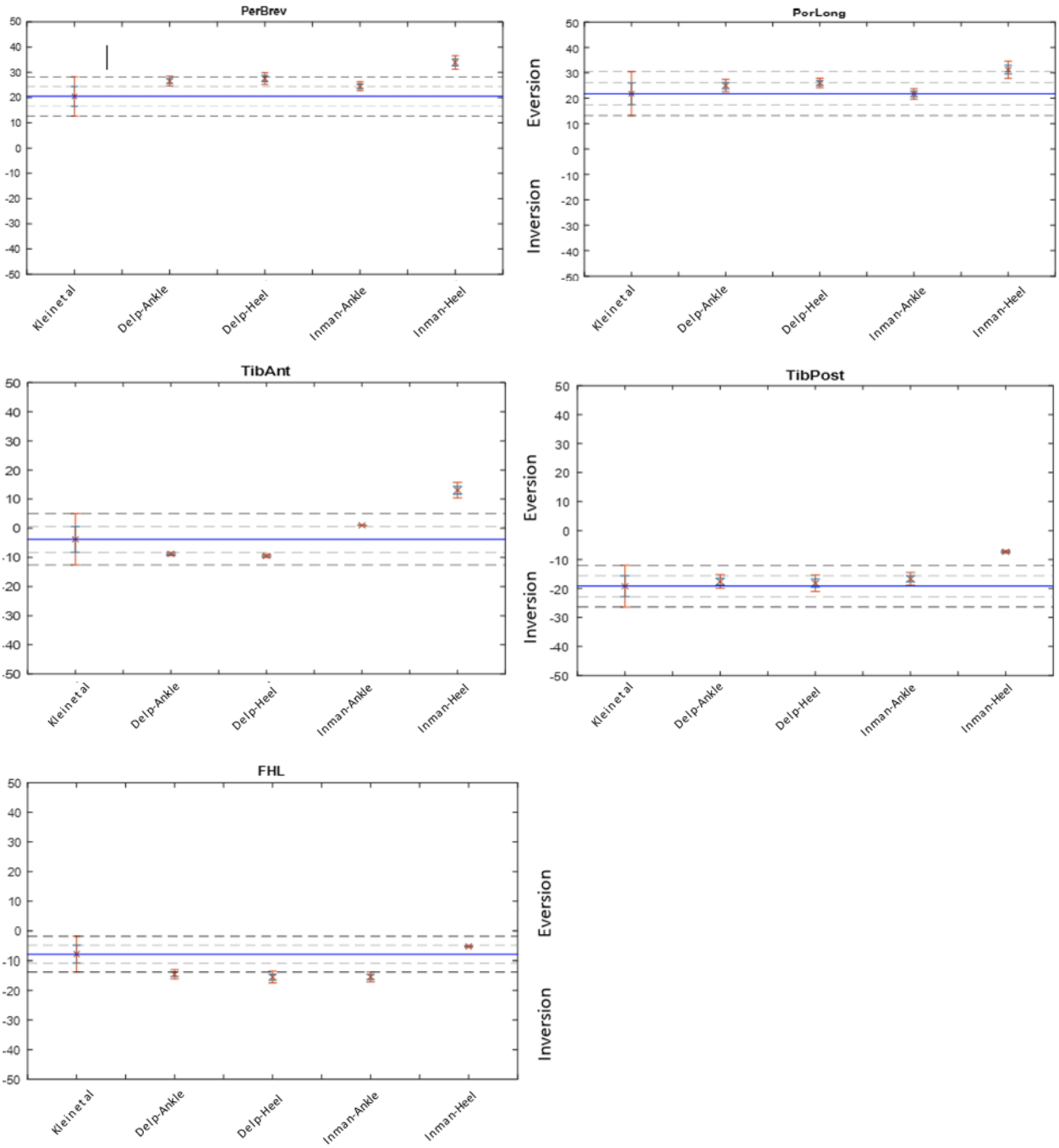

Figure 3-2: Comparison between the Klein et al. average muscle moment arm (blue line) and the subtalar joint location/orientation combinations. Pale dotted line indicates 1std away from Klein average, and black dotted line indicates 2std. Muscles with comparison include: (a) PerBrev, (b) PerLong, (c) TibAnt, (d) TibPost, and (e) FHL.

The joint angles show no significant differences for any of the joints (knee, ankle, or subtalar joint) between subtalar joint orientations, both in the default heel location and with the origin at the ankle. The models did significantly vary in peak subtalar joint moment predictions between Delp and Inman orientations, both with the heel (p=0.02) and ankle (p=0.03) origin locations. In both cases, the Inman orientations produced much larger moments, with maximum values reaching just under .6 N*m/BW (Figure 3-3). This is in comparison to the Delp orientation models that both produce similar subtalar joint moments that reach a maximum value closer to only .25 N*m/BW.

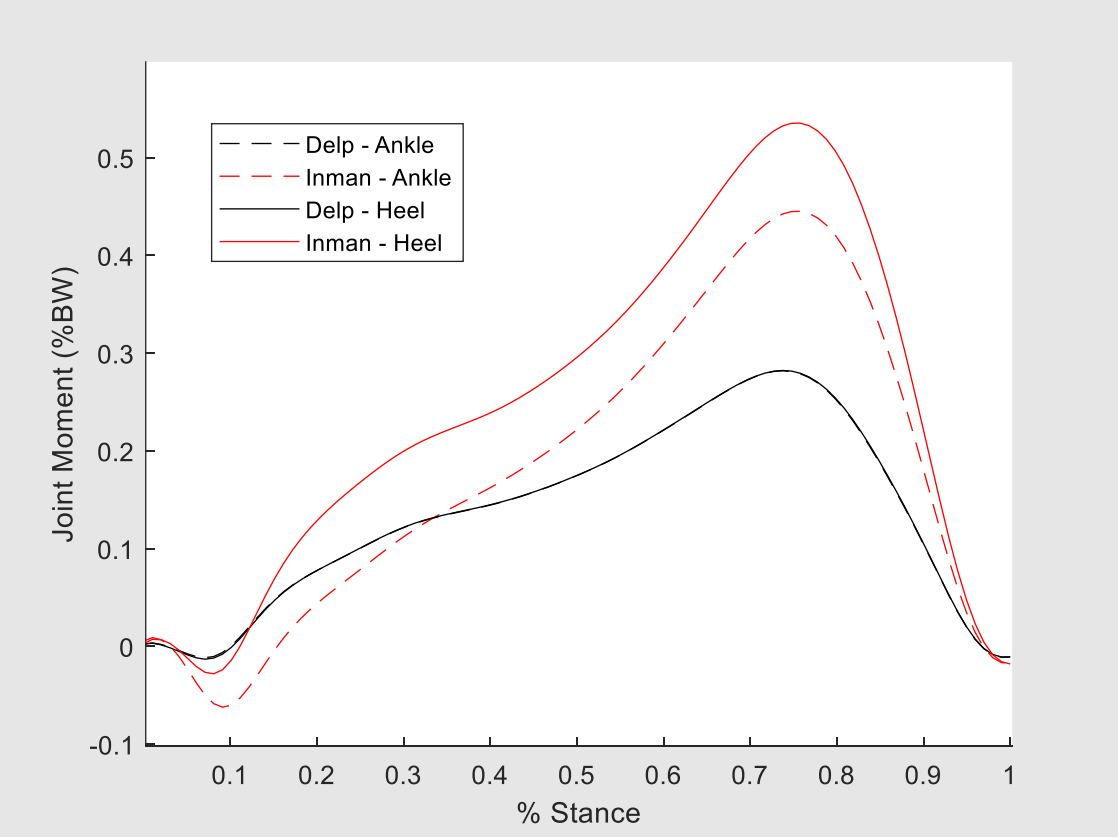

Figure 3-3: Subtalar joint moment comparison of the subtalar joint axis definition models.

3.3b INFLUENCE OF JOINT ORIGIN LOCATION

Unlike in the Delp models, which were very similar in results not depending on location, modifying the location of the origin to get the Inman-Ankle model, resulted in muscle moment arms that fall within the 2 std deviation range established before for the five muscles previously mentioned. This shows that compared to changes in subtalar joint axis orientation, the effect of moving the origin location was more variable. When the default Delp orientation was used, shifting the origin location resulted in slightly less extreme invertor/evertor moment values, seen by the average muscle moment arms (Table 3-2). By setting the origin location at the Ankle, the Delp orientation resulted in values that were closer to zero, though the differences seen between Heel and Ankle origin locations were minimal. However, the differences in muscle moment arms due to origin location were significant when the Inman orientation was implemented. For many of the muscles, the new origin location (Ankle) resulted in moments arms that more closely matched those calculated from the Delp models. This can be seen in the Tibialis Posterior muscle (Figure 3-4a), where the Delp-Ankle, Delp-Heel, and Inman-Ankle models all seem to overlap while the Inman-Ankle model has a more positive moment arm. The Tibialis Anterior (Figure 3-4b) however, did not return values that closely matched with either Delp model when the Ankle origin location was set for the Inman STJ orientation model. Instead, the Inman-Ankle Tibialis Anterior muscle moment arm is somewhere in between that of Inman-Heel and the Delp models (-Heel and -Ankle). When comparing these calculated mean moment arms to *in vitro* measurements, the Inman-Ankle model more closely matches the Delp models as well as the Klein et al. (1996) mean values (Klein et al., 1996). After changing the origin location to being in line with the ankle, the Inman axis orientation model no longer results in values that fall

outside of the 2std dev range as reported by Klein et al. (1996) for the same five muscles (TibAnt, TibPost, PerLong, PerBrev, FHL) (Figure 3-2).

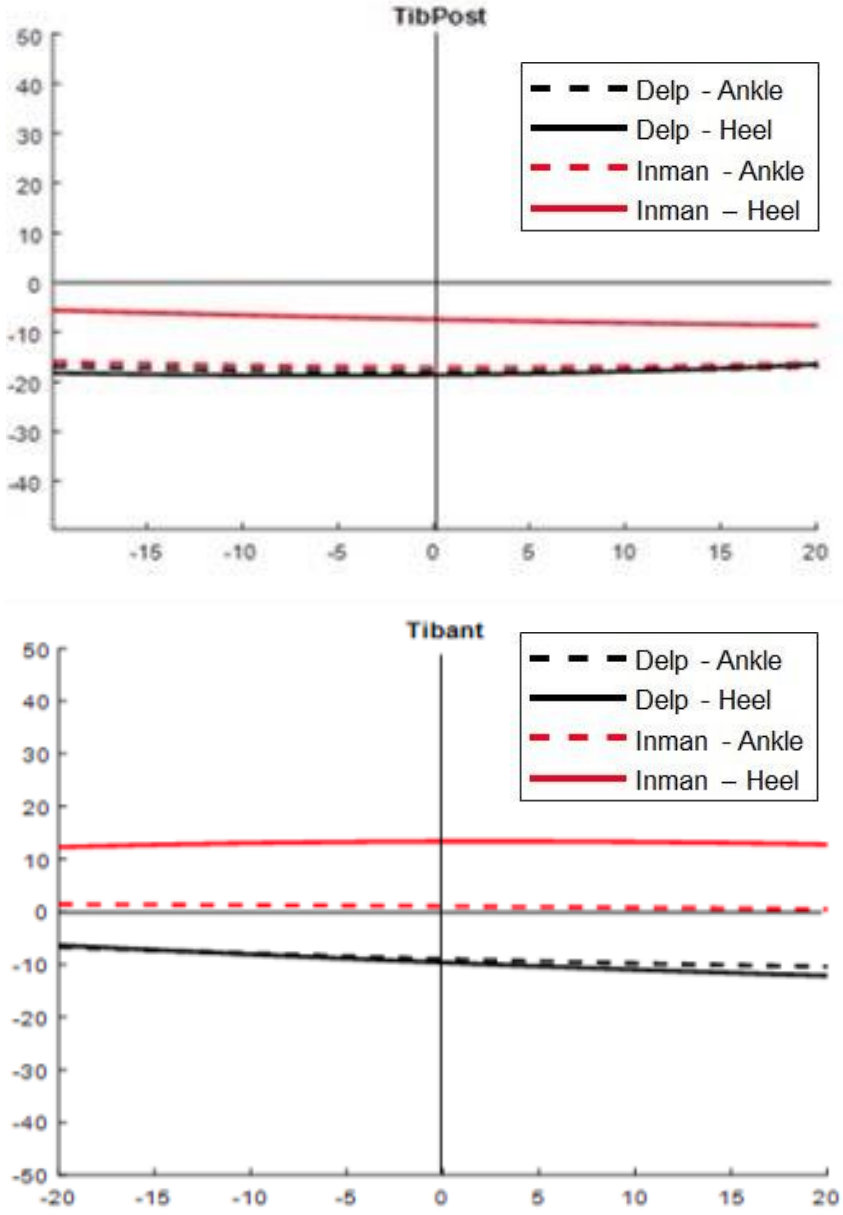

Figure 3-4: Muscle moment arm comparisons of the (a) Tibialis Posterior and (b) Tibialis Anterior. Convention of sign for the muscle moment arms for the subtalar joint are such that positive indicates an eversion moment, while negative indicates an inversion moment.

Similar to the muscle moment arms being similar between Delp orientation models even when the origin location was adjusted, the joint kinematics and joint moments for all the joints of the lower extremity show little to no differences. However, there were significant differences seen in subtalar joint moments between Inman orientation models (Figure 3-3). By moving the origin location from the heel to the ankle, the subtalar joint moment significantly decreased ($p=0.01$).

3.4 DISCUSSION

The purpose of this study was to establish the effect that both factors of joint definition, origin location and axis orientation, have on muscle moment arms of the subtalar joint as well as the effect these changes have on the prediction of joint angles and moments of the knee, ankle, and subtalar joint. Moving the subtalar joint axis origin location from the Heel (distal calcaneus) to the Ankle (talocrural joint) resulted in less extreme invertor/evertor moment arms for all the muscles that cross the subtalar joint for the Delp orientation. These differences however are not significant. This is likely because the axis of rotation for the Heel location extends through the talus and intersects with where the Ankle location origin is. Thus, the STJ axes are coincident, despite the difference in their origin locations (Figure 3-5a). The slight differences in muscle moment arms may be a result of the ~.06 m large differences in joint origin location. The knee, ankle, and subtalar joint angles and moments between Delp-Heel and Delp-Ankle model produce similar results further highlighting that the two axes are practically the same. For this reason, it may be sufficient to keep the origin location at the distal heel when using the Delp orientation.

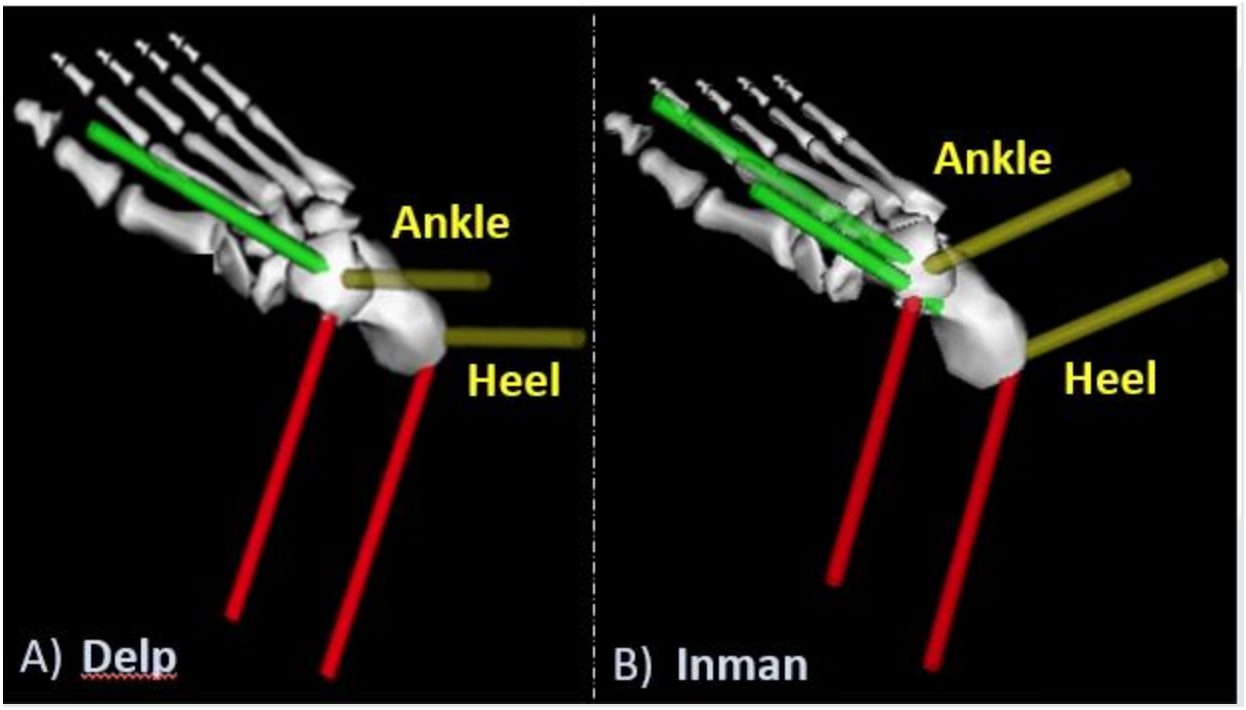

Figure 3-5: A comparison of how subtalar joint orientation affects the axis along which 1DOF rotation of STJ occurs (green). OpenSim Lai model with overlapped distal calcaneus location (Heel) and talocrural joint origin location (Ankle) with (A) OpenSim's default STJ orientation (Delp) at both locations and (B) Inman orientation at both locations.

This study shows that if the STJ axis orientation is modified, the origin location should be considered first. When defining the STJ orientation based on Inman's mean inclination/deviation angles, the origin location dramatically influenced how the 1 DOF rotational axis crosses through the talus (Figure 3-5b) (Delp et al., 1990; Isman and Inman, 1969). The axis of rotation between the Inman-Heel and Inman-Ankle models are no longer overlapping, thus affecting subtalar joint moment and muscle functions actuating the joint. This is especially seen when comparing Inman-Heel and Inman-Ankle STJ moments, which are both significantly different from each other, as well as being significantly larger than the identical Delp orientation model predictions (Figure 3-3). When using the Inman orientation, moving the location of the axis origin to the intermalleolar axis results in smaller peak subtalar joint moments as well as the muscle moment

arm values matching closer to the Delp model's calculations for all five muscles (Table 3-2). For many of the muscles, the Inman-Ankle modified model almost overlaps the Delp orientation (-Heel and -Ankle) models' moment arms (Figure 3-4a).

There are three muscles that do not closely follow the Delp orientation curves when the Inman-Ankle model subtalar joint definitions are set. These muscles are the Tibialis Anterior, EDL, and EHL which together make up the ankle dorsiflexor functional group. The muscle moment arm values for these muscles decrease as the relative distance to the axis origin shortens by moving the location to the ankle. Interestingly, the Inman orientation models (-Ankle and -Heel) both show the tibialis anterior muscle acting as an evertor, seen by the positive moment arm values, while the Delp orientation shows this same muscle acting in an opposite role (and more appropriate role), as an inverter (Figure 3-6). The differences in function can be resolved by looking at Figure 3-7 which shows the differences in subtalar joint axis orientation and location in relation to muscle tendon insertion when the joint axis is manipulated. There is almost no change between relative location of the muscles and subtalar joint axis when the Delp orientation (green) is used, no matter the origin location. However, when the Inman orientation (blue) is used, there is a noticeable difference in the skew of the axis depending on which origin location is implemented. This drastic change of the relationship between the subtalar joint axis and muscle insertions when the Inman orientation is used, leads to the Tibialis Anterior and EHL to be located laterally in relation to the subtalar joint axis when the -Ankle origin location is set, thus providing an eversion muscle action. This shows that special attention needs to be paid to how the subtalar joint is characterized, to make sure the muscles are functioning as they do in situ.

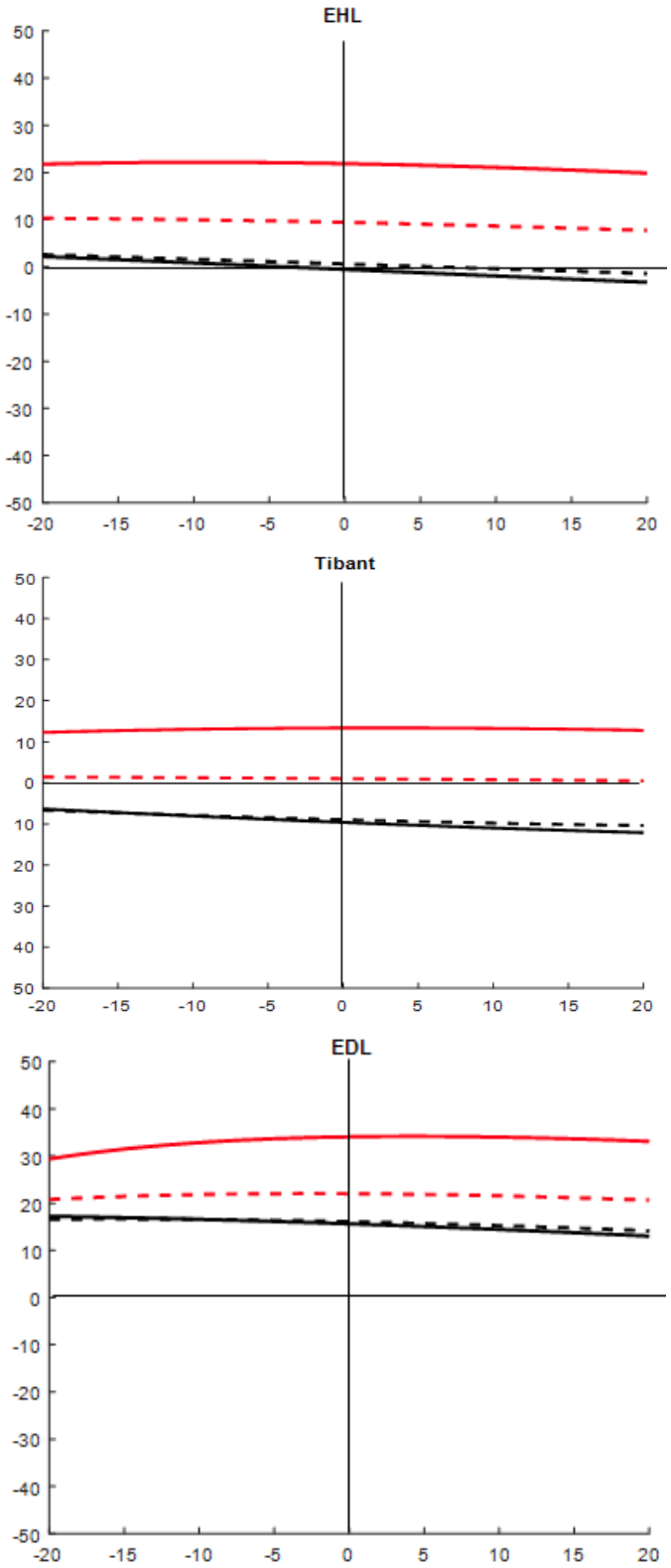

Figure 3-6: Muscle moment arm moment arm vs subtalar angle curves for the Inman-Ankle (red-dotted line), Inman-Heel (red-solid line), Delp-Ankle (black-dotted line), and Delp-Heel (black-solid line) models for Ankle Dorsiflexor functional group.

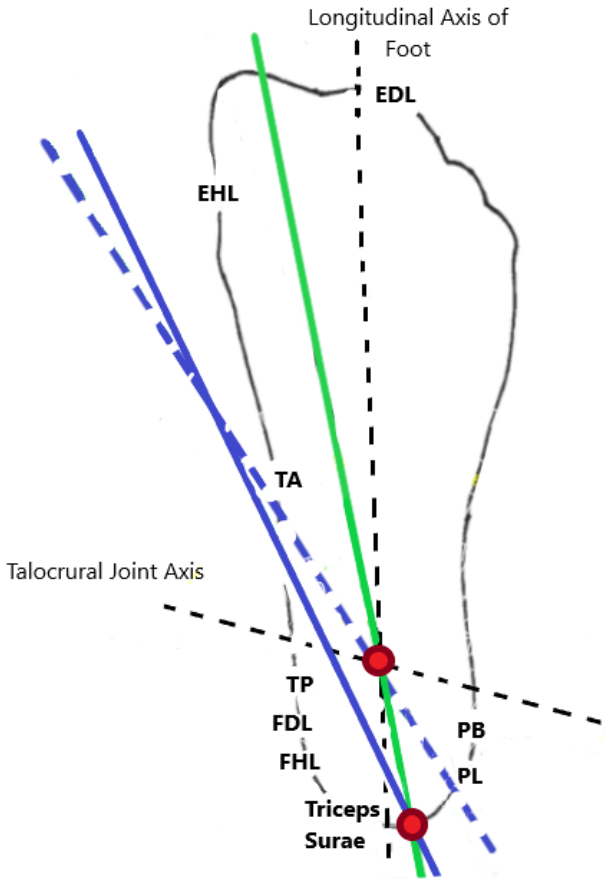

Figure 3-7: Relationship between subtalar joint axis and surrounding muscle insertions when using Delp (green) or Inman (blue) orientations. Dotted line represents through -Ankle origin location, solid through -Heel.

3.5 CONCLUSION

In this study, the effects of Delp and Inman orientations on model definition (muscle moment arms) and model joint analysis (kinematics and kinetics) were evaluated. The results show that the default model is sufficient for biomechanical analysis when using a generic subtalar joint axis; however, if a subject-specific axis is to be considered, the origin location of the subtalar joint axis should be addressed first. The orientations chosen in this study were compared as they represent the most commonly used (Delp) and referenced (Inman) subtalar joint orientations. However, these orientations were determined by way of computational

estimates and in non-weightbearing cadaveric studies, respectively. The subtalar joint orientation has been shown to vary depending on the evaluation method (i.e. cadaver, computational, weight-bearing CT (Fernandez et al., 2020) as well as varying throughout the subtalar joint's range of motion (Lundberg and Svensson, 1993). Realistic conditions like these should be considered to understand the true muscle moment arm and how it relates to its function. Future work should investigate how subject specific definitions of the subtalar joint axis definition may be appropriate for feet with deformities or during dynamic tasks, like cutting or walking on uneven terrain, that involve significant inversion/eversion subtalar joint motion.

CHAPTER 4: THE EFFECT OF SUBTALAR AXIS ORIENTATION ON LOWER KINETIC CHAIN ESTIMATES OF WALKING AND RUNNING

4.1 INTRODUCTION

The subtalar joint is primarily responsible for load transmittance during the beginning part of stance as well as allowing for flexibility needed for sloped walking or uneven terrain (Beimers et al., 2008; Taylor et al., 2001). This is possible due to the joint's unique tri-planar motion of pronation/supination. However, frequently biomechanical models simplify this as a rotation around a single degree of freedom axis (Nichols et al., 2016). The orientation of the subtalar joint axis is defined with coordinates that represent inclination and deviation angles established in the literature (Delp et al., 1990; Isman and Inman, 1969). Realistic musculoskeletal models, using either a generic-axis based on literature or subject-specific axis consideration, rely on accurate joint axis definition as this plays an influential part in computation of muscle and joint forces and motions (Lewis et al., 2006; Nichols et al., 2017).

The action of a muscle is determined by the muscle's moment arm, or relative location and distance of attachments in relation to the joint axis (Klein et al., 1996; Spoor et al., 1990). The location of the subtalar joint axis has a significant effect on lower-foot muscle moment arms and resulting subtalar joint moment estimates (Chapter 3); however, these differences may be more evident when the subtalar joint orientation is skewed. Because the subtalar joint is the lower part of the kinetic chain, its orientation may affect other joint analyses further up the chain. It is unknown if the musculoskeletal models are more sensitive to changes in subtalar joint axis inclination or deviation angles. To investigate this, the separate contributions should be

manipulated one at a time to their maximum and minimum reported values (Delp et al., 1990; Isman and Inman, 1969) while keeping the opposite angle definition constant.

The subtalar joint axis was initially defined during passive motions using non-weight bearing *in vitro* analysis. From a study of 46 cadavers, Isman and Inman (1969) concluded mean inclination and deviation angles of 42° and 23° that fall within their respective ranges of 20-68° and 4-47°.. In recent years, with the aid of modern imaging techniques, it has been determined that these ranges may not be realistic definitions of subtalar join axis for normal population during weight-bearing. *In vivo,* CT evaluations have shown that the deviation angle of the subtalar joint is estimated to much lower values during simulated and full weight-bearing with averages reported around 6° (Beimers et al., 2008; Fernandez et al., 2020). This is in part due to the change in relative motion of the talus and calcaneus between open-chain and closed-kinetic-chain motion (Rockar, 1995). *In vivo* weightbearing studies have determined the helical axis to be much lower in deviation angle compared to *in vitro* non-weightbearing study (Delp et al., 1990; Isman and Inman, 1969) and different still from mathematical models that find the orientation by the intersection of the distal talus and distal calcaneus locations (Delp et al., 1990; Isman and Inman, 1969). It is important to analyze the various joint orientation estimate techniques to understand the fidelity of using passive or computational axis definition for simulation of weight-bearing and dynamic motion.

Previous evaluation comparing the computation-based axis (Delp et al., 1990; Isman and Inman, 1969) and orientation based on *in vitro* passive motion (Delp et al., 1990; Isman and Inman, 1969) showed significantly larger subtalar joint moments between subjects when Inman's mean inclination/deviation angles were implemented in the musculoskeletal model (Noginova et al., 2018). The same study concluded that as the complexity of motion increased, from walk to

run, so did the significant difference in subtalar joint moment outputs between orientation models. These differences can be attributed to: (1) larger vertical forces acting on the body during running, (2) increased speed, as well as (3) substantial change in biomechanics ranging from joint motion, leg stiffness, and joint reaction force (Chan and Rudins, 1994; Hamner and Delp, 2013). With these changes to biomechanics that depend on running speed, it is important to understand the role of the subtalar joint as load-acceptor and how the joint transmits the stresses to the rest of the joints of the kinetic chain.

Musculoskeletal models allow for the simulation and prediction of muscle and joint forces during dynamic analysis. Since these rely on the accuracy of axis definition, analyzing the isolated contribution of inclination/deviation angles as well as best realistic orientation estimates helps in understanding how the orientation and dynamic loading of the subtalar affects the lower kinetic chain during active motion. Therefore, the purposes of this study are (1) to determine how the inclination and deviation angles separately affect the musculoskeletal model's sensitivity in estimating joint rotations, moments, and contact force for the knee, ankle, and subtalar joint as well as (2) determine how the differences in STJ axis orientation are affected by degree of dynamic motion (walking vs running).

4.2 METHODS

Experimental data for this study was obtained from two open-source datasets. Overground walking data for 3 subjects with instrumented tibia implant was obtained from the open-source Grand Knee Challenge (2013, 2014, 2016). Using the Lai full-body model in OpenSim (SimTK, Stanford, CA, v3.3), adjusted models were created by scaling by anthropometric measures for each subject based on the modified Cleveland Clinic marker set

used to define body segment lengths (Fregly et al., 2012). These were then simplified to include the pelvis and lower extremity (right leg for 4th and 6th competition, left leg for 3rd) (Lai et al., 2017). Along with the *in vivo* knee loads acquired from the instrumented implant (eTibia), marker trajectory, and ground reaction force (GRFs) were obtained from the GKC competition dataset for three trials of normal gait for each subject. Similarly, a dataset of running at various speeds was obtained through open-access resources (Hamner and Delp, 2013). From this dataset, three subjects were chosen, and motion capture data, including skin marker trajectory and ground reaction forces (GRF), were obtained for running speeds of 2 m/s and 5 m/s (Hamner and Delp, 2013). The dataset also includes pre-established subject-specific models that were scaled based on Hamner's custom marker set consisting of 54 reflective markers worn during the running tasks (Hamner and Delp, 2013). These full-body models were then adjusted to include the pelvis and lower right limb. Both the Hamner and Lai models were validated for walking and running and had identical lower segment (ankle, subtalar, mtp) definitions.

The default ankle and subtalar joint axis definition in the Lai and Hamner model match that as first established by Delp (Delp et al., 1990; Hamner and Delp, 2013; Lai et al., 2017). This coordinate system axis has its origin location found at the most disto-lateral aspect of the calcaneus with orientation of the axis pointing up and inward through the talus with inclination and deviation angles of 37.2° and 8.7°, respectively. Because the origin location of the subtalar joint axis significantly affects the model's muscle function, especially when the subtalar joint orientation does not match the default (Paper 1), the Lai and Hamner model both have been modified to have the subtalar joint origin location found at the intermalleolar axis.

To evaluate how sensitive the model is to changes in STJ inclination/deviation angles, the STJ orientations of the Lai walking model were modified to reflect what happens when these are

taken to their maximum/minimum values as defined by Inman while keeping the other at the default (Table 4-1) (Delp et al., 1990; Isman and Inman, 1969)..

	Delp	IncMin	IncMax	DevMin	DevMax	Inman
Inclination	37.2°	21°	69°	37.2°	37.2°	42°
Deviation	8.7°	8.7°	8.7°	4°	47°	23°

Table 4-1: Subtalar joint orientation models, used in analysis of normal gait, and their respective inclination/deviation angles.

In the Hamner running models, the subtalar joint orientations were modified to match experimental helical axis findings. For running speeds of 2 m/s and 5 m/s, the Delp and Inman orientations were compared to helical axis estimates gathered from *in vivo* weight-bearing CT(Fernandez et al., 2020). Table 4-2 below shows the STJ models analyzed for running tasks as well as the conditions of the study in which the orientations were determined.

	Delp	Inman	CT
	mathematical	*In vitro*, non-weightbearing	*In vivo*, weightbearing
Inclination	37.2°	42°	43°
Deviation	8.7°	23°	6°

Table 4-2: Subtalar joint orientation models, used in analysis of running at 2 m/s and 5 m/s, and their respective inclination/deviation angles.

Using OpenSim's toolbox and a custom-built MATLAB (MathWorks, Natick, MA, USA, R2019b) code, inverse kinematics, inverse dynamics, and joint reaction force analyses were computed for the joints of the lower extremity, including: the knee, ankle, and subtalar joint. For

all walking trials, there was no weighting of marker tasks added when solving the inverse kinematic computations. Conversely, for all three running subjects with pre-scaled models, the weighting scheme was kept as it was originally obtained from the dataset. The MATLAB code also determined the swing vs stance phase of gait based on measured GRF and normalizes the results to 100 points which represent the percent of the stance phase.

The walking trials with the varied STJ orientations (Table 4-1) were compared to the Delp orientation model, which is used as "standard". Since the *in vivo* CT orientation matches both the Delp and Inman orientations in one angle component, the three orientation models are all compared to one another to highlight the contribution of inclination/deviation angles at both speeds of running (Table 4-2). Discrete variables from stance phase, such as mean, peak, and ROM values were compared with different orientations and during walking and running using Student's two-tailed paired t-tests performed in SPSS (IBM Corp, Armonk, NY, version 27) with significance set at $p < 0.05$.

4.3 RESULTS

4.3.a. EFFECT OF ANGLE

Changing the musculoskeletal model's definition of subtalar joint axis inclination (Figure 4-1) or deviation angle (Figure 4-2) did not significantly affect any of the joint rotations computed for the joints of the lower kinetic chain (i.e., knee, ankle, and subtalar joint). There are also minimal differences in knee and ankle joint moments when comparing the Delp and Inman orientation models to those representing Inclination/Deviation (Figures 4-3a&b and 4-4a&b) max/min models.

Peak subtalar joint moments were significantly different between the ‘standard’ Delp orientation and all other analyzed subtalar joint orientation models (i.e. DevMax, DevMin, IncMax, IncMin, Inman) (Figures 4-3c and 4-4c). The largest and smallest peak subtalar joint moments came from the manipulation of the orientation angles to their maximum range values (Table 4-3), with DevMax resulting in a peak of .76 N*m/BW seen during the late part of stance, and IncMax resulting in only .09 N*m/BW.

Figure 4-1: The effect of inclination angle on (a) knee, (b) ankle, and (c) subtalar **joint rotations** comparing IncMax and IncMin to default Delp and most commonly reference Inman orientation.

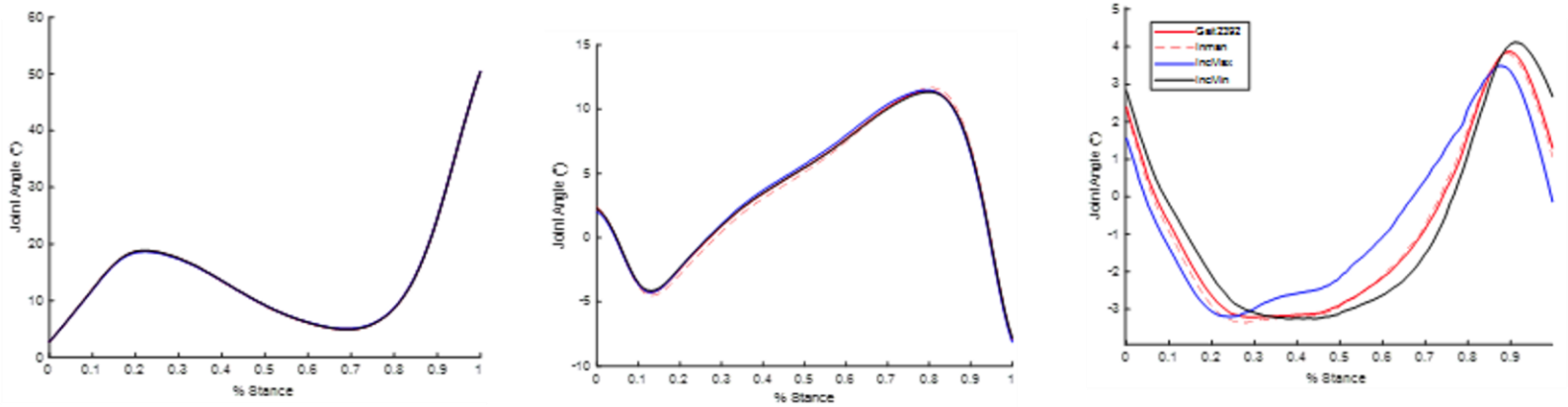

Figure 4-2: The effect of deviation angle on (a) knee, (b) ankle, and (c) subtalar **joint rotations** comparing DevMax and DevMin to default Delp and most commonly reference Inman orientation.

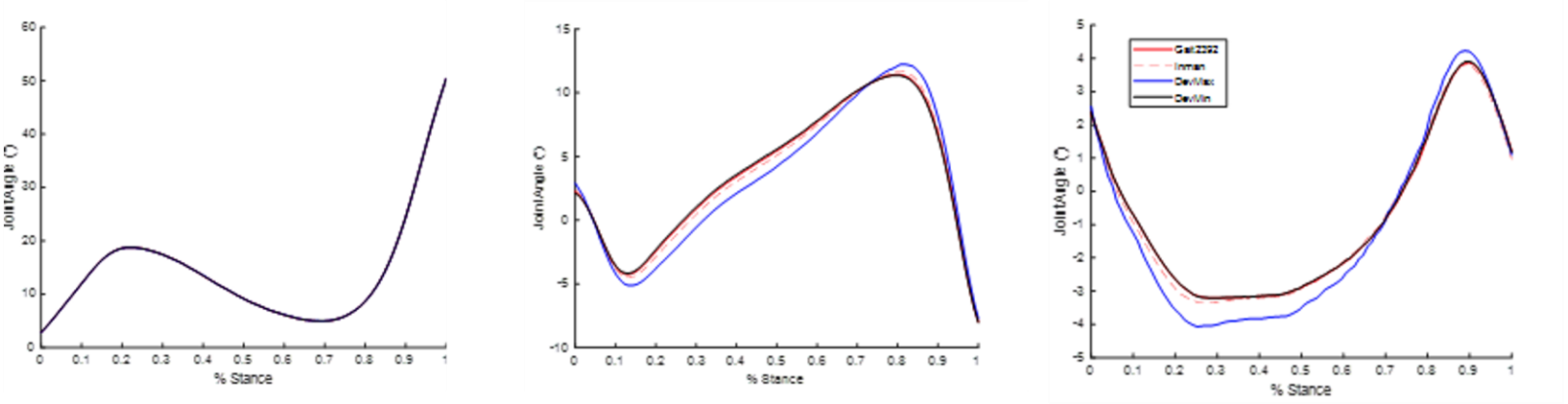

—Figure 4-3: The effect of deviation angle on (a) knee, (b) ankle, and (c) subtalar **joint moment** comparing DevMax and DevMin to default Delp and most commonly reference Inman orientation.

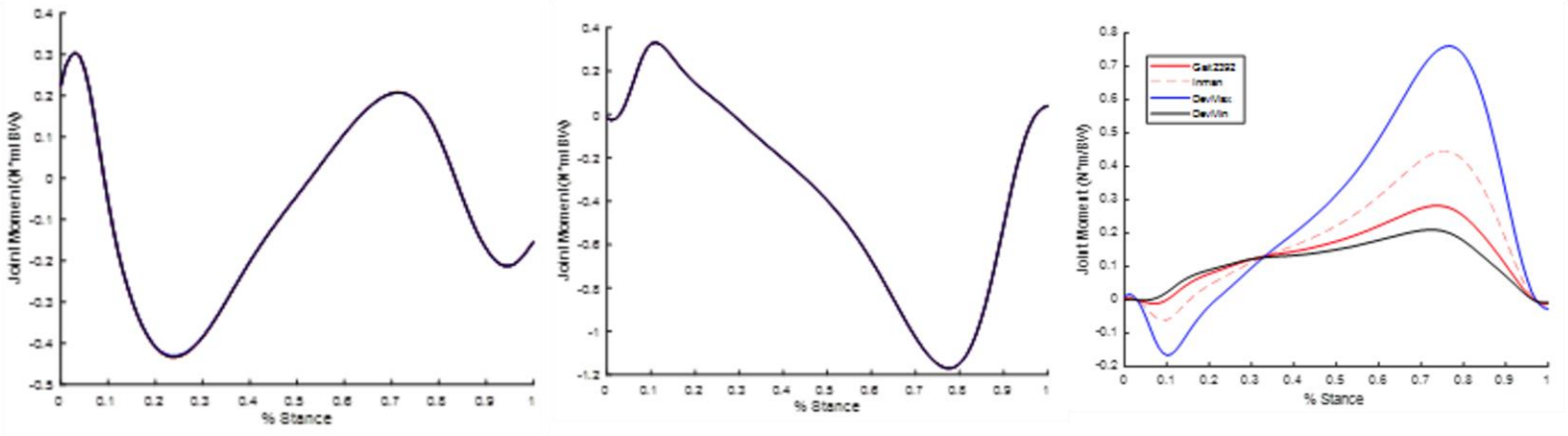

Figure 4-4: The effect of inclination angle on (a) knee, (b) ankle, and (c) subtalar **joint moment** comparing IncMax and IncMin to default Delp and most commonly reference Inman orientation.

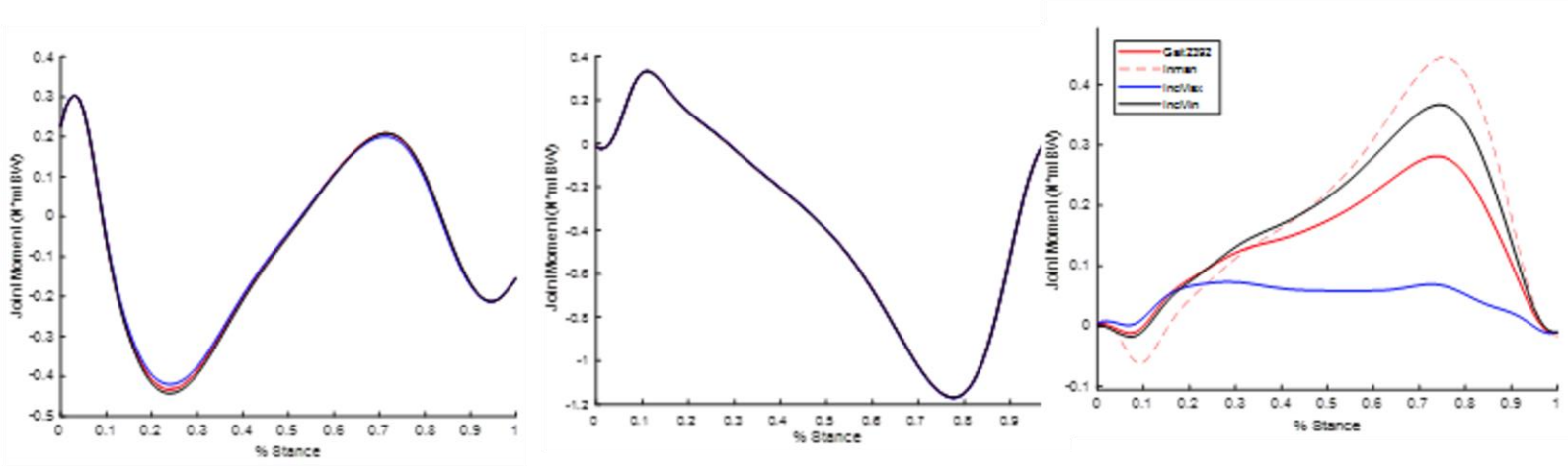

In comparison, the minimum inclination and deviation orientation models resulted in peak values of 0.37 N*m/BW and 0.22 N*m/BW. These are both much closer to the default Delp model which results in peak subtalar moment estimates of approximately .29 N*m/BW.

		DevMax	DevMin	Delp	IncMax	IncMin	Inman
Knee	Peak (N*m/BW)	0.22	0.22	0.22	0.22	0.23	0.22
Ankle	Peak (N*m/BW)	0.35	0.35	0.35	0.35	0.35	0.35
Subtalar	Peak (N*m/BW)	**0.76**	**0.22**	0.29	**0.09**	**0.37**	**0.45**
	Significance (p score)	**p=0.01**	**p=0.02**	***	**p < 0.01**	**p < 0.01**	**p=0.02**

Table 4-3: Peak moment values (N*m/BW) for the knee, ankle, and subtalar joint during walking for each subtalar joint orientation model. Bold values indicate significant differences in comparison to the 'standard' represented by *** in the table.

The joint contact force calculated at the knee, ankle, and subtalar joint does not significantly differ for any of the joints when the deviation angle is taken to the maximum and minimum values as described by Inman (Figure 4-5) (Isman and Inman, 1969). Manipulating the inclination angle of the model to its' maximum reported value, the loading pattern of the ankle and subtalar joints are observably different (Figures 4-5 and 4-6b&c) with the IncMax model producing significantly lower peak reaction force ($p<0.01$) during the second half of stance.

Figure 4-5: The effect of deviation angle on knee, ankle, and subtalar joint **total contact force** comparing DevMax and DevMin to default Gait2392 orientation and most commonly reference Inman orientation.

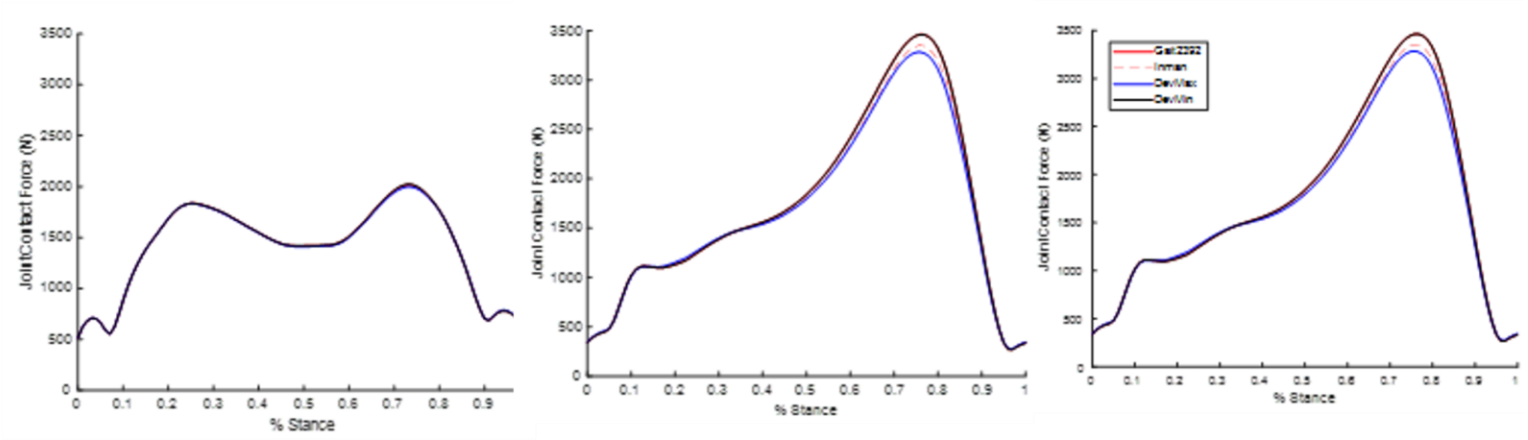

Figure 4-6: The effect of inclination angle on knee, ankle, and subtalar joint **total contact force** comparing IncMax and IncMin to default Gait2392 orientation and most commonly reference Inman orientation.

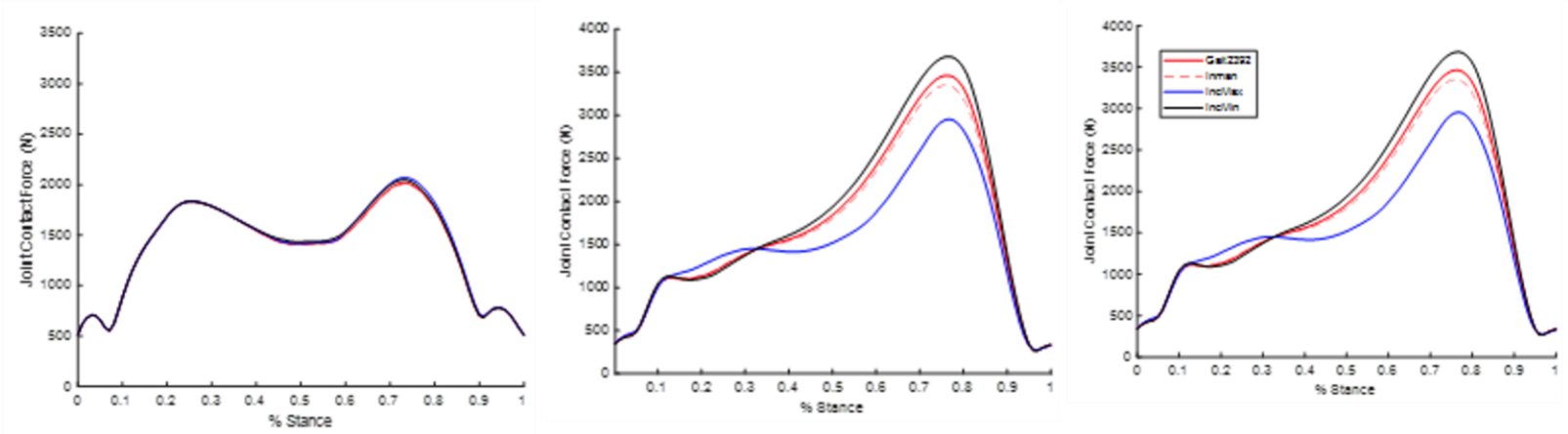

4.3.b. WALKING VS RUNNING

Similar to walking conditions, neither running at 2.0 m/s nor 5.0 m/s produced statistically significant differences in computed generalized angle coordinates for any joint when comparing between models with default Delp axis orientation, Inman's mean, or subtalar joint axis orientation determined from weight-bearing CT (Figure 4-7).

Variances in peak knee and ankle joint moments were also non-significant between orientation models, not dependent on running speed (Figure 4-8a&b). However, when comparing the subtalar joint moment calculations, there are significant differences in peak values as deviation angles increase (Figure 4-8c) (Table 4-4) and this is consistent for gait and both speeds of running. For all joints of the lower kinetic chain. the peak moment values also increased as the motion complexity and speed increased (i.e. walk to run, run 2.0 to run 5.0). The peak estimated values for the knee and ankle increased by 6x when transitioning from walk to run while only a 1.5x increase was calculated for these joints between running at a slower speed to a faster one (Table 4-4).

Figure 4-7: Comparison of computed (a) knee, (b) ankle, and (c) subtalar joint angles between subtalar joint orientation models of walking (DevMin, Delp, Inman) and running (CT, Delp, Inman) at varying speed of motion: Walking (black), Run 2.0 m/s (blue), Run 5.0 m/s (red).

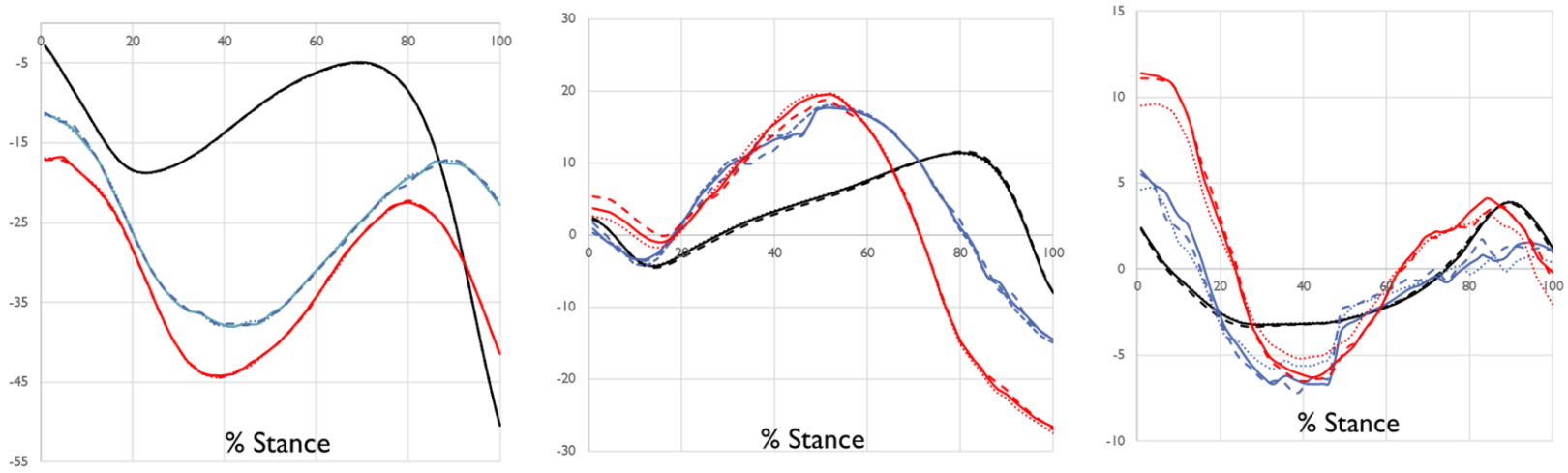

Figure 4-8: Comparison of computed (a) knee, (b) ankle, and (c) subtalar joint moments between subtalar joint orientation models of walking (DevMin, Delp, Inman) and running (CT, Delp, Inman) at varying speed of motion: Walking (black), Run 2.0 m/s (blue), Run 5.0 m/s (red).

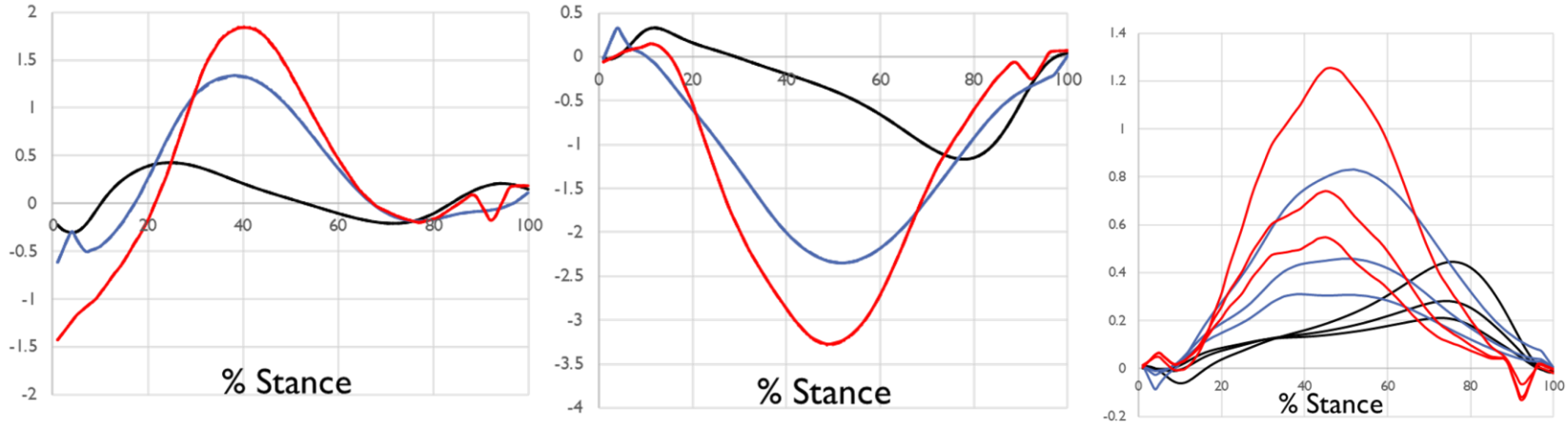

Table 4-4: Peak moment estimates (N*m/BW) of the knee, ankle, and subtalar joint for each orientation model analyzed for walking, running at 2.0 m/s, and running at 5.0 m/s. Bold values represent significant differences in comparison to the 'standard' represented by *** in the table.

		Walking				Running at 2 m/s				Running at 5 m/s		
		DevMin	Delp	Inman		CT	Delp	Inman		CT	Delp	Inman
Knee	Peak (N*m/BW)	0.22	0.22	0.22		1.37	1.38	1.37		2.00	1.99	1.99
Ankle	Peak (N*m/BW)	0.35	0.35	0.35		-2.36	-2.36	-2.36		-3.52	-3.51	-3.52
STJ	Peak (N*m/BW)	**0.22**	0.29	**0.45**		**0.35**	**0.48**	**0.84**		**0.58**	**0.78**	**1.31**
	Significance (p value)	**p=0.02**	***	**p=0.02**		***	**p=0.02**	**p=0.02**		***	**p=0.03**	**p=0.01**
						p=0.02	***	**p=0.02**		**p=0.03**	***	**p=0.01**

Analysis of running did not produce any significant differences for either speed in knee, ankle, nor subtalar joint reaction forces between the default Delp model and DevMin/CT or Inman orientation models. As speed or complexity of motion increased, so did peak joint reaction values (Figure 4-9). Knee contact force curve has an observable double hump loading pattern during walking (Figure 4-9a) that has the second peak nearly 3x bodyweight. As the speed increases from walk to run and then run 2.0 m/s to 5.0 m/s, the double peak becomes singular with a high of 10x body weight. The ankle and subtalar joint contact forces are similar in value and show an increase of peak force from 5x bodyweight to nearly 12x as the speed increases to a 5.0 m/s run (Figure 4-9 b&c).

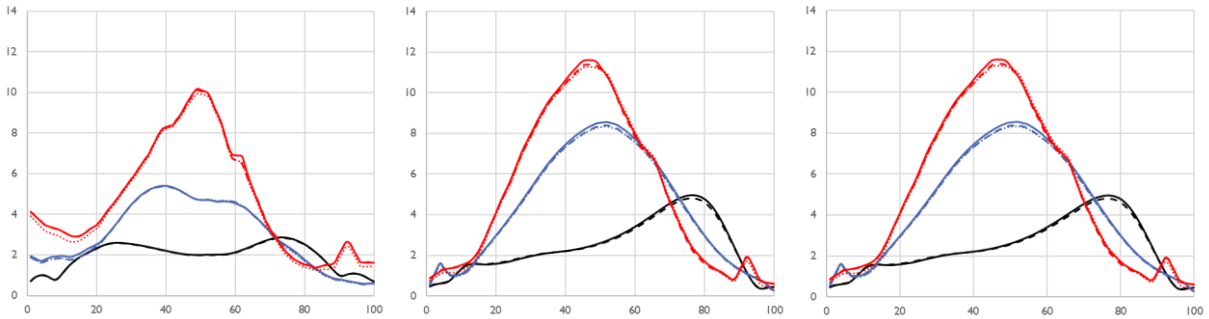

Figure 4-9: Comparison of computed (A) knee, (B) ankle, and (C) subtalar joint reaction force between subtalar joint orientation models of walking (DevMin, Delp, Inman) and running (CT, Delp, Inman) estimated during stance phase of varying speed of motion: Walking (black), Run 2.0 m/s (blue), Run 5.0 m/s (red).

4.4 DISCUSSION

The purpose of this study was to determine how the inclination and deviation angles of the subtalar joint axis orientation affected joint calculations (angles, moments, and reaction force) of the subtalar joint as well as the adjacent joints of the lower kinetic chain, primarily the

ankle and knee. These differences were analyzed across varying degree of dynamic motion, walking and running.

4.4.a. EFFECT OF ANGLE

The generalized coordinates computed are identical for the knee for each modified subtalar joint orientation model, with some slight but not significant differences seen at the ankle and subtalar joint (Figures 4-1 and 4-2) when the inclination and deviation angles are separately modified. Generally speaking, the kinematics match well with *in vivo* measurements of knee, ankle, and subtalar joint angles collected using intracortical bone pins during walking (Arndt et al., 2004; Reinschmidt et al., 1997). While the changes in the joint motion are not remarkably different, there is an observable increase in overall range of motion of the ankle and subtalar joint during stance. The differences, specifically when the deviation angle is modified (Figure 4-2 b&c), support the suggestion that as deviation angle from the sagittal plane increases, so does the amount of dorsiflexion-plantarflexion motion that the hindfoot can produce (Budny, 2004; Chan and Rudins, 1994; Kirby, 1987). Conversely, changes to the inclination angle mostly affect the timing of subtalar joint eversion (Figure 4-1c). In a normal foot, gradual eversion occurs until approximately 30% of stance where a progressive inversion motion follows until ~90% stance phase of the gait cycle (Birch and Deschamps, 2014). The findings of this study suggest that as the inclination angle of the subtalar joint axis relative to the horizontal axis increases, the faster the foot inverts during the stance phase. The minute differences between subtalar joint orientation models did not affect joints further up the kinetic chain, i.e. the knee.

No observable differences were seen in the knee or ankle joint moment distribution when the inclination or deviation angle were manipulated to their maximum and minimum range values (Figures 4-3 and 4-4 a&b). The moment curves for these joints match previous modeling

and in vivo based studies reporting knee and ankle moments during walking (Kirtley et al., 1985; Malaquias et al., 2017; Winter et al., 1990). In evaluating the subtalar joint moment during, it has been reported to have peak moment values between .2 and .7 N*m/kg depending on varus/valgus alignment and added degrees of freedom to the foot (Kakihana et al., 2005; Malaquias et al., 2017). In this study, the change in both inclination or deviation angle significantly affected the peak subtalar joint moment values (Figures 4-3c and 4-4c). The orientation models with maximum angle representation (DevMax and IncMax) resulted in the largest and smallest peak subtalar joint moment values with .76 N*m/BW and .09 N*m/BW, respectively (Table 4-3). In comparison, the minimum orientation models (DevMin and IncMin) resulted in moderate peak subtalar joint moment values that more closely matched the default Delp model of .28 N*m/BW. This supports the observation that while the default Delp orientation does fall within Inman's range like reported in the literature, it falls on the lower end of the range for both inclination and deviation angles (Delp et al., 1990; Isman and Inman, 1969). The knee contact forces have been evaluated in musculoskeletal models for varying motions (walking, running, etc.) and the effect of changing parameters of the knee (Andersen, 2018; Ding et al., 2016; Hast and Piazza, 2013; Knarr and Higginson, 2015). However, to the author's knowledge, there has been no analysis of how changes to the subtalar joint axis affects loads of the ankle and knee. The results of this study show that there are not any significant differences in peak knee contact forces when the subtalar joint axis orientation is manipulated (Figures 4-5a and 4-6a). All selected orientation models produce a double hump knee loading with peak total contact force at 2000 N, or 2.5BW. Similar knee loading shape and peak values have been reported in the literature from investigators using the same GKC dataset (Andersen, 2018; Chen et al., 2016; Hast and Piazza, 2013). The only subtalar joint orientation model that resulted in significantly different contact

force estimates was the IncMax model that produced significantly lower peak ankle and subtalar joint contact forces seen in the late stance of the gait cycle (Figure 4-6 b&c). The peak value was just under 3000N in the IncMax model, while the standard Delp model predicted estimates of around 3500N. In bodyweight, this is a difference between 4.22BW and 4.95BW, respectively. There are no reported subtalar joint contact force estimates in the literature, but the ankle and subtalar joint have very similar loading curves and values and so the two can be compared directly. It has been reported in the ankle that the compressive forces fall anywhere between 3.5-4.5BW or 4500-5000N during the stance phase in normal feet (Dettwyler et al., 2004; Procter and Paul, 1982). While there are significant differences between the two model orientations for the subtalar and ankle contact force estimates, they are both within previously reported values of normal feet.

4.4.b. WALKING VS RUNNING

When analyzing the effect of subtalar joint axis orientation during running, models were chosen that closely follow realistic axis representations found through *in vitro* passive evaluation (Delp et al., 1990; Isman and Inman, 1969), *in vivo* weightbearing CT imaging (CT), and the default musculoskeletal orientation found geometrically (Delp et al., 1990; Isman and Inman, 1969).

The only measure to result in significant differences for this motion due to changes in subtalar joint orientation definition is the subtalar joint moment. This is true for both running speeds (2.0 m/s and 5.0 m/s) (Figure 4-8c). When comparing across the three subtalar orientations models, for both walking and running, the Inman model always resulted in the largest subtalar joint moments, followed by Delp model orientation and then DevMin/CT (Table 4-4). For all speeds, the peak subtalar joint moments were 1.3x smaller for the DevMin/CT than

the Delp orientation model and simultaneously 2x smaller than Inman model which has the largest peak value, likely due to having the largest deviation angle of all three models. It was seen in the first part of this study that deviation angle has a significant effect on peak subtalar joint moment values. Comparing between speeds, there is an increase in peak moment values for the knee and ankle as complexity and speed increase. Transitioning from walking to running results in both knee and ankle moments to increase by nearly 6 times. This occurs due to the substantially different biomechanics that is observed during running (Chan and Rudins, 1994). Overall investigators have reported changes in ground reaction force, muscle activity, joint motion and moments. It has been determined that for running, the differences are primarily based on the speed, with jogging being considered around 2.0 m/s and full speed walking at 4-5 m/s (Chan and Rudins, 1994; Hamner and Delp, 2013). Increasing the running speed from 2.0 m/s to 5.0 m/s resulted in a 1.45-1.5x increase in peak knee and ankle moment values.

There were no significant differences in running between the three subtalar joint orientation models for lower kinetic chain rotations and loading. The joint reaction forces for all models match previous reports that as speed increases, specifically from walking to running the double-hump knee loading becomes a solidary larger peak with vertical forces nearly doubling (Chan and Rudins, 1994). This is seen in Figure 4-9a, as the speed increases the double-peaks seen at the beginning and end part of stance phase form into one larger peak 10x BW with peak value at 50% stance. The ankle joint contact forces also support previous findings that during running, the localized forces estimated at the ankle are nearly 13 times body weight (Chan and Rudins, 1994).

4.5. CONCLUSION

In this study, the effect of subtalar joint orientation definition on varying dynamic motions was evaluated for the measures of joint angles, moment, and reaction force for the joints of the lower kinetic chain. The sensitivity of the model to changes in inclination and deviation angle was tested by manipulating the subtalar joint axis definition to reflect the minimum/maximum as established by Inman. Realistic subtalar joint orientations determined by varying methodologies (mathematical, *in vitro*, and *in vivo*) were also compared for all joint measures at increasing speeds, from walk to jog to run. Across all speeds, the subtalar joint moment was significantly different between all analyzed subtalar joint orientation models. The larger peak subtalar joint moment is a result of increase in deviation of the subtalar joint from the midline of the foot. There was a significant difference observed in peak ankle and subtalar joint reaction force when comparing IncMax model to default orientation. However, since IncMax represents the largest values of the range determined by Inman, the axis definition may not be very realistic for the average human subtalar joint axis (Delp et al., 1990; Isman and Inman, 1969). The results of this study show that the established musculoskeletal models, Lai and Hamner, are valid for simulating knee and ankle measures during straight walking and running on even ground as they are not sensitive to changes at the subtalar joint. One limitation of this study is that the DOF of the model is very simplified. The knee, ankle, and subtalar joints in both Lai and Hamner model have just 1DOF. The rotation around the subtalar joint axis is normally characterized by tri-planar motion. By simplifying the joints to just 1DOF, it is difficult to determine the contribution of each of the three rotational degrees of freedom (frontal/ sagittal/and transverse planes) and how the changes in inclination/deviation angles will affect motion in each plane as well as overall subtalar joint motion. Another limitation is that both

walking and running are mainly sagittal plane-based activities, with the subtalar joint only contributing ~6-10° of motion (Hicks et al., 2015). To better evaluate the subtalar joint and the effect that changes to joint axis definition have on its function, more dynamic motion in other planes should be observed, such as cutting or walking on uneven terrain in which supination/pronation is necessary for stability and load acceptance.

CHAPTER 5: THE EFFECT AND VALIDATION OF SUBTALAR JOINT INCLUSION IN MUSCULOSKELETAL MODELS DURING WALKING AND RUNNING

5.1 INTRODUCTION

Musculoskeletal models allow for assessment of subject-specific measures that we cannot easily obtain during in vivo data collection. However, it is the responsibility of researchers to validate the results of their simulations to make sure they do in fact reflect human motion/loads (Hicks et al., 2015). Validation can be done directly or indirectly. Direct validation involves comparing the simulated results to measures collected simultaneously. In dynamic musculoskeletal models, direct validation occurs through instrumented implants or electromyographic signals (EMG). Even with EMG being used as a method of direct comparison, it has been determined in previous literature that, while EMG does allow for qualitative assessment of onset/offset timing and muscle pattern, it is not a very good predictor of joint contact loading output (Anderson and Pandy, 2001; Hicks et al., 2015; Meyer et al., 2013). Therefore, it allows for direct validation of muscle activation but not for validating the resulting joint reaction analysis that uses estimated muscle activations as input to internal loads applied to the joint in question. Indirect validation involves comparing results to previously validated values or measures collected in other subjects/studies. Validation allows the researcher to determine how sensitive and accurate their models are to changes in joint definition.

Knee joint forces have been estimated through musculoskeletal modeling in numerous studies (Correa et al., 2011; Gardinier et al., 2013; Meyer et al., 2013; Sasaki and Neptune, 2010). In the past, validation of these has been possible through comparisons of *in vivo* measurements like EMG. With the introduction of instrumented implant, direct comparison of

joint contact predictions to the implanted load cell readings allows researchers to understand the comprehensive forces in real time. The GKC introduced by Fregly et al. (2012) in 2010 encourages ‘competitors’ to use the included force-measuring knee implant and concurrently collected EMG data to critically evaluate and validate their own models. These *in vivo* measures have allowed investigators to evaluate the inter-subject differences in knee loading during various tasks (bouncy gait vs smooth gait, sit to stand, etc.) as well as how to modify their own models to attain the most accurate computations (blind vs unblind) (Chen et al., 2014; Ding et al., 2016; Jung et al., 2016; Lundberg et al., 2013). However, since all participants from the GKC dataset required a bi-lateral total knee replacement, there are limitations in the motions available (i.e. running). Even with simpler tasks such as walking, the subjects may have different muscle loading patterns to accommodate for the unhealthy knee. Therefore, using EMG in concert with in vivo loading measures can broaden understanding of muscle action in non-healthy individuals and how EMGs can be used to validate musculoskeletal models when in vivo joint measures are not available.

Sensitivity of musculoskeletal models to subtalar joint axis origin location (Chapter 3) and axis orientation (Chapter 4) have been previously concluded. These studies showed significant changes in muscle moment arms and subtalar joint moment estimates during dynamic motion. However, the models with modified subtalar joint axes have yet to be validated for contact force estimates of the knee as well as sensitivity to inclusion of the subtalar joint during dynamic analysis. It is often a “rule of thumb” to lock the subtalar and mtp joint during dynamic analysis, such as inverse kinematics and inverse dynamics, to minimize errors and computation (Falisse et al., 2018). However, since the subtalar joint takes on much of load acceptance during stance phase as well as allows for motion in three planes, locking the joint may not give an

accurate representation of the loads being transmitted across the lower kinetic chain during weight-bearing.

The purpose of this study was to validate the models of walking and running as it relates to their accuracy of estimating knee joint contact forces as well as assess the sensitivity of musculoskeletal models to the inclusion of the subtalar joint as these are often left locked when performing dynamic simulations.

5.2 METHODS

In this study, walking data were obtained from three years of the GKC competition (2012, 2013, 2016). For each of these subjects (SC, JW, DM), the data included anthropometric information, marker trajectory, ground reaction force (GRF), EMG signals, and measured loads from an instrumented knee implant. A musculoskeletal modeling software, OpenSim (3.3v), was used to import the modified Cleveland Clinic marker-set used in the GKC data to define subject body segment length. From the parameters of length and subject weight, a full-body model (Lai et al., 2017) was adjusted to include just the pelvis and lower instrumented limb (left for subject SC, and right for subjects JW and DM). To evaluate the importance of the subtalar joint in a more dynamic task, 3 subjects running at 2.0 m/s were selected from an open-source resource (SimTK). The included data subject-specific models (Hamner and Delp, 2013), marker trajectory, ground reaction force (GRF), and raw EMG of major knee and ankle muscles. The obtained pre-scaled models were based on custom 54 retroreflective marker-set that was then adjusted to include the pelvis and lower right limb for each participant.

For all subject-specific models, the location of the subtalar joint axis was modified such that the origin location was located on the talus, at the midpoint of the intermalleolar axis. For

this study, three STJ orientations were analyzed for walking and running: default Delp, Inman, and DevMin(walking)/CT (running). Both the DevMin orientation model and CT orientations (Fernandez et al., 2020) can be related to one another as both have moderate inclination angles with deviation angles on the low end of range established by Isman and Inman (1969). The table below shows the inclination/deviation angles for each listed orientation model (Table 5-1). Using OpenSim's toolbox and a custom-built MATLAB (MathWorks, Natick, MA, USA, R2019b) code, biomechanical analysis for all subjects and orientations included inverse kinematics, inverse dynamics, static optimization, and joint reaction analysis, with the subtalar joint locked and unlocked. Stance phase for both normal gait and running were defined by GRF and normalized to 100 points which represents the percent of stance phase.

	Delp (both)	Inman (both)	DevMin (walking)	CT (running)
	geometrical	*In vitro*, non-weightbearing	*In vitro*, Inman range	*In vivo*, weightbearing
Inclination	37.2°	42°	37.2°	43°
Deviation	8.7°	23°	4°	6°

Table 5-1: Subtalar joint orientation models used in analysis of walking and running at 2 m/s with their respective inclination/deviation angles.

The EMG signals from both open-source datasets were transformed to muscle activation following a previously reported method of filtering and rectifying (Lloyd and Besier, 2003). The raw EMG signals were processed by first passing them through a high pass fourth order

Butterworth filter of 450 Hz to remove soft tissue artifact. Then it was full wave rectified so that all values were positive, and finally sent back through a second filter of 5Hz. Resulting EMG curves and muscle activations were compared for the Gastrocnemius (GasLat and GasMed), Soleus, and Tibialis Anterior (TibAnt), as those are the muscles that cross the ankle joint complex. The muscle activations that were reported from the static optimization analysis were directly validated by comparing to the provided measured EMG for 2-3 cycles of gait and normal running. The curves are compared qualitatively based with a focus on onset/offset timing and general shape. Along with the muscles that were measured through EMG, the following muscles' activations were also compared in this study between locked and unlocked STJ conditions: Peroneus Longus (PerLong), Peroneus Brevis (PerBrev), Flexor Hallucis Longus (FHL), Flexor Digitorum Longus (FDL), and Tibialis Posterior (TibPost).

To directly validate the musculoskeletal orientation models for analyzing walking, root-mean-square error (RMSE) and Pearson's correlation coefficient (p^2) were calculated between measured *in vivo* instrumented knee implant load (eTibia) and the model's predicted knee joint contact forces. These were done separately for each subject obtained from GKC, comparing the unlocked RMSE and correlation estimates to one overall locked estimate, since the values between all locked subtalar orientations are within .5N. Following guidelines set by Walter, corrolation was evaluated based on score as: poor (0.0-0.5), moderate (0.5-0.7), good (0.7-0.9), or strong (0.9-1.0) (Andersen, 2018; Walter et al., 2015). Simultaneously collected EMG were also used as a secondary method of validating the model's accuracy in muscle activation and joint reaction analysis. Since the estimated knee contact forces cannot be directly validated for the running model to *in vivo* loads, the predicted values will be validated using EMG. The EMG-to-activation patterns will be compared between walking and running datasets. If there is good

approximation for both, then the validity of the walking data can be used to conclude that the knee joint loads are similarly accurate. To assess the sensitivity of the models to the inclusion of the subtalar joint, two-tailed paired t-tests were performed in SPSS (IBM Corp, Armonk, NY, V27) with significance set at 0.05. The t-tests compared discrete variables, such as mean and peak values, between locked and unlocked subtalar joint conditions for all of the joints of the lower kinetic chain, from the subtalar joint to the knee.

5.3 RESULTS

Each of the subjects from the GKC were modeled for self-selected speeds of walking with three separate subtalar joint orientations, as well as with locked and unlocked conditions. The resulting knee contact predictions were compared to measured loads obtained through an instrumented knee implant (Figure 5-1). The RMSE values ranged from .42 to .83 BW across all three subjects for all of stance phase (Table 5-2).

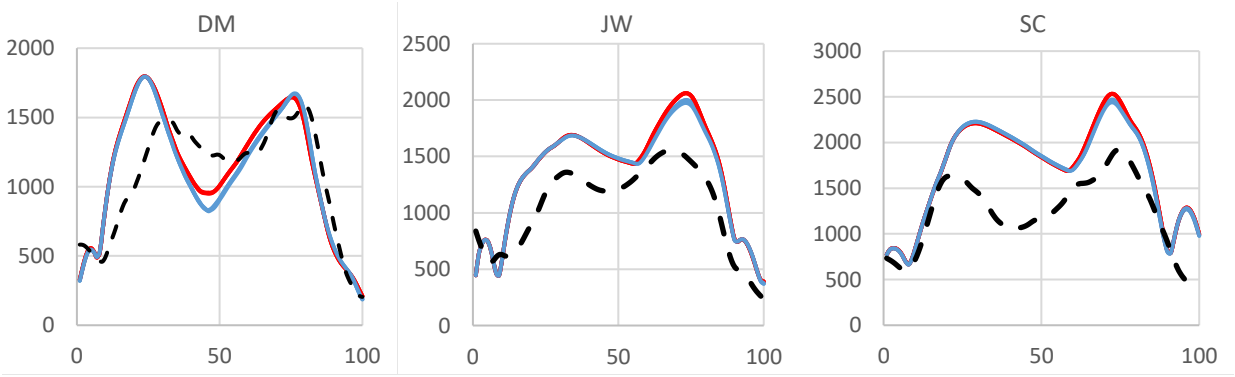

Figure 5-1: Comparison of knee force estimates of subtalar joint orientations models, locked (red) and unlocked (blue), to measured knee loads (dotted black line) for three separate subjects of GKC.

		DevMin	Delp	Inman	locked
DM	RMS (N)	298.93	298.44	299.37	289.5
	RMS/BW	0.44	0.44	0.44	0.42
	p2	0.75	0.75	0.75	0.77
JW	RMS (N)	342.06	341.43	336.48	356
	RMS/BW	0.52	0.52	0.51	0.54
	p2	0.93	0.93	0.93	0.94
SC	RMS (N)	565.11	564.44	562.24	571.9
	RMS/BW	0.82	0.82	0.82	0.83
	p2	0.82	0.82	0.82	0.83

Table 5-2: Calculated RMS and correlation (p^2) values for three subjects from the Grand Knee Challenge, comparing three subtalar joint orientation models (DevMin, Delp, Inman) that were left unlocked and a model with the subtalar joint locked during dynamic analysis.

Even with high RMSE values per bodyweight seen in subject SC, there was good correlation for all subjects when comparing the loading pattern of the simulated values to the measured knee loads. The range of correlation values was between 0.75 to 0.93. According to the scoring metric established by Walter et al (2015), these correlation values fall into the good (0.7-0.9) and strong (0.9-1.0) evaluations (Table 5-2)..

While there was large variability shown in the range of RMSE and p^2 values subject to subject, the differences in intra-subject comparison between subtalar joint orientations was minimal. The largest difference in RMS error between the DevMin, Delp, and Inman orientations when the subtalar joint was left unlocked was 5.58N, a difference of nearly .008 BW. The biggest difference seen for each subject comes from the comparison of the locked subtalar joint to the unlocked conditions. While these are still small, the locked condition showed a slight increase in RMS error for subjects JW and SC while the error decreased from 0.44 to 0.42 for subject DM (Table 5-2). The correlation values increased for all subjects by 0.01 or 0.02 when the subtalar joint was locked during dynamic analysis of normal gait.

There is good agreement for all the muscles that were measured with EMGs, both seen in

the walking and running dynamic tasks, when compared to the model's predicted activations (Figure 5-2). In other words, there was a good match on the timing and overall shape of excitation pattern between the curves. For all the muscles with EMG to validate with, the subtalar joint orientation models all provided very similar activation patterns when left unlocked.

Figure 5-2: EMG-to-activation comparisons of the subtalar joint orientation models for the muscles, (a) GasLat (b) GasMed (c) Soleus and (d) TibAnt muscles for walking and running tasks. In vivo EMG measures (black) are compared against subtalar joint locked (red) and unlocked (blue) model conditions.

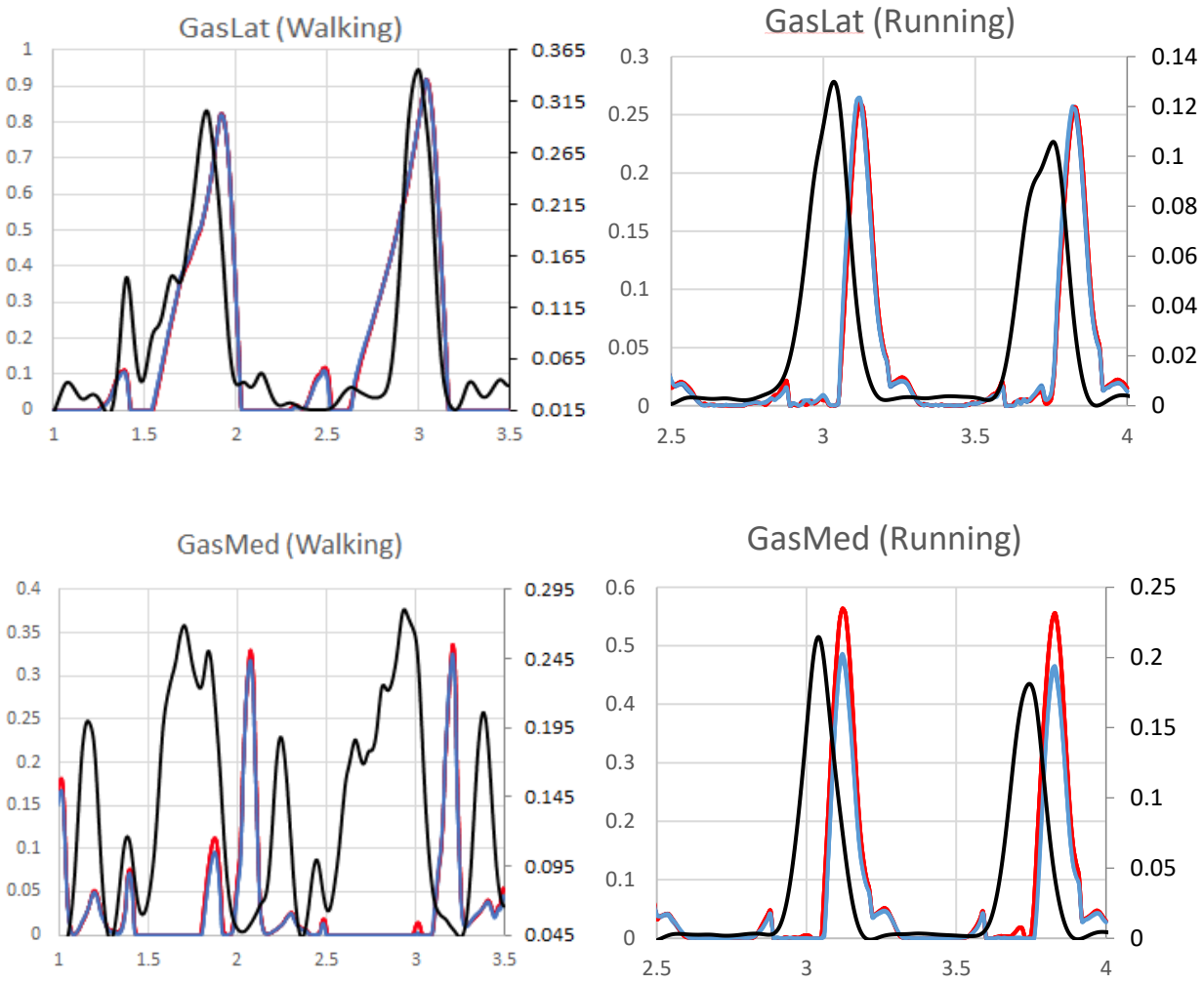

Figure 5-2: continued

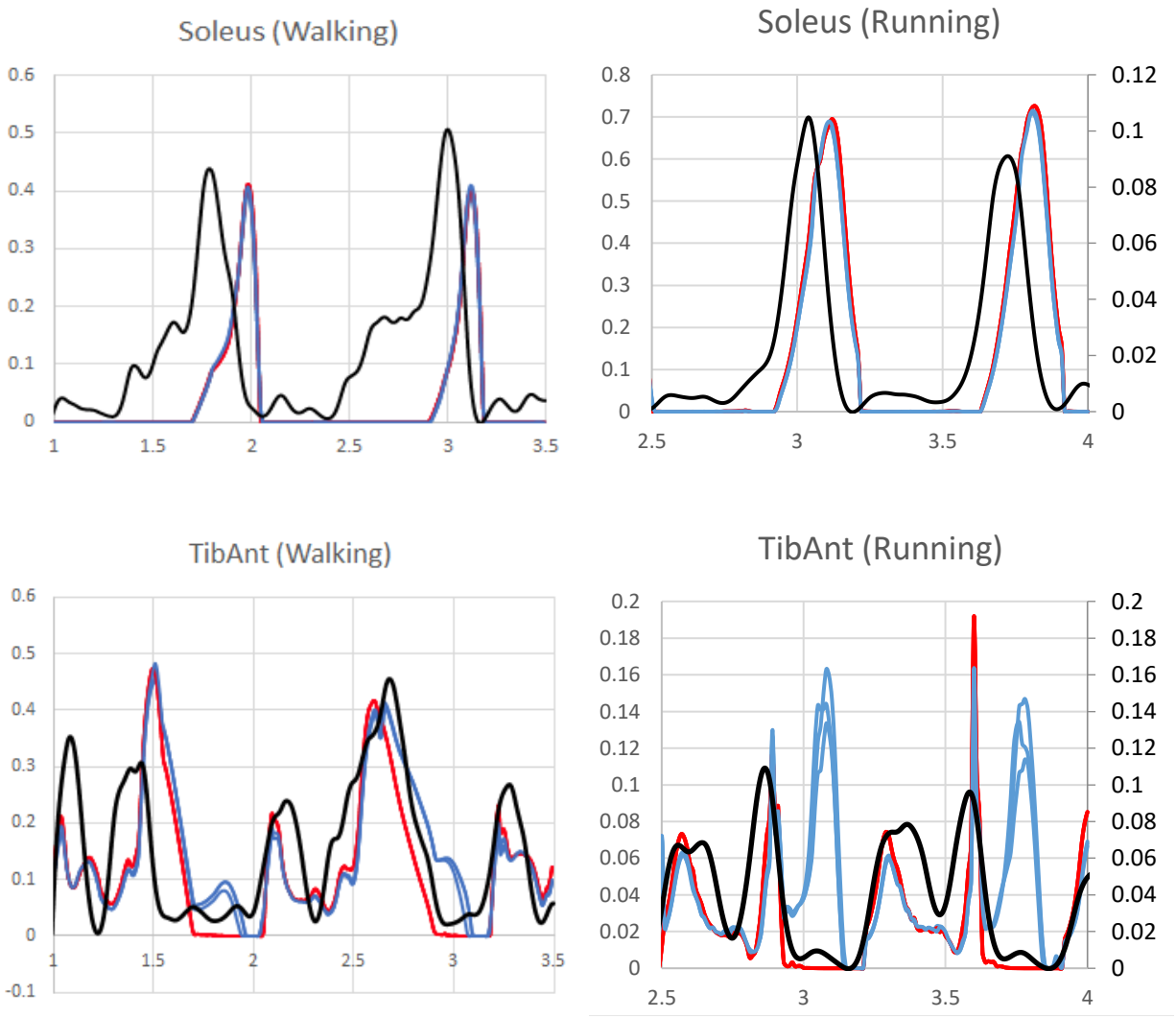

The Tibialis Anterior muscle activation predictions match the timing and shape of the *in vivo* EMG for much of the gait cycle (Figure 5-2d); however, there is a notable difference between locked (red) and unlocked (blue) models indicated with an extra peak in the middle of stance. This peak coincides with the time during stance in which a strong inversion action is prescribed to the subtalar joint. Since the Tibialis Anterior functions as an ankle invertor, the muscle is activated during dynamic motion with the subtalar joint left unlocked. When the subtalar joint is locked in a model, there is no inversion/eversion of the foot. Therefore, the static optimization analysis has no need to activate the muscles for that action. This difference between subtalar joint inclusion conditions is also seen in the activation patterns of the other ankle invertors and evertors, such as: Peroneus Longus, Peroneus Brevis, Flexor Digitorum Longus, Flexor Hallucis Longus, and Tibialis Posterior, though there are no EMGs to compare to (Figure 5-3).

Figure 5-3: Muscle activation comparison of locked (red) and unlocked (blue) subtalar joint in dynamic analysis of walking and running. Muscles examined are (a) TibPost, (b) PerLong, (c) PerBrev, (d) FDL, and (e) FHL.

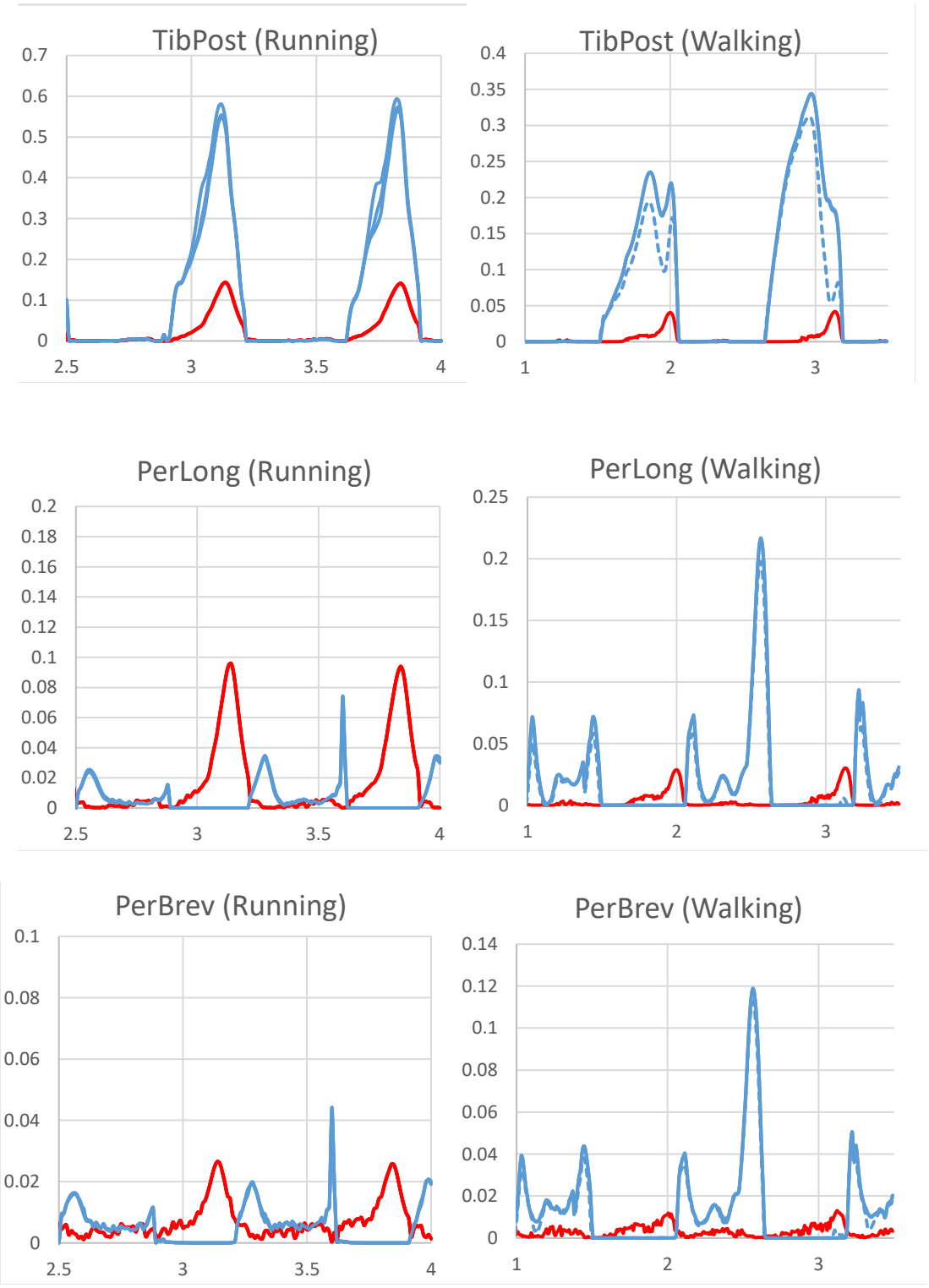

Figure 5-3: continued

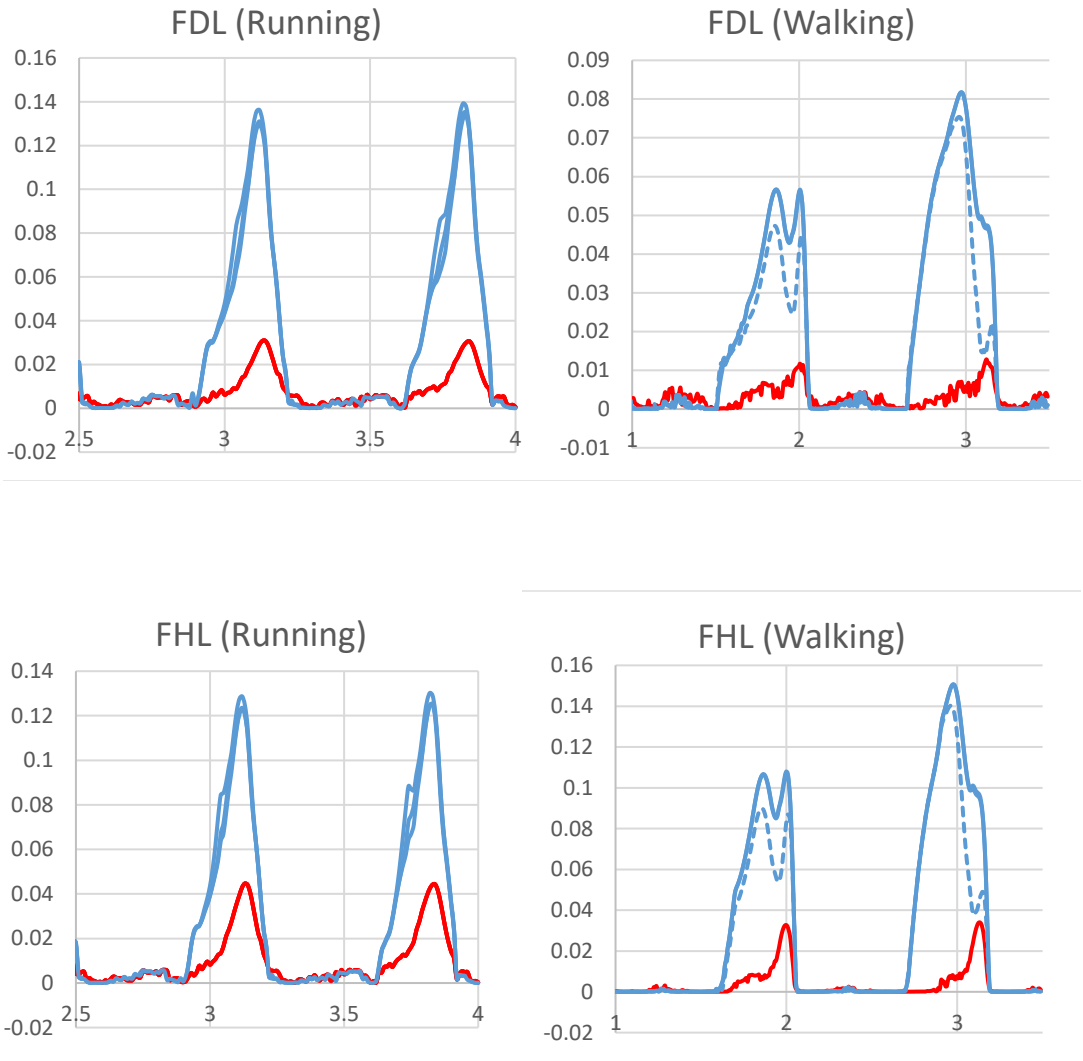

The differences between locked and unlocked subtalar joint conditions were also quantified during dynamic simulation of walking and running. Peak ankle and subtalar joint contact forces were significantly higher when the subtalar joint was left unlocked in analysis of walking, compared to locked conditions for all subtalar joint orientation models (Figure 5-4). All locked models had the same peak subtalar joint contact force at 3.84 N/BW (Table 5-3). The Delp and DevMin orientations were identical, overlapping for the entire stance phase of the graph (Figure 5-4) and have peak values at 4.95 N/BW.

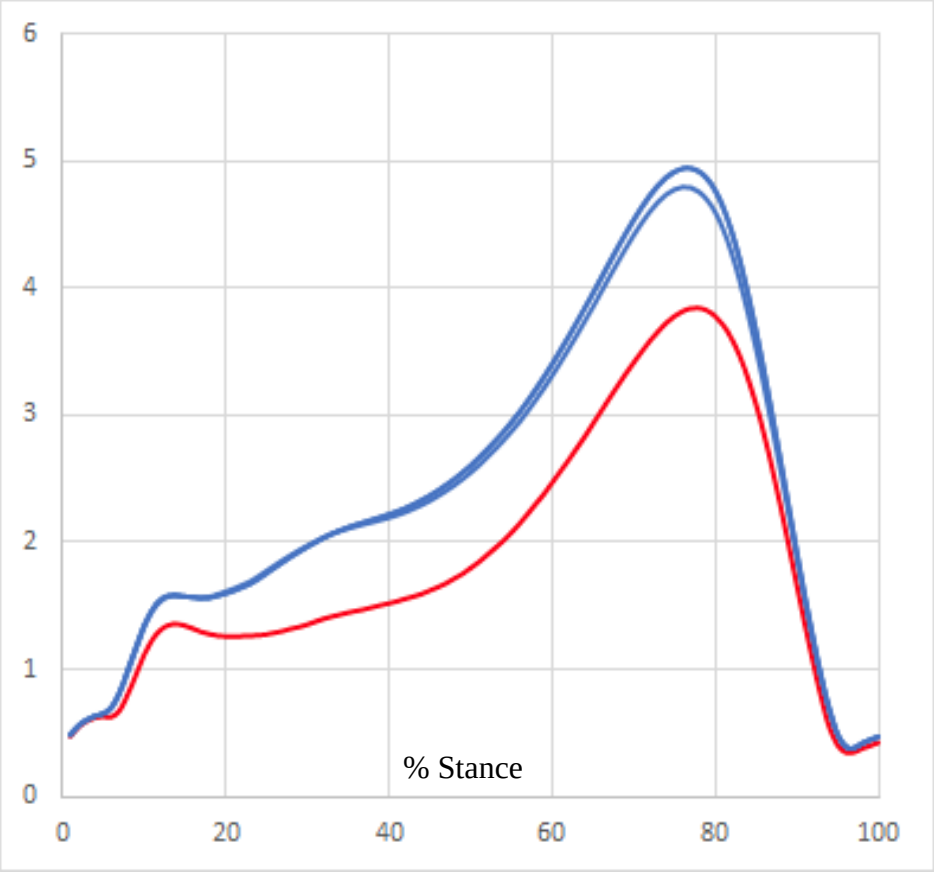

Figure 5-4: Musculoskeletal model prediction of subtalar joint contact forces (N/BW) for stance phase of gait with the subtalar joint locked (red) and unlocked (blue).

	DevMin (N/BW)	Delp (N/BW)	Inman (N/BW)
locked	3.84	3.84	3.84
unlocked	4.95	4.95	4.80
significance	**p=0.03**	**p=0.03**	**p=0.05**

Table 5-3: Peak subtalar joint contact force (N/BW) estimated during walking from the orientation models with the subtalar joint locked and unlocked. Significance set at $p<0.05$

During running, the significant differences were no longer at the ankle and subtalar joint but at the knee (Figure 5-5). The overall peak knee joint contact forces were evaluated for the entire stance phase of running and were found to be significantly higher for the Delp and Inman orientation models when the subtalar joint was kept locked (Table 5-4). Separate analyses of the first and second peaks of the knee loading pattern also yielded significant differences between subtalar joint inclusion conditions across all subtalar joint orientations.

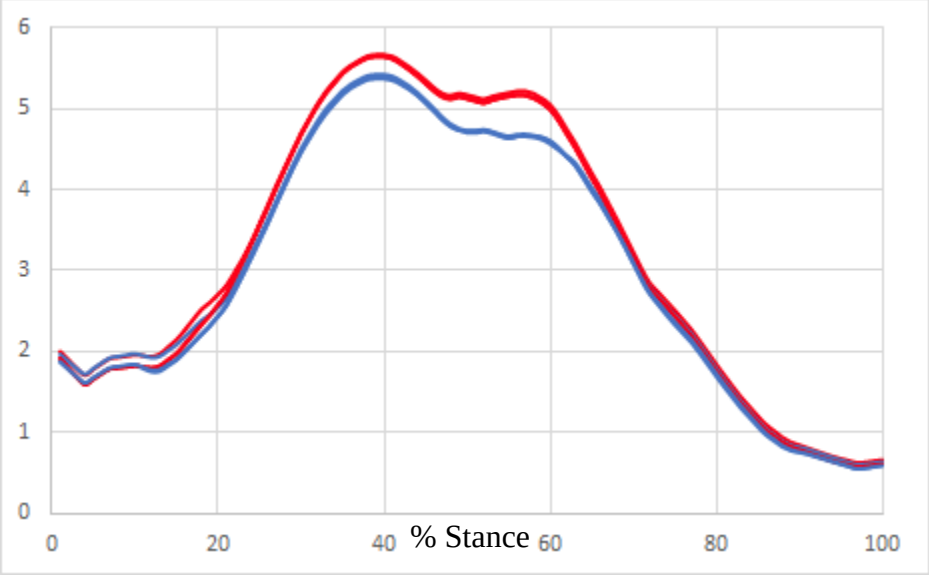

Figure 5-5: Musculoskeletal model prediction of knee joint contact forces for running at 2.0 m/s with the subtalar joint locked (red) and unlocked (blue).

	CT			Gait2392			Inman		
	Lock (N/BW)	Unlock (N/BW)	p value	Lock (N/BW)	Unlock (N/BW)	p value	Lock (N/BW)	Unlock (N/BW)	p value
Total peak	5.88	5.60	0.06	5.93	5.65	**0.05**	5.88	5.57	**0.04**
Peak 1	5.78	5.52	**0.04**	5.82	5.56	**0.04**	5.78	5.50	**0.02**
Peak 2	5.19	4.81	**0.04**	5.23	4.81	**0.05**	5.19	4.79	**0.01**

Table 5-4: Total, first, and second peak comparisons of knee joint contact forces between subtalar joint orientation models with and without the subtalar joint included during analysis of 2 m/s running.

5.4 DISCUSSION

The purposes of this study were to use direct and indirect validation to determine the accuracy of musculoskeletal models to predict joint forces of the lower kinetic chain during walking and running, as well as evaluate the sensitivity of the models to changes in subtalar joint axis definitions when they are included in dynamic simulations. Subject-specific musculoskeletal models were created to evaluate 3 subjects walking, and 3 different subjects running.

In evaluating the results from simulating gait, direct validation is made possible by comparison between estimated knee contact forces and *in vivo* measured knee loads from instrumented tibial implants. The root-mean-square (RMS) for two of the subjects falls within values that have been previously reported by researchers using the GKC data to validate their changes in their models. Subject DM had a predicted RMS of .44 (~299N) across all unlocked subtalar joint axis orientation models, with an RMS of .42 (~289N) when the subtalar joint was kept locked (Table 5-2). Since the subtalar joint is locked from moving from the neutral position, the orientation of its' rotational axis does not matter, and all locked conditions result in similar results. Previous literature reported similar RMS values of .484 for this subject when evaluating blind vs unblind model predictions (Ding et al., 2016) as well as RMS ranges of .37-.51

depending on smooth or bouncy gait (Jung et al., 2016). The models of the subject from the 4th competition (JW) produce similar RMS values of .51-.52 (~340 N) for the knee contact loads across the stance phase of gait. This falls within the previously reported RMS ranges of .32-.653 RMS (Chen et al., 2016; Ding et al., 2016; Lin et al., 2018). In this study, subject SC had reported RMS values of 0.82 (~564 N) across all subtalar joint orientation models. This is nearly double the reported RMS values that previous studies have concluded, which range from .24 to .61, but most reports have RMS values around ~.30-.40 (Chen et al., 2016; Kinney et al., 2013; Knarr and Higginson, 2015; Lin et al., 2018; Lundberg et al., 2013).

Even though the RMS value for SC is higher than what has been previously reported, the Pearson's correlation for each of the three subjects from the GKC are within acceptable values. This is based on the scale established for correlation values as well as comparisons with previously reported values (Walter et al., 2015). According to the scale, subjects DM and SC fall within the “good” criteria (0.7-0.9) with scores of .75-.77 and .82-.83, respectively (Table 5-2). In studies comparing bouncy and smooth gait, the correlation of subject DM was also reported to be within the good criteria with a mean of .748 (Ding et al., 2016; Jung et al., 2016). Similarly, previous studies have reported a range of correlation for subject SC that falls within .74-.94(Chen et al., 2016). In a summary from the GKC competition, Kinney reported that the winners from the third year of the competition (of subject SC) found correlation values falling between 82-.89 (Kinney et al., 2013). The findings of this study match closely with the results of the GKC competition winners with a correlation of .82. When Chen et al (2016). evaluated their model for subject JW during normal walking conditions, the estimated knee contact load matched measured with a correlation ranged between 0.76-0.81. The findings of this study show a higher correlation between predicted and measured knee loads. When comparing the model

output measures for knee joint contact force to *in vivo*, the correlation for subject JW falls within the "strong" (0.9-1.0) correlation criteria with a correlation coefficient of 0.93-.94. Because the RMS and/or correlation coefficients fall within acceptable ranges that have been previously reported, it can be concluded that the musculoskeletal models are valid for estimating knee joint contact forces during normal gait.

The next question is if these same musculoskeletal models are just as valid to estimate knee contact forces during more dynamic tasks, such as running, when there are no *in vivo* measurements collected simultaneously from instrumented knee implant. One way to determine this is by comparing how well the models predict muscle activation patterns, during both motions, and how closely these match to the EMG signals collected concurrently. Both the walking and running datasets include EMG signals of the Gastrocnemius (lateral and medial), Soleus, and Tibialis Anterior. For all of these major ankle muscles, the EMG collected is a very close match to the predicted muscle activations from the static optimization analysis. There is a slight time delay seen in running from when the EMG signal is picked up and this is consistently the same time delay for all muscles (Figure 5-2a). The time delay in the EMG during walking had already been accounted for before analyzing through OpenSim. However, there is still a longer delay seen in the Gastrocmedius and Soleus muscles during cycles of walking (Figure 5-2 b&c). Because the subjects from the GKC needed total knee replacement, it can be assumed that their muscles have been affected in comparison to healthy and active runners from the running dataset. While there is a delay in muscle activation for these two muscles during walking, the overall shape of the activation still looks similar and can be concluded to be valid. Other researchers that have compared EMG to model activatiaons of GasLat, GasMed, Soleus, and TibAnt muscles have also relied on qualitative assessment to determine how well the model

predictions match measured outputs (Chen et al., 2014; Hamner and Delp, 2013; Lin et al., 2018; Walter et al., 2015). The EMG-to-activation comparisons in this study match closely with that from Chen et al (2014). In both studies, the predicted the Tibialis Anterior muscle produced a smaller peak in the middle of stance phase and there was a slight delay in peak medial Gastrocnemius activation in comparison to the peak of the measured EMG. The authors of that study determined that the predicted activations were consistend with transformed EMG(Chen et al., 2014). Since the running dataset shows just as good of a match in EMG-to-muscle activation comparison, if not a better one than what is seen in the walking dataset, it can be assumed that the musculoskeletal model will do just as well in predicting knee contact loads of running as compared to walking.

The subtalar joint is often left out of biomechanical models or held “locked” in a neutral position during dynamic analysis. In doing so, the major contributions of the subtalar joint to overall ankle-complex inversion and eversion are being ignored. This is seen by the qualitative differences in muscle activations of the FHL, FDL, TibPost, and TibAnt (Figure 5-3). For these muscles, there is a large activation seen during the stance phase that is not seen when the subtalar joint is locked. This makes sense as these muscles are known as the primary foot invertors, and when the subtalar joint is “locked” or kept neutral, there would be no activation coming from these muscles as there would be when the subtalar joint is left unlocked and able to perform its function of inversion. Similarly, there are differences seen in the Peroneals (PerLong and PerBrev) when comparing between subtalar joint inclusion conditions. The differences seen in locked vs unlocked for these muscles has to do with a shift in activation timing rather than by peak activations observed. The Peroneal muscles in the unlocked subtalar joint models show muscle activations that occur later in the stance phase that relate closely to eversion of the foot.

When the subtalar joint is held locked, it is grouped with the talocrural and together treated as a 1DOF joint so the only activations that would be seen for these muscles would occur as part of dorsiflexion motion.

The comparisons between muscle activations cannot be normalized and are qualitative based on patterns seen in the figures, however, there were quantitatively significant differences found between locked and unlocked subtalar joint models when comparing contact force predictions from joint reaction analysis. When analyzing the motion of straight path walking, there were significant differences in peak talocrural and subtalar joint contact forces between locked and unlocked conditions for all subtalar joint orientation models (Figure 5-4). For all orientations, the unlocked condition resulted in larger compressive forces at the joints of the ankle than when the subtalar joint is left out, or locked. With increased complexity of motion with speed, i.e. walking to running, the subtalar joint compressive loads were no longer significantly affected by subtalar joint inclusion. This is likely because the subtalar joint acts as a rigid body during running to allow for quick push-off to the next swing phase. However, the findings of this study show that the inclusion of the subtalar joint in models affects joints within the kinetic chain, i.e. the knee (Figure 5-5) during dynamic tasks. Analysis of both peaks of the knee loading pattern resulted in significant differences between locked and unlocked subtalar joint conditions, not dependent on axis orientation (Table 5-4). For both peaks, the locked condition resulted in larger knee joint reaction forces, with the difference being more notable during the second peak around ~60% of the stance phase of running. The significant differences between the locked and unlocked joint reaction analysis could be due to the differences in muscle activations between inclusion conditions. While the ankle invertor/evertor muscles activations and relative contributions are small in comparison to the larger measured activations

of gastrocnemius and soleus, together the function units may be enough to ellicit the significant change.

One limitation of this study is that there is no way to easily measure and validate the ankle muscles through non-invasive EMG or the internal joint contact forces through implants like is possible for the knee. This study concludes through indirect validation that the knee contact loads can be accurately predicted using the musculoskeletal models validated for walking. When running data is made available for subjects with instrumented knee implants, it should be used to directly validate the results of musculoskeletal models to confirm that they can accurately predict knee loads for various dynamic tasks. In the current literature, many investigators make qualitative assessments of the EMG and estimated muscle activation comparisons. Future work should focus on establishing a standard or quantifiable way of comparing measured EMG and predicted muscle activations that can be used by all researchers evaluating validity based on EMGs alone. Furthermore, the datasets used in this study evaluated walking and running in a straight path on even ground. Since the subtalar joint is a major contributor to inversion/eversion, validation of motions such as cutting or walking on uneven ground may better capture the importance of inclusion during dynamic analysis.

5.5 CONCLUSION

This study showed that the musculoskeletal models created from openly available datasets can accurately approximate knee contact loads for walking, by directly validating using instrumented knee implant loads. The validity of the musculoskelal model during gait was used to evaluate if the model would be just as accurate in predicting knee loads during a more dynamic task, such as running. This was done by comparing EMG-to-muscle activation

relationships between both tasks of major knee and ankle muscles. Since the models predict muscle activation just as well during running as they do during walking, then we can conclude that the musculoskeletal models will be able to estimate knee contact loads within good approximation.

This study also showed that for both walking and running, the models are sensitive to the inclusion of the subtalar joint during dynamic simulations. This is an important result as the mtp and subtalar joint are often left locked in biomechanical analyses. The results show that there are significant differences in muscle activations for the foot invertors (FHL, FDL, TibPost, TibAnt) as well as evertors (Peroneals). Since the main difference between inverse dynamics and joint reaction analysis is the consideration from muscle forces, the combined differences of the function groups together may account for the significant difference in talocrural and subtalar joint contact force during walking and significant knee contact force during running. A limitation of this study is that there is no way to easily measure and validate the ankle muscles through non-invasive EMG or the internal joint contact forces through implants like is possible for the knee. This study concludes through indirect validation that the knee contact loads can be accurately predicted using the musculoskeletal models validated for walking. Future work should focus on establishing a standard or quantifiable way of comparing measured EMG and predicted muscle activations that can be used by all researchers evaluating validity based on EMGs alone. Also, when running data is available for subjects with instrumented knee implants, it should be used to directly validate the results of musculoskeletal models to confirm that they can accurately predict knee loads for various dynamic tasks.

CHAPTER 6: CONCLUSION AND SUMMARY

The subtalar joint is responsible for stabilizing the foot as it transmits load during heel strike to toe off to the rest of the lower kinetic chain as well as adapting the foot to sloped or uneven terrain walking. The mobility provided by the subtalar joint is due to the combined tri-planar motion of pronation/supination. Musculoskeletal models often simplify the subtalar joint by leaving it out of models, "locking" it with the ankle, or treating the multi-axial rotations as just a 1 DOF axis of rotation that acts as a hinge. When the subtalar joint is accounted for in biomechanical analyses, the axis definition may not adequately represent realistic approximations. This serves as a possible problem in modeling as the function of surrounding muscles and motion of the subtalar joint is dependent on the descriptions in relation to the subtalar joint axis. There is a growing trend in biomechanical modeling to create subject specific models, thus, it is critical to consider the definition of the subtalar joint axis in computational modeling. Understanding how best to define the subtalar joint axis is important to be able to validate musculoskeletal model during dynamic simulations, like walking or running.

The overall goal of this dissertation was to evaluate the sensitivity of musculoskeletal models to changes in subtalar joint axis definition and determine how valid they are at computing muscle and joint measures during dynamic tasks of walking and running through direct and indirect comparisons. This problem was addressed with three separate studies aimed at comparing results from inverse kinematics, inverse dynamics, static optimization, and joint reaction analyses when there were changes to subtalar joint: (1) coordinate system origin location, (2) axis orientation, and (3) inclusion consideration (locked vs unlocked). The musculoskeletal models were validated using direct comparison to *in vivo* measures obtained during normal gait of knee joint load through instrumented tibial implant and muscle activations

through EMG collection. Indirect comparisons included relating the computed results to previously reported literature and previously validated models. The findings of this dissertation conclude that when the subtalar joint is included in a musculoskeletal model and the axis orientation is going to be modified to reflect subject-specific axes or inclination/deviation angles that match *in vivo* weight-bearing conditions, then the accuracy in origin location of the axis should be considered first.

Moving the location of the subtalar joint axis origin from the back side of the heel (-Heel) to the ankle (-Ankle) significantly affects the average muscle moment arms of many of the key ankle muscles (peroneus brevis, tibialis posterior, and tibialis anterior). This significance is seen when modifying the subtalar joint axis orientation to match Inman's mean inclination/deviation angles. The default orientation used, established by Delp geometrically, finds the subtalar joint orientation as the intersecting line between the points defining the distal heel and distal talus. While this resulting axis with inclination (37.2°) and deviation angles (8.7°) fall within the range as defined by Inman, it still greatly varies from the mean of 42° and 23°, respectively (Delp et al., 1990; Isman and Inman, 1969). When using the origin location on the base of the heel, change in orientation affects where and how the subtalar joint axis crosses through the talus. With the large variation in deviation angle seen in Inman's axis, the muscles such as the tibialis anterior and EHL fall on the lateral aspect of the axis. This gives the muscles that invert the ankle the function of ankle evertors in these models. Moving the origin location to the ankle origin reduces the average muscle moment arms values to more realistic measures as the moment arm distance is closer. Even with the ankle location, the difference in orientations between Delp and Inman models, primarily in the deviation angle, results in very slight evertor action from the tibialis anterior and EHL. As seen in Chapter 3, the choice in subtalar joint coordinate system

origin location significantly affects muscle moment arm, but it also affects the sensitivity of musculoskeletal models when there are changes to joint axis orientation and inclusion.

When using the origin location at the heel, knee joint reaction forces during walking were found to be significantly different at the second peak of the knee loading curve for all the models in which the deviation angles were manipulated (DevMax -0.03, DevMin -0.02, and Inman –0.03). Lower down the kinetic chain, the ankle and STJ reaction forces were both significantly different for DevMin and Inman with p=0.01 for both. This is also seen in more dynamic tasks, running at 2.0 and 5.0 m/s, where both peaks of the knee contact force distribution had significantly different values when comparing CT and Inman orientations. These two models have similar inclination angles but highly differ in deviation angles. All of these differences in joint reaction force predictions seen across the three speeds of motion disappeared when the updated ankle location was utilized for the subtalar joint origin. In other words, if the corrected -Ankle origin location is used when evaluating knee and ankle joint contact forces, then the choice in subtalar joint orientation does not bring about any significant changes in knee and ankle contact forces. Therefore, a generic orientation would be acceptable. However, the results in Chapter 4 show that the choice in subtalar joint orientation, not dependent on origin location, does significantly affect subtalar joint moment calculations for all orientation models compared to the default orientation. The results show that the model with the largest deviation angle produces the largest peak STJ moment (DevMax for walking, Inman for running), while the model with the largest inclination has the smallest peak subtalar joint moment (IncMax for walking, CT for running).

The origin location also affects how significant inclusion of the subtalar joint is during dynamic analysis. When keeping the location of the STJ origin at the heel, there are significant

differences for DevMax (p=0.04) and Inman (p=0.05) models when comparing between locked and unlocked knee joint reaction estimates. In the ankle/subtalar joint, the DevMax (p=0.03), IncMin (.01) and Inman (p=0.00) models produce significantly different contact forces between STJ inclusion conditions while walking. During running 2 m/s, there were significant differences in peak knee joint loads between locked and unlocked old-origin locations for Inman and CT models (p=0.03). Even with the origin location moved, there are still significant differences in gait model comparisons between locked and unlocked conditions, though the models that are significantly affected are different. Where before DevMax was significantly different when the Heel location was used, with the Ankle origin location implemented, the models that are significantly different locked vs unlocked are DevMin, Delp, and IncMin and only for the ankle/subtalar joint contact forces. Conversely, during running, the significant differences between locked and unlocked subtalar joint models were seen for both peaks of the knee loading curve across all subtalar joint orientation models. Furthermore, when the origin location is found at the ankle, "locking" the subtalar joint also shows significant differences in major invertor/evertor muscle activation patterns that are computed during static optimization. This supports the conclusion that locking the joint treats it and the adjacent ankle as just one-joint complex. These differences in muscle activation likely work together as functional muscle units and contribute to the significant differences in subtalar/ankle and knee joint contact forces seen during walking and running, respectively. The findings show that even when using realistic *in vivo* weightbearing inclination/deviation angles, there are significant differences not just in the subtalar joint but in the following knee joint when the subtalar joint is locked. Therefore, the subtalar joint is vital to the transmission of loads to the surrounding joints of the kinetic chain.

The origin location also affects how significant inclusion of the subtalar joint is during dynamic analysis. When keeping the location of the STJ origin at the heel, there are significant differences for DevMax (p=0.04) and Inman (p=0.05) models when comparing between locked and unlocked knee joint reaction estimates. In the ankle/subtalar joint, the DevMax (p=0.03), IncMin (.01) and Inman (p=0.00) models produce significantly different contact forces between STJ inclusion conditions while walking. During running 2 m/s, there were significant differences in peak knee joint loads between locked and unlocked old-origin locations for Inman and CT models (p=0.03). Even with the origin location moved, there are still significant differences in gait model comparisons between locked and unlocked conditions, though the models that are significantly affected are different. Where before DevMax was significantly different when the Heel location was used, with the Ankle origin location implemented, the models that are significantly different locked vs unlocked are DevMin, Delp, and IncMin and only for the ankle/subtalar joint contact forces. Conversely, during running, the significant differences between locked and unlocked subtalar joint models were seen for both peaks of the knee loading curve across all subtalar joint orientation models. Furthermore, when the origin location is found at the ankle, “locking” the subtalar joint also shows significant differences in major invertor/evertor muscle activation patterns that are computed during static optimization. This supports the conclusion that locking the joint treats it and the adjacent ankle as just one-joint complex. These differences in muscle activation likely work together as functional muscle units and contribute to the significant differences in subtalar/ankle and knee joint contact forces seen during walking and running, respectively. The findings show that even when using realistic *in vivo* weightbearing inclination/deviation angles, there are significant differences not just in the

subtalar joint but in the following knee joint when the subtalar joint is locked. Therefore, the subtalar joint is vital to the transmission of loads to the surrounding joints of the kinetic chain.

The data obtained in this study also came with in vivo measures which allow for direct validation between musculoskeletal model's predictions and realistic values. RMS and correlation values were calculated for each of the three walking subjects between knee joint reaction forces in OpenSim and the eTibia knee loads measured from instrumented knee implants. The computed results fell within previously reported values RMS and correlation scoring standards. Through this data we can confidently conclude that our musculoskeletal model is valid for computing muscle and joint measures during walking. Both walking and running datasets also provided skin EMG data to compare to muscle activations of major knee and ankle muscles. When evaluating how the EMG-to-activation comparisons match for both motions, it was determined that the musculoskeletal model does just as well at predicting the muscle patterns while running as it does during normal gait. Using the established validity of the model during walking as indirect validation, it can be concluded that the model will be able to accurately predict knee joint loads during running.

Future work from this dissertation should focus on using in vivo collected knee loads during running to directly validate the predicted values from musculoskeletal models to fully understand the internal and external forces acting within the knee during stance phase. Similarly, one limitation of this study is that due to the muscles relative size and depth within the leg, there is no easily accessible and noninvasive way (i.e. skin EMG) of measuring the finer ankle muscles' activations or the *in vivo* ankle and subtalar joint contact forces to validate against predicted. Another limitation of this study is that the motion analyzed, walking and running, primarily occur in the sagittal plane. Since the subtalar joint is involved in contributing to foot

inversion/eversion, it is necessary to evaluate the importance of the joint during more complex motions. Therefore, future work will aim to evaluate the inclusion of the subtalar joint in musculoskeletal models during simulation of cutting or walking on uneven terrain, where the role of the subtalar joint is more prominent.

REFERENCES

Almonroeder, T., Willson, J.D., Kernozek, T.W., 2013. The Effect of Foot Strike Pattern on Achilles Tendon Load During Running. Annals of Biomedical Engineering 41, 1758-1766.

Andersen, M.S., 2018. How sensitive are predicted muscle and knee contact forces to normalization factors and polynomial order in the muscle recruitment criterion formulation. International Biomechanics 5, 88-103.

Anderson, F.C., Pandy, M.G., 2001. Static and dynamic optimization solutions for gait are practically equivalent. Journal of Biomechanics 34, 153-161.

Arndt, A., Westblad, P., Winson, I., Hashimoto, T., Lundberg, A., 2004. Ankle and Subtalar Kinematics Measured With Intracortical Pins During the Stance Phase of Walking. Foot & Ankle International 25, 357-364.

Aynardi, M., Pedowitz, D.I., Raikin, S.M., 2015. Subtalar Instability. Foot and Ankle Clinics 20, 243-252.

Baeyens, J.P., Cattrysse, E., Roy, P.V., Clarys, J.P., 2005. Measurement of three-dimensional intra-articular kinematics: methodological and interpretation problems. Ergonomics 48, 1638-1644.

Bahr, R., Pena, F., Shine, J., Lew, W.D., Engebretsen, L., 1998. Ligament force and joint motion in the intact ankle: a cadaveric study. Knee Surgery, Sports Traumatology, Arthroscopy 6, 115-121.

Ball, K.A., Greiner, T.M., 2008. On the problems of describing joint axis alignment. Journal of Biomechanics 41, 1599-1603.

Beimers, L., Tuijthof, G.J.M., Blankevoort, L., Jonges, R., Maas, M., Dijk, C.N.v., 2008. In vivo range of motion of the subtalar joint using computed tomography. Journal of Biomechanics 41, 1390-1397.

Berme, N., Cappozzo, A., Meglan, J., 1990. Rigid body mechanics as applied to human movement studies. Biomechanics of human movement: Applications in rehabilitation, sports and ergonomics, 89-102.

Birch, I., Deschamps, K., 2014. Dynamic in Vivo Subtalar Joint Kinematics Measured Using a Skin Marker-Based Protocol: A Face Validity Study. Journal of the American Podiatric Medical Association 104, 357-364.

Bogert, A.J.v.d., Smith, G.D., Nigg, B.M., 1994. In Vivo Determination of the Anatomical Axes of the Ankle Joint Complex: An Optimization Approach. Journal of Biomechanics 27, 1477-1488.

Bonnel, F., Toullec, E., Mabit, C., Tourne, Y., Sofcot, 2010. Chronic ankle instability: Biomechanics and pathomechanics of ligaments injury and associated lesions. Orthopaedics & Traumatology: Surgery & Research 96.

Brantigan, J.W., Pedegana, L.R., Lippert, F.G., 1977. Instability of the Subtalar Joint: Diagnosis by Stress Tomography in Three Cases. The Journal of Bone & Joint Surgery 59.

Brockett, C.L., Chapman, G.J., 2016. Biomechanics of the ankle. Journal of Orthopaedic Trauma 30, 232-238.

Brown, K.M., Bursey, D.E., Arneson, L.J., Andrews, C.A., Ludewig, P.M., Glasoe, W.M., 2009. Consideriation of digitization precision when building local coordinate axes for a foot model. Journal of Biomechanics 42, 1263-1269.

Budny, A., 2004. Subtalar joint instability: current clinical concepts. Clinics in Podiatric Medicine and Surgery 21, 449-460.

Carson, M.C., Harrington, M.E., Thompson, N., O'Connor, J.J., Theologis, T.N., 2001. Kinematic analysis of a multi-segment foot model for research and clinical applications: a repeatability analysis. Journal of Biomechanics 34, 1299-1307.

Chan, C.W., Rudins, A., 1994. Foot Biomechanics During Walking and Running. Mayo Clinic Proceedings 69, 448-461.

Chen, Z., Zhang, X., Ardestani, M.M., Wang, L., Liu, Y., Lian, Q., He, J., Li, D., Jin, Z., 2014. Prediction of in vivo joint mechanics of an artificial knee implant using rigid multi-body dynamics with elastic contacts. Proceedings of the Institution of Mechanical Engineering, Part H 228, 564-575.

Chen, Z., Zhang, Z., Wang, L., Li, D., Zhang, Y., Jin, Z., 2016. Evaluation of a subject-specific musculoskeletal modelling framework for load prediction in total knee arthroplasty. Medical Engineering and Physics 38, 708-716.

Choisne, J., Hoch, M.C., Bawab, S., Alexander, I., Ringleb, S.I., 2013. The Effects of a Semi-Rigid Ankle Brace on a Simulated Isolated Subtalar Joint Instability. Journal of Orthopaedic Research 31, 1869-1875.

Choisne, J., Ringleb, S.I., Samaan, M.A., Bawab, S.Y., Naik, D., Anderson, C.D., 2012. Influence of kinematic analysis methods on detecting ankle and subtalar joint instability. Journal of Biomechanics 45, 46-52.

Close, J.R., Inman, V.T., Poor, P.M., Todd, F.N., 1967. The Function of the Subtalar Joint. Clinical Orthopaedics and Related Research 50, 159-180.

Correa, T.A., Baker, R., Graham, H.K., Pandy, M.G., 2011. Accuracy of generic musculoskeletal models in predicting the functional roles of muscles in human gait. Journal of Biomechanics 44, 2096-2105.

Delp, S.L., Loan, J.P., Hoy, M.G., Zajaz, F.E., topp, E.L., Rosen, J.M., 1990. An Interactive Graphics-Based Model of the Lower Extremity to Study Orthopaedic Surgical Procedures. IEEE Transactions on Biomedical Engineering 37, 757-767.

Dettwyler, M., Stacoff, A., Quervain, I.A.K.-d., Stussi, E., 2004. Modelling of the ankle joint complex. Reflections with regards to ankle prostheses. Foot and Ankle Surgery 10.

Ding, Z., Nolte, D., Tsang, C.K., Cleather, D.J., Kedgley, A.E., Bull, A.M.J., 2016. In Vivo Knee Contact Force Prediction Using Patient-Specific Musculoskeletal Geometry in a Segment-Based Computational Model. Journal of Biomechanical Engineering 138, 021018.

Engsberg, J.R., 1987. A Biomechanical Analysis of the Talocalcaneal Joints - In Vitro. Journal of Biomechanics 20, 429-442.

Falisse, A., Rossom, S.v., Gijsbers, J., Steenbrink, F., 2018. OpenSim Versus Human Body Model: A Comparison Study for the Lower Limbs During Gait. Journal of Applied Biomechanics 34, 496-502.

Fernandez, M.P., Hoxha, D., Chan, O., Mordecai, S., Blunn, G.W., Tozzi, G., Goldberg, A., 2020. Centre of Rotation of the Human Subtalar Joint Using Weight-Bearing Clinical Computed Tomography. Scientific Reports 10.

Fregly, B.J., Besier, T.F., Lloyd, D.G., Delp, S.L., Banks, S.A., Pandy, M.G., D'Lima, D.D., 2012. Grand challenge competition to predict in vivo knee loads. Journal of Orthopaedic Research 30, 503-513.

Fujii, T., Kitaoka, H.B., Watanabe, K., Luo, Z.-P., An, K.-N., 2010. Ankle Stability in Simulated Lateral Ankle Ligament Injuries. Foot & Ankle International 31, 531-537.

Gardinier, E.S., Manal, K., Buchanan, T.S., Snyder-Mackler, L., 2013. Minimum detectable change for knee joint contact force estimates using an EMG-driven model. Gait & Posture 38, 1051-1053.

Grood, E.S., Suntay, W.J., 1983. A Joint Coordinate System for the Clinical Description of Three-Dimensional Motions: Application to the Knee. Journal of Biomechanical Engineering 105, 136-144.

Hamner, S.R., Delp, S.L., 2013. Muscle contributions to fore-aft and vertical body mass center accelerations over a range of running speeds. Journal of Biomechanics 46, 780-787.

Hast, M.W., Piazza, S.J., 2013. Dual-Joint Modeling for Estimation of Total Knee Replacement Contact Forces During Locomotion. Journal of Biomechanical Engineering 135, 021013.

Hicks, J.L., Uchida, T.K., Seth, A., Rajagopal, A., Delp, S.L., 2015. Is My Model Good Enough? Best Practices for Verification and Validation of Musculoskeletal Models and Simulations of Movement. Journal of Biomechanical Engineering 137, 020905.

Irmischer, B.S., 2017. Hip Mechanics of Unilateral Drop Landing. Old Dominion University
Isman, R.E., Inman, V.T., 1969. Anthropometric Studies of the Human Foot and Ankle. Bulletin of Prosthetics Research, 97-129.

Ito, K., Hosoda, K., Shimizu, M., Ikemoto, S., Nagura, T., Seki, H., Kitashiro, M., Imanishi, N., Aiso, S., Jinzaki, M., Ogihara, N., 2017. Three-dimensional innate mobility of the human foot bones under axial loading using biplane X-ray fluoroscopy. Royal Society Open Science 4, 171086.

Jastifer, J.R., Gustafson, P.A., 2014. The subtalar joint: Biomechanics and functional representations in the literature. The Foot, 203-209.

Jenkyn, T.R., Nicol, A.C., 2007. A multi-segment kinematic model of the foot with a novel definition of forefoot motion for use in clinical gait analysis during walking. Journal of Biomechanics 40, 3271-3278.

Jung, Y., Phan, C.-B., Koo, S., 2016. Intra-Articular Knee Contact Force Estimation During Walking Using Force-Reaction Elements and Subject-Specific Joint Model. Journal of Biomechanical Engineering 138, 021016.

Kakihana, W., Akai, M., Nakazawa, K., Takashima, T., Naito, K., Torii, S., 2005. Effects of Laterally Wedged Insoles on Knee and Subtalar Joint Moments. Archives of Physical Medicine and Rehabilitation 86.

Keefe, D.T., Haddad, S.L., 2002. Subtalar instability: Etiology, diagnosis, and management. Foot and Ankle Clinics 7, 577-609.

Kinney, A.L., Besier, T.F., D'Lima, D.D., Fregly, B.J., 2013. Update on Grand Challenge Competition to Predict in Vivo Knee Loads. Journal of Biomechanical Engineering 135, 021012.
Kirby, K.A., 1987. Methods for Determination of Positional Variations in the Subtalar Joint Axis. Journal of the American Podiatric Medical Association 77, 228-234.

Kirtley, C., Whittle, M.W., Jefferson, R.J., 1985. Influence of walking speed on gait parameters. Journal of Biomedical Engineering 7, 282-288.

Kjaersgaard-Andersen, P., Wethelund, J.-O., Nielsen, S., 1987. Lateral Talocalcaneal Instability Following Section of the Calcaneofibular Ligament: A Kinesiologic Study. Foot & Ankle International 7, 355-361.

Klein, P., Mattys, S., Rooze, M., 1996. Moment Arm Length Variations of Selected Muscles Acting on Talocrural and Subtalar Joints During Movement: An In Vitro Study. Journal of Biomechanics 29, 21-30.

Knarr, B.A., Higginson, J.S., 2015. Practical approach to subject-specific estimation of knee joint contact force. Journal of Biomechanics 48, 2897-2902.

Lai, A.K.M., Arnold, A.S., Wakeling, J.M., 2017. Why are Antagonist Muscles Co-activated in My Simulation? A Musculoskeletal Model for Analysing Human Locomotor Tasks. Annals of Biomedical Engineering 45, 2762-2774.

Langelaan, E.J.v., 1983. A kinematical analysis of the tarsal joints. An X-ray photogrammetric study. Acta Orthopaedic Scandinavica 204, 1-269.

Leardini, A., Stagni, R., O'Connor, J.J., 2001. Mobility of the subtalar joint in the intact ankle complex. Journal of Biomechanics 34, 805-809.

Leitch, J., Stebbins, J., Zavatsky, A.B., 2010. Subject-specific axes of the ankle joint complex. Journal of Biomechanics 43, 2923-2928.

Lewis, G.S., Cohen, T.L., Seisler, A.R., Kirby, K.A., Sheehan, F.T., Piazza, S.J., 2009. In vivo tests of an improved method for functional location of the subtalar joint axis. Journal of Biomechanics 42, 146-151.

Lewis, G.S., III, H.S.S., Piazza, S.J., 2006. In Vitro Assessment of a Motion-Based Optimization Method for Locating the Talocrural and Subtalar Joint Axes. Journal of Biomechanical Engineering 128, 596-603.

Lewis, G.S., Kirby, K.A., Piazza, S.J., 2007. Determination of subtalar joint axis location by restriction of talocrural joint motion. Gait & Posture 25, 63-69.

Lin, Y.-C., Walter, J.P., Pandy, M.G., 2018. Predictive Simulations of Neuromuscular Coordination and Joint-Contact Loading in Human Gait. Annals of Biomedical Engineering 46, 1216-1227.

Lloyd, D.G., Besier, T.F., 2003. An EMG-driven musculoskeletal model to estimate muscle forces and knee joint moments in vivo. Journal of Biomechanics 36, 756-776.

Lundberg, A., Svensson, O.K., 1993. The axes of rotation of the talocalcaneal and talonavicular joints. The Foot 3, 65-70.

Lundberg, A., Svensson, O.K., Nemeth, G., Selvik, G., 1989. The Axis of Rotation of the Ankle Joint. The Journal of Bone & Joint Surgery 71, 94-99.

Lundberg, H.J., Knowlton, C., Wimmer, M.A., 2013. Fine Tuning Total Knee Replacement Contact Force Prediction Algorithms Using Blinded Model Validation. Journal of Biomechanical Engineering 135, 021015.

Maceira, E., Monteagudo, M., 2015. Subtalar Anatomy and Mechanics. Foot and Ankle Clinics 20, 195-221.

Maheshwari, J., 2014. Analysis of the Human Musculoskeletal System and Simulation-Based Design of Assistive Devices Using OpenSim. Birla Institute of Technology and Science, pp. 1-45.

Malaquias, T.M., Silveira, C., Aerts, W., Groote, F.d., Dereymaeker, G., Sloten, J.V., Jonkers, I., 2017. Extended foot-ankle musculoskeletal models for application in movement analysis. Computer Methods in Biomechanics and Biomedical Engineering 20, 153-159.

Manter, J.T., 1941. Movements of the Subtalar and Transverse Tarsal Joints. The Anatomical Record 80, 397-410.

McCullough, M.B.A., Ringleb, S.I., Arai, K., Kitaoka, H.B., Kaufman, K.R., 2011. Moment Arms of the Ankle Throughout the Range of Motion in Three Planes. Foot & Ankle International 32, 300-306.

McMaster, M., 1976. Disability of the Hindfoot after Fracture of the Tibial Shaft. The Journal of Bone & Joint Surgery 58, 90-93.

Meyer, A.J., D'Lima, D.D., Besier, T.F., Lloyd, D.G., Jr., C.W.C., Fregly, B.J., 2013. Are External Knee Load and EMG Measures Accurate Indicators of Internal Knee Contact Forces during Gait. Journal of Orthopaedic Research 31, 921-929.

Michelson, J., Hamel, A., Buczek, F., Sharkey, N., 2004. The Effect of Ankle Injury on Subtalar Motion. Foot & Ankle International 25, 639-646.

Nichols, J.A., Roach, K.E., Fiorentino, N.M., Anderson, A.E., 2016. Predicting tibiotalar and subtalar joint angles from skin-marker data with dual-fluoroscopy as a reference standard. Gait & Posture 49, 136-143.

Nichols, J.A., Roach, K.E., Fiorentino, N.M., Anderson, A.E., 2017. Subject-Specific Axes of Rotation Based on Talar Morphology Do Not Improve Predictions of Tibiotalar and Subtalar Joint Kinematics. Annals of Biomedical Engineering 45, 2109-2121.

Noginova, J.M., Bennett, H.J., Samaan, M.A., Ringleb, S.I., Year The Effects of Subtalar Axis Orientation on Kinematics and Kinetics During Dynamic Motion. In American Society of Biomechanics.

Parr, W.C.H., Chatterjee, H.J., Soligo, C., 2012. Calculating the axies of rotation for the subtalar and talocrural joints using 3D bone reconstructions. Journal of Biomechanics 45, 1103-1107.

Pearce, T.J., Buckley, R.E., 1999. Subtalar Joint Movement: Clinical and Computed Tomography Scan Correlation. Foot & Ankle International 20, 428-432.

Pellegrini, M.J., Glisson, R.R., Wurm, M., Ousema, P.H., Romash, M.M., Nunley, J.A., Easley, M.E., 2016. Systematic Quantification of Stabilizing Effects of Subtalar Joint Soft-Tissue Constraints in a Novel Cadaveric Model. The Journal of Bone & Joint Surgery 98, 842-848.

Piazza, S.J., 2005. Mechanics of the Subtalar Joint and Its Function During Walking. Foot and Ankle Clinics 10, 425-442.

Procter, P., Paul, J.P., 1982. Ankle Joint Biomechanics. Journal of Biomechanics 15, 627-634.

Reinschmidt, C., Bogert, A.J.v.d., Lundberg, A., Nigg, B.M., Murphy, N., Stacoff, A., Stano, A., 1997. Tibiofemoral and tibiocalcaneal motion during walking: external vs. skeletal markers. Gait & Posture 6, 98-109.

Reule, C.A., Alt, W.W., Lohrer, H., Hochwald, H., 2011. Spatial orientation of the subtalar joint axis is different in subjects with and without Achilles tendon disorders. British Journal of Sports Medicine 45, 1029-1034.

Rockar, P.A., 1995. The Subtalar Joint: Anatomy and Joint Motion. Foot/Ankle Therapy & Research 21, 361-372.

Root, M.L., Weed, J.H., Sgarlato, T.E., Bluth, D.R., 1966. Axis of Motion of the Subtalar Joint: An Anatomical Study. Journal of the American Podiatry Association 56, 149-155.

Sasaki, K., Neptune, R.R., 2010. Individual Muscle Contributions to the Axial Knee Joint Contact Force during Normal Walking. Journal of Biomechanics 43, 2780-2784.

Sheehan, F.T., Seisler, A.R., Siegel, K.L., 2007. In Vivo Talocrural and Subtalar Kinematics: A Non-invasive 3D Dynamic MRI Study Foot & Ankle International 28, 323-335.

Sherman, M.A., Seth, A., Delp, S.L., Year What is a Moment Arm? Calculating Muscle Effectiveness in Biomechanical Models Using Generalized Coordinates? In Proceedings of the ASME Design Engineering Technical Conferences.

Siegler, S., Chen, J., Schneck, C.D., 1988. The Three-Dimensional Kinematics and Flexibility Characteristics of the Human Ankle and Subtalar Joints - Part I: Kinematics. Journal of Biomechanical Engineering 110, 364-373.

SimTK, SimTK, https://simtk.org/.

Spoor, C.W., Leeuwen, J.L.v., Meskers, C.G.M., Titulaer, A.F., Huson, A., 1990. Estimation of Instantaneous Moment Arms of Lower-Leg Muscles. Journal of Biomechanics 23, 1247-1259.

Spoor, C.W., Veldpaus, F.E., 1980. Rigid body motion calculated from spatial co-ordinates of markers. Journal of Biomechanics 13, 391-393.

Stagni, R., Leardini, A., O'Connor, J.J., Giannini, S., 2003. Role of Passive Structures in the Mobility and Stability of the Human Subtalar Joint: A Literature Review. Foot & Ankle International 24, 402-409.

Taylor, M.K.F., Bojescul, C.J.A., Howard, R.S., Mizel, M.S., McHale, C.K.A., 2001. Measurement of Isolated Subtalar Range of Motion: A Cadaver Study. Foot & Ankle International 22, 426-432.

Wade, F.E., Lewis, G.S., Piazza, S.J., 2019. Estimates of Achilles tendon moment arm differ when axis of ankle rotation is derived from ankle motion. Journal of Biomechanics 90, 71-77.

Walter, J.P., Korkmaz, N., Fregly, B.J., Pandy, M.G., 2015. Contribution of Tibiofemoral Joint Contact to Net Loads at the Knee in Gait. Journal of Orthopaedic Research 33, 1054-1060.

Winter, D.A., Patla, A.E., Frank, J.S., Walt, S.E., 1990. Biomechanical Walking Pattern Changes in the Fit and Healthy Elderly. Physical Therapy 70, 340-347.

Woltring, H.J., Huiskes, R., Lange, A.d., 1985. Finite Centroid and Helical Axis Estimation from Noisy Landmark Measurements in the Study of Human Joint Kinematics. Journal of Biomechanics 18, 379-389.

Wong, Y., Kim, W., Ying, N., 2005. Passive motion characteristics of the talocrural and the subtalar joint by dual Euler angles. Journal of Biomechanics 38, 2480-2485.

Wright, D.G., Desai, S.M., Henderson, W.H., 1964. Action of the Subtalar and Ankle-Joint Complex During the Stance Phase of Walking. The Journal of Bone & Joint Surgery 46, 361-464.

Wu, G., Cavanagh, P.R., 1995. ISB Recommendations for Standardization in the Reporting of Kinematic Data. Journal of Biomechanics 28, 1257-1261.

Wu, G., Siegler, S., Allard, P., Kirtley, C., Leardini, A., Rosenbaum, D., Whittle, M., D'Lima, D.D., Cristofolini, L., Witte, H., Schmid, O., Stokes, I., 2002. ISB recommendation on definitions of joint coordinate system of various joints for the reporting of human joint motion - part I: ankle, hip, spine. Journal of Biomechanics 35, 543-548.

Ying, N., Kim, W., Wong, Y., Kam, B.H., 2004. Analysis of passive motion characteristics of the ankle joint complex using dual Euler angle parameters. Clinical Biomechanics 19, 153-160.

VITA

Julia Noginova

EDUCATION

PHD IN BIOMEDICAL ENGINEERING DECEMBER 2021
Old Dominion University, Norfolk, VA
BACHELOR OF SCIENCE Major: **PHYSICS** Concentration: **Medical Physics** MAY 2014
George Mason University, Fairfax, VA

Certifications: Biosafety and Biosecurity (BSS), OSHA Bloodborne Pathogens, Human Subjects Research (HSR), and Responsible Conduct of Research (RCR)

Memberships: American Society of Biomechanics (2014 – Present), Gamma Phi Beta (2011 – Present)

EXPERIENCE

OLD DOMINION UNIVERSITY, NORFOLK, VA SEPTEMBER 2014 – DECEMBER 2021
Biomechanics Research: Graduate Research Assistant
Educational Research: Research Assistant
TA & Lab Supervisor

PUBLICATIONS

Noginova, J., Hoch, M. C., Weinhandl, J., Bawab, S., Ringleb, S. I. Anterior Cruciate Ligament Sectioning Alters Center of Pressure with the Tibiofemoral Joint: An In Vitro Study. Journal of Musculoskeletal Research. 2019.

Ringleb, S. I., Pazos, P., **Noginova, J**., Cima, F., Ayala, O., Kaipa, K., Kidd, J., Gutierrez, K. (2021). The Influence of Participation in a Multi-Disciplinary Collaborative Service-Learning Project on the Effectiveness of Team Members in a 100-level Mechanical Engineering Class. American Society of Engineering Education (ASEE 2021) Annual Conference and Exposition, Virtual.

PRESENTATIONS

International

Noginova, J. **M.,** Bennett, H. J., Samaan, M. A., Ringleb, S. I. The Effects of Subtalar Axis Orientation on Kinematics and Kinetics During Walking and Running. IFAB, NY, 2018. Podium presentation.

Noginova, J.**M**., Bennett, H.J., Ringleb, S.I. Does Including the Subtalar Joint Affect the Kinetics in the Ankle and Knee in a Musculoskeletal Model of Running? XXVII ISB, Canada, 2019. Oral Presentation.

National

Noginova, J. M., Bennet, H. J., Ringleb, S. I. Consideration of Subtalar Joint Axis Location in Dynamic Musculoskeletal Model. ASB, Virtual, 2021. Podium presentation.

Noginova, J. M., Bennett, H. J., Samaan, M. A., Ringleb, S. I. The Effects of Subtalar Axis Orientation on Kinematics and Kinetics During Dynamic Motion. ASB, MN, 2018. Rapid Podium presentation.

Noginova, J., Hartley, E., Hoch, M., Ringleb, S. I. Measurement of Interjoint Pressure in the Midfoot Using Novel Sensors. ASB, CO, 2017. Poster presentation.

Noginova, J., Hoch, M., Weinhandl, J., Bawab, S., Ringleb, S. I. How Does the Anterior Cruciate Ligament Affect Center of Pressure? ASB, NC, 2016. Poster presentation.